WOOD AND FIBER SCIENCE

The Sustainable Natural Materials Journal

Volume 56, Number 4_2024 *(ISSN 0735-6161)*

Open Access

JOURNAL OF THE

SWST – International Society of Wood Science and Technology

WOOD AND FIBER SCIENCE

WOOD AND FIBER SCIENCE is published quarterly in January, April, July, and October by the Society of Wood Science and Technology, P.O. Box 6155, Monona, WI 53716-6155

There are three classes of membership (electronic only) in the Society: Members – dues $150; Retired Members – dues $75; Student Members – dues $25. We also have a membership category for individuals from Emerging Countries where individual members pay $30, individual students pay $10; Emerging Group of 10 pay $290, and Student Groups of 10 pay $90. Institutions and individuals who are not members pay $300 per volume (electronic only). Applications for membership and information about the Society may be obtained from the Executive Director, Society of Wood Science and Technology, P.O. Box 6155, Monona, WI 53716-6155 or found at the website http://www.swst.org.

Site licenses are also available with a charge of:
- $300/yr for single online membership, access by password and email
- $500/yr for institutional subscribers with 2–10 IP addresses
- $750/yr for institutional subscribers with 11–50 IP addresses
- $1000/yr for institutional subscribers with 51–100 IP addresses
- $1500/yr for institution subscribers with 101–200 IP addresses
- $2000/yr for institutions subscribers with over 200 IP addresses.

New subscriptions begin with the first issue of a new volume. All subscriptions are to be ordered through the Executive Director, Society of Wood Science and Technology. The Executive Director, at the Business Office shown below, should be notified 30 days in advance of a change of email address.

Business Office: Society of Wood Science and Technology, P.O. Box 6155, Monona, WI 53716-6155.
Editorial Office: jeff.morrell@oregonstate.edu

EDITORIAL AND PUBLICATION POLICY

Wood and Fiber Science as the official publication of the Society of Wood Science and Technology publishes papers with both professional and technical content. Original papers of professional concern, or based on research of international interest dealing with the science, processing, and manufacture of wood and composite products of wood or wood fiber origin will be considered.

All manuscripts are to be written in US English, the text should be proofread by a native speaker of English prior to submission. Any manuscript submitted must be unpublished work not being offered for publication elsewhere.

Papers will be reviewed by referees selected by the editor and will be published in approximately the order in which the final version is received. Research papers will be judged on the basis of their contribution of original data, rigor of analysis, and interpretations of results; in the case of reviews, on their relevancy and completeness.

As of January 1, 2022, Wood and Fiber Science will be an online only, Open Access journal. There will be no print copies. Color photos/graphics will be offered at no additional cost to authors. The Open Access fee will be $1800/article for SWST members and $2000/article for nonmembers. The previous five years of articles are still copyright protected (accept those that are identified as Open Access) and can be accessed through member subscriptions. Once a previous article has reached its 5th anniversary date since publication, it becomes Open Access.

Technical Notes

Authors are invited to submit Technical Notes to the Journal. A Technical Note is a concise description of a new research finding, development, procedure, or device. The length should be **no more than two printed pages** in WFS, which would be five pages or less of double-spaced text (TNR12) with normal margins on 8.5 x 11 paper, including space for figures and tables. In order to meet the limitation on space, figures and tables should be minimized, as should be the introduction, literature review and references. The Journal will attempt to expedite the review and publication process. As with research papers, Technical Notes must be original and go through a similar double-blind, peer review process.

On-line Access to *Wood and Fiber Science* Back Issues

SWST is providing readers with a means of searching all articles in *Wood and Fiber Science* from 1968 to present Articles from 1968 to 2019 are available to anyone, but in order to see 2019 to 2021 articles you must have an SWST membership or subscription. SWST members and subscribers have full search capability and can download PDF versions of the papers If you do not have a membership or subscription, you will not be able to view the full-text pdf.

Visit the SWST website at http://www.swst.org and go to Wood & Fiber Science Online. Click on either SWST Member Publication access (SWST members) or Subscriber Publication access (Institution Access). All must login with their email and password on the HYPERLINK "http://www.swst.org" www.swst.org site, or use their ip authentication if they have a site license.

As an added benefit to our current subscribers, you can now access the electronic version of every printed article along with exciting enhancements that include:

- IP authentication for institutions (only with site license)
- Enhanced search capabilities
- Email alerting of new issues
- Custom links to your favorite titles

(ISSN 0735-6161)
CODEN WOOFAJ

WOOD AND FIBER SCIENCE

JOURNAL OF THE SOCIETY OF WOOD SCIENCE AND TECHNOLOGY

VOLUME 56 DECEMBER 2024 NUMBER 4

CONTENTS

Articles

CHARACTERIZATION OF BONDLINES IN CROSS-LAMINATED TIMBER MADE WITH PRESERVATIVE-TREATED LUMBER

Cody Wainscott
Graduate Student
Department of Wood Science and Engineering, Oregon State University, Corvallis, OR
E-mail: cody.wainscott@oregonstate.edu

Matthew J. Konkler
Senior Faculty Research Assistant II
Department of Wood Science and Engineering, Oregon State University, Corvallis, OR
E-mail: matthew.konkler@oregonstate.edu

Scott Noble
Senior Project Manager
Kaiser + Path Architecture, Portland, OR
E-mail: scott@kaiserpath.com

Joey Valenti
Chief Executive Officer
The Albizia Project, LLC, Wahiawa, HI
E-mail: joey@albiziaproject.com

Jeffrey J. Morrell
Emeritus Faculty
Department of Wood Science and Engineering, Oregon State University, Corvallis, OR
E-mail: jeff.morrell@oregonstate.edu

*Gerald Presley**
Assistant Professor
Department of Wood Science and Engineering, Oregon State University, Corvallis, OR
E-mail: gerald.presley@oregonstate.edu

(Received March 28)

Abstract. The number of mass timber construction projects is rapidly increasing in North America but this technology encounters durability issues where termites are present. One method for minimizing this risk is to incorporate termiticidal treatments into mass timber elements. This study examined the impact of cross-laminated timber (CLT) pre and post layup treatment on bond line integrity. Douglas-fir 2 × 6-in. lumber or CLT panel sections were pressure treated with 1) borates or 2) propiconazole, tebuconazole, imidacloprid, permethrin, and iodopropynyl butylcarbamate (PTIP), or 3) dip treated with a mixture of propiconazole, tebuconazole, and imidacloprid + borate (PTIB). CLT panels were manufactured using melamine formaldehyde or polyurethane resins. The impact of preservative treatment on bondline integrity was tested by delamination and block shear tests. Adhesive penetration was also measured using fluorescence microscopy and surface wettability was measured using a contact angle analyzer. Planing-treated lumber before use in CLT panel assembly reduced actives by 57-94% compared with unplaned lumber containing the same treatment. Panels made with borate-treated lumber were more easily delaminated than panels composed of PTIP-treated wood. Microscopic evaluation of CLT bondlines showed greater resin penetration in panels made with PTIP-treated wood; however, penetration was highly variable across specimens. Borate-containing treatments increased surface wettability which may have contributed to reduced treated

* Corresponding author

panel performance. The results help define the challenges associated with incorporating biocidal treatments into panels and identify some mechanisms by which they reduce performance.

Keywords: CLT, preservative, bondline, melamine formaldehyde, polyurethane.

INTRODUCTION

Cross-laminated timber (CLT) is an engineered timber product composed of an uneven number of layers (usually three, five, or seven layers) of lumber glued together in alternating layers offset 90° from one another (Brandner et al 2016; APA 2018). The current form of CLT was first developed in Austria in the 1990s and has gained global use as a sustainable building material (Brandner et al 2016). CLT was first used in building construction in the United States in the early 2000s (França et al 2018). Because it is made from wood, CLT sequesters CO_2 from the atmosphere during its service life. The technology also boasts several other advantages including reduced construction time, easier construction clean-up, strength-to-weight performance comparable to concrete or steel, good seismic and fire performance, and reduced energy consumption (Mallo et al 2014; Crawford and Cadorel 2017; Shahan et al 2021; Ayanleye et al 2022).

CLT is a material whose biological components are degradable if they are wetted above the fiber saturation point (~28% MC) at a wide range of temperatures between 5 and 40°C. It is estimated that the annual loss of wooden materials from biodegradation in the United States is around $5 billion and CLT-based structures will factor into these totals as they age (Ayanleye et al 2022). CLT is largely used for structural wall and floor/ceiling assemblies in buildings in interior protected applications that equate to American Wood Protection Association (AWPA) Use Categories 1 and 2. These exposures face limited risks of wetting and fungal decay provided the vapor barriers and cladding remain functional and intact, but interior framing materials such as CLT are at risk for termite attack. North America is home to several large population centers in tropical and subtropical areas where high annual rainfall and temperatures lead to greater decay risk than those found in Northern Europe (Forest Products Laboratory 2021). Additionally, the southern continental United States and Hawaii harbor a number of subterranean termite species, the most economically important wood-destroying insects (Goodell and Nielson 2023). Hawaii is the only U.S. state to require that all structural timber elements be preservative treated to a specific preservative retention and this requirement will apply to mass timber structures (Hawaii amended 2018 IBC section 2303.1.9).

Wood products can be protected from fungal or termite attacks with chemical treatments applied to wood topically or by pressure treatment (Oliveira et al 2018). The AWPA specifies chemical retention levels for UC1 and UC2 that are sufficient for protection against fungal decay and wood-destroying insects as well as a special level for protection against Formosan termites which requires higher chemical loadings for borate-based treatments (AWPA 2021). However, incorporating fungicidal or termiticidal treatments in CLT can be problematic due to the potential for chemical interactions with wood adhesives and the size of panels relative to commercial treating vessels. Preservatives can be incorporated into CLT panels by using pressure-treated wood to manufacture panels (prelayup treatment) or by applying biocide to panels after a layup by pressure or nonpressure processes (postlayup) (França et al 2018; Wang et al 2018). Lamination using dowels avoids the use of adhesives and should enable the use of pressure-treated lamellae in dowel-laminated timber construction without compromising structural performance. However, dowel-laminated timber is not as widely manufactured in North America as CLT. As a result, termite treatment solutions will have to be incorporated into CLT manufacturing or building management for these materials to penetrate the market more broadly.

Although chemical treatments can prevent fungal and insect attacks, they can also adversely affect CLT panel performance (Tascioglu et al 2003). Postlayup treatments can be applied to whole

panels with no need to resurface the treated Panels. However, pressure treatment is limited to panels smaller than the treatment vessel diameter (usually under 2-3 m in diameter). These processes are also limited to organic solvent-based treatments because of the risk of swelling and subsequent deformation. Prelayup treatments can be used to produce panels of any dimension, but the requirement to plane the lumber shortly before resin application removes much of the preservative reducing durability and creating chemically treated wastes. Preservatives can also interfere with resin curing, resulting in reduced bondline performance (Cai et al 2022).

A number of factors influence adhesive penetration into wood including wood species, surface characteristics, porosity, surface tension, and pH. Resin characteristics that can affect performance include molecular weight, viscosity, pH value, and curing additives. Excessive adhesive penetration can result in a starved bondline while insufficient penetration produces a thick bondline, with both events leading to an adhesive failure (Kamke and Lee 2007; Ciglian and Reinprecht 2022). The addition of preservatives can further affect adhesive bonding development (Kamke and Lee 2007; Faria et al 2020; Lim et al 2020; Ayanleye et al 2022; Ciglian and Reinprecht 2022; Alade et al 2023).

While preservative treatment may be necessary for the performance of CLT in areas with a substantial risk of termite attack, it will be important to confirm that the treatments do not adversely affect glue line bond properties. The objective of this study was to evaluate the effects of pre and postlayup treatments on bondline integrity of Douglas-fir CLT panels.

MATERIALS AND METHODS

Materials

Untreated CLT panels were made with coastal Douglas-fir 2 × 6-in. nominal lumber obtained in western Oregon. All treated lumber was also made from coastal Douglas-fir. Borate-treated lumber used to make panels was obtained from a commercial facility in western Oregon and was treated with a solution of sodium octaborate tetrahydrate. PTIB-treated lumber was obtained from a commercial facility and was dip-treated in a solution of disodium octaborate tetrahydrate augmented with propiconazole, tebuconazole, and imidacloprid. PTIP-treated wood was pressure treated in a commercial facility using a proprietary solution containing propiconazole, tebuconazole, imidacloprid, permethrin, iodopropynyl butyl carbamate (IPBC), and minor amounts of borates. All lumber used for CLT panel construction in this study was commercially available stock material and contained random proportions of heartwood and sapwood.

Melamine formaldehyde (MF) adhesive was a commercially available preparation that required a hardener to be mixed before application. Polyurethane (PUR) adhesive was a commercially available single-component adhesive that required a primer to be applied to the wood before adhesive application.

CLT Panel Fabrication

CLT panels were made using 51 × 152 mm nominal (2 × 6-in.) Douglas-fir lumber that was either untreated, dip-treated, or pressure-treated with one of three preservative systems and one of two resin systems. All lumber used for panel manufacture was planed 1.6 mm (1/16th in.) before layup using a Leadermac LMC-460PL 4-side planer/molder (Blaine, WA). Three ply 1.52 × 2.44 m (5 × 8 ft) panels were made for each treatment in addition to three untreated panels at the Tall Wood Design Institute at Oregon State University. Panels were glued with either MF or PUR resin in combination with treated or untreated wood as shown in Table 1. The resin was applied using a custom APQUIP Co. resin applicator equipped for one and two-component resin systems (Monterey, CA). Lumber was passed through a resin curtain calibrated to deliver a specified application rate. MF was applied via a two-part applicator with a 1.5:1 resin:catalyst ratio at a rate of 367 g/m^2. Assembly time was 75 min at 21°C, and press time was 5 h at 0.83 MPa (120 psi). The one-part polyurethane was

Table 1. Preservative treatments and resin types used to produce nine three-ply, 5 × 8 ft Douglas-fir CLT panels examined in this study.

Lumber preservative treatment	Preservative components	Adhesive
Postlayup treatments (PTIP)	Propiconazole, tebuconazole, imidacloprid, permethrin, iodopropynyl butyl carbamate	Melamine formaldehyde
Postlayup treatments (borates)	Disodium octaborate tetrahydrate	Melamine formaldehyde
Postlayup treatments (PTIB)	Borates + propiconazole, tebuconazole, imidacloprid	Melamine formaldehyde
Control	Untreated control	Melamine formaldehyde
Organic pressure treatment (PTIP)	Propiconazole, tebuconazole, imidacloprid, permethrin, iodopropynyl butyl carbamate	Melamine formaldehyde
Borate pressure treatment (borates)	Disodium octaborate tetrahydrate	Melamine formaldehyde
Borate/organic diptreatment (PTIB)	Borates + propiconazole, tebuconazole, imidacloprid	Melamine formaldehyde
Organic pressure treatment (PTIP)	Propiconazole, tebuconazole, imidacloprid, permethrin, iodopropynyl butyl carbamate	Polyurethane
Borate pressure treatment (borates)	Disodium octaborate tetrahydrate	Polyurethane
Borate/organic diptreatment (PTIB)	Borates + propiconazole, tebuconazole, imidacloprid	Polyurethane

applied at a rate of 137 g/m^2 to boards that had previously been wetted with a 5% primer solution at 20 g/m^2. Adhesive application rates followed manufacturer recommendations, and these were assumed to be comparable with current industry standards at the time. Lumber was arranged into crosslams randomly with no attempt to normalize laminae for heartwood and sapwood content across panels. Lumber was arranged on a 2.44 × 3.05 m (8 × 10 ft) Minda laboratory CLT press (Minden, Germany). Assembly time was 60 min at 20°C and press time was 2.5 h at 0.83 MPa (120 psi) with pressure applied on the top and sides.

Nine CLT panels were produced for this study. Three panels were made using untreated Douglas-fir lumber and were subsequently cut into nine 457 × 762 mm (18 × 30-in.) subpanels each. Six test subpanels from each were treated with one of three preservative treatments described in the section "Preservative Treatment". Two of the postlayup treated panels per treatment were retained at OSU for testing. The remaining subpanels were treated and sent to Hawaii for separate termite testing.

The remaining 6 panels were produced using pressure or dip-treated lumber that was planed before assembly. Two panels were made per treatment type, one using MF resin and another using PUR resin as described above. The preservative treatments used are described in Table 1.

Preservative Treatment

Lumber for the prelayup treatments and test panels used for postlayup preservative treatments were treated on a commercial scale treating plants using pressure or nonpressure processes.

Borate pressure treatment was performed in a commercial cylinder using disodium octaborate tetrahydrate (DOT) to the AWPA U1 Formosan termite retention level for borates of 6.7 kg/m^3 (0.42 pcf) DOT. Lumber and test panels were treated using a full cell process with a 30 min vacuum at -11.9 kPa (26 in Hg) followed by filling the cylinder with a 10% w/w DOT solution. The pressure was applied at 598 kPa (88 psi) within 15 s and then raised to an average of 931 kPa for about 14 min to the target retention. The pressure was reduced to 102 kPa (15 psi) over 60 s and the cylinder was drained before pulling a final vacuum of -11.9 kPa (26 in Hg). Net absorption by gauge was 1693 L (448 gal). The full cross

section of borate pressure-treated lumber was penetrated with borates as assessed by the treater.

PTIB dip treatment was carried out by soaking lumber or test panels in a treating solution containing 1.8% PTI and 11% DOT. The treatment targeted a DOT retention of 1.9 kg/m^3 (0.12 pcf). Lumber and test panels were immersed in the treating solution at 43.3°C (110°F) for 15 min PTI retention calculated by solution uptake was 0.37 kg/m^3 (0.021 pcf). The full cross section of PTIB dip-treated lumber was penetrated with borates as assessed by the treater.

PTIP treatment was done in a commercial facility producing lumber used for interior applications in Hawaii. Retentions targeted were suitable for Formosan termite exposure in Hawaii and chemical penetration was assessed at the treating facility.

The active ingredients in lumber or test panels treated with these systems were quantified in the outer 0.4-in. (10 mm) assay zone using the appropriate AWPA standard. Materials were assayed for borates while propiconazole and tebuconazole were assessed for PTIB and PTIP. The assay zone of lumber from each treatment was ground to 20 mesh in a Wiley Mill before analysis. Borates were quantified using the Azomethine method, AWPA standard A65 (AWPA 2021). Propiconazole and tebuconazole were quantified in the organics-containing treatments by high-performance liquid chromatography using a modified version of AWPA standard A48 (AWPA 2021). Permethrin, imidacloprid, and IPBC were not quantified in the organic treatment and the azole fraction was used as a measure of total chemical retention (Table 2). The Formosan termite standard listed includes a sum of propiconazole, tebuconazole, and imidacloprid; however, imidacloprid was not assayed in lumber used in this study.

Bondline Strength Characterization Using Delamination and Block Shear

Three specimens were collected from each 18 × 30-in. subpanel for a total of 12 blocks per treatment according to guidelines outlined in the ANSI/APA PRG-320 standard (APA 2018). One exception to this was for the postlayup treated panels where triplicate samples were only sourced from three of the four replicates per treatment. This was due to unbonded regions after manufacturing in some of the test panels that

Table 2. Retentions of borates, azoles, and imidacloprid in the 0.4-in. (10 mm) AWPA assay zone in pre and postlayup treatments alongside Formosan termite standard retentions listed by AWPA. Prelayup treatments were planed before panel fabrication and show a % percent preservative loss in this assay zone compared with unplaned treated lumber from the same facility.

Treatment	Planed/unplaned	Sample type	Resin system	Boron retention levels (kg/m^3)	% Loss vs unplaned lumber	Tebuconazole (kg/m^3)	% Loss vs unplaned lumber	Propicon azole (kg/m^3)	% Loss vs unplaned lumber	Total azole (kg/m^3)
AWPA formosan termite standard				4.5		0.08		0.08		0.21
Untreated	Planed	Untreated Panel	MF	0.31[a]		0.00		0.01		0.01[a]
Borate	Unplaned	Lumber	N/A	31.90		N/A		N/A		N/A
PTIB	Unplaned	Lumber	N/A	1.98		0.10		0.20		0.30
PTIP	Unplaned	Lumber	N/A	3.47		0.03		0.16		0.19
Borate	Unplaned	Postlayup treated	MF	27.68[c]		N/A	N/A	N/A		N/A
PTIB	Unplaned	Postlayup treated	MF	1.27[b]		0.13	−23.53	0.23		0.36[b]
PTIP	Unplaned	Postlayup treated	MF	2.58[b]		0.07	−97.06	0.31		0.38[b]
Borate	Planed	Prelayup treated	MF	13.42[c]	57.93	N/A	N/A	N/A	N/A	N/A
PTIB	Planed	Prelayup treated	MF	0.12[a]	93.94	0.00	100.00	0.01	96.98	0.01[a]
PTIP	Planed	Prelayup treated	MF	1.21[b]	65.13	0.02	29.41	0.17	−10.97	0.20[a]
Borate	Planed	Prelayup treated	PUR	10.46[c]	67.21	N/A	N/A	N/A	N/A	N/A
PTIB	Planed	Prelayup treated	PUR	0.22[a]	88.89	0.03	70.59	0.05	73.87	0.08[b]
PTIP	Planed	Prelayup treated	PUR	2.32[b]	33.14	0.06	−64.71	0.19	−23.87	0.25[c]

prevented the selection of sound test specimens for delamination and block shear tests. Two 3 × 6 in. (76 × 152 mm) by panel thickness samples were taken from near opposing corners at least 1.5 in. (38 mm) from the panel edge and one sample was taken from the center of the panel. Each sample was cut into two paired 3 × 3-in. (76 × 76 mm) samples. One of the samples was reserved for a block shear test and the other for a delamination test. Delamination test specimens were weighed and inspected for preexisting bond issues and marked accordingly before being submerged in water and subjected to a -70 ± 20 kPa (21 ± 6 in Hg) vacuum stage for 30 min, followed by a 520 ± 20 kPa pressure stage for 2 h. The saturated specimens were oven-dried at 70.0 ± 0.1°C for about 14 h until MC was reduced to about 10-15% w/w before soaking. After drying, each specimen was visually inspected for bondline separation and measured using a ±0.01 mm caliper. Delamination was calculated according to Eq 1:

$$D\ \% = \frac{X - L}{L} \times 100\% \qquad (1)$$

where D % is the percentage of delamination of the sample, X is the measured (mm) delamination of the bondline, and L is the total bondline length (mm) before being placed in the pressure vessel. In addition, samples were graded as pass/fail according to the PRG-320 criteria where all specimens must contain less than 5% delamination, otherwise, the whole panel from which samples are taken fails to meet the requirements (APA 2018). A total of 12 blocks were taken from two prelayup panels and nine from postlayup panels within each resin-treatment combination.

Block shear tests were performed according to the ASTM D905 method referred to in PRG-320. Tests were performed on 3 × 3-in. (76 × 76 mm) specimens sampled from the same location as paired specimens tested for delamination. The specimens were then cut into a stair step shape according to ASTM D905. An Instron universal testing machine (Norwood, MA), equipped with a 10kN capacity load cell with an accuracy of ±0.4 N was used to load each bond surface to failure. The ultimate load was recorded. After testing, wood failure (WF) was assessed on both sides of the fractured bond surfaces by illuminating the broken surface with ultra-violent light and photographing the surface. Image J was used to determine the percentage of the surface that contained MF or PUR resin, indicative of adhesive failure, using the plugin Trainable Weka Segmentation (version 3.8.5).

Microscopic Examination of the Bondline

Microscopic analysis of bondline integrity for each treatment listed in Table 1 was done on 25 × 25 × 25 mm blocks taken from near the panel edges (3 on each side) and the panel center (three total). Each sample contained two bondlines and the sections were microtomed to produce 90-μm thick sections across both bondlines in the sample for a total of 18 thin sections per treatment. Each bondline section was dyed with safranin-o red and placed on a glass slide with coverslip (Bastani et al 2016). Samples were then examined under a fluorescent microscope to observe adhesive penetration into the wood using a 40× objective with an excitation wavelength of 450-490 nm. Average cell depth was determined by counting the number of cells from the bondline containing adhesive and dividing by the number of cell rows visible in the photo. Penetration was only measured in the CLT lamina visible in cross section under the microscope.

Surface Wettability

Wettability was measured on treated boards after planing using a Biolin Scientific contact angle analyzer to measure resin droplet contact angle with the wood surfaces by the sensile drop method on all of the treated materials except for PTIP due to loss of samples before the completion of the experiment. The planed boards had ∼1.5 mm planed off to represent the process used to manufacture CLT with the treated wood. The boards were cut into 1-in. × 5 $^1/_2$-in. samples conditioned at 65% RH and 20°C for over a week before testing. The contact angle was examined with MF, PUR resins, and water using a

19-gauge syringe to place drops on the tangential early wood surface of each specimen. Three replicate drops were placed on opposite sides of each specimen for a total of six measurements per piece. The surface tension of the resins was measured by the pendant drop method at 22°C and 65% RH using Young-Dupré Eq 2. Surface energy was found for each treated and nontreated surface.

$$SE = ST_a(1 + \text{Cos}(Ø)) \quad (2)$$

where SE is the surface free energy of the wood surface, ST_a is the surface tension of the adhesive droplet, and the cos (Ø) is the contact angle of the liquid drop formed on the wood surface.

Statistics

The data were subjected to an analysis of variance (ANOVA) among the control and resin/preservative treatment combinations at $\alpha = 0.05$, using the Excel statistical package. All average data are shown with ± 1 SD.

RESULTS AND DISCUSSION

Effect of Planing on Chemical Retention of Wood Treatments

Planing is necessary for all lumber used in the manufacture of CLT to ensure boards fit together flush and to create an activated surface to facilitate bond development. This is a problem for the use of pressure-treated or dip-treated Douglas-fir lumber in CLT because most of the preservative chemical is loaded near the surface of the wood in the outer 10 mm (0.4-in.) assay zone for 50 mm (2-in.) thick lumber. Chemical retention data for the different treatments used in this study are shown in Table 2 along with the calculated losses due to planing relative to nonplaned control lumber of the same treatment. Major losses were seen in the prelayup treatment due to the planing step (Table 1). Planing removed 33-94% of the borates in the AWPA assay zone for the prelayup treatments while borate losses where the principle active preservatives losses ranged from 57 to 94%. The greatest losses were seen in the borate-PTI dip treatment which were 89-94%. This is because nonpressure treatments result in lower penetration leaving the vast majority of preservative in dip-treated lumber in the very outer layers where it was planed off. It is important to note that despite losing 58-67% of the original borates in the AWPA assay zone due to planing, prelayup panels pressure treated with borates still contained more than double the AWPA retention level for Formosan termites. This suggests that despite planing, the borate-treated lumber used in this study would still effectively resist Formosan termite attack.

Nearly all of the azoles in the AWPA assay zone were lost from the PTI dip-treated wood due to planing. This indicates low levels of preservative penetration in the dip treatment which is to be expected. Azole levels in the PTIP treatment were higher in planed panels than the nonplaned controls, except tebuconazole in the MF panel. These observations suggest that retentions were still sufficient to maintain Formosan termite protection.

Preservative retentions tend to be higher near the surface and planing removes this material. If the 10 mm assay zone specified in the AWPA Standards is used to measure retentions, then the assay zone on the planed boards is likely to have a lower retention in what becomes the new assay zone. These data indicate that the planing of treated wood for CLT manufacture results in chemical waste and may also result in reduced preservative retentions in the resulting panels. However, retention levels for most of the prelayup pressure treatments after planing were still above those specified for protection against Formosan termites. This is especially notable with the azole retention levels for the PTIP treatment after planing.

It must be noted that retentions on unplaned material were not measured in the same boards used in the CLT layup although they were prepared at the same time. Thus, there may be some variations between the boards. This explains why azole retentions were higher for planed material for some of the prelayup-treated PTIP panels.

Delamination

Some panels had areas with considerable delamination that were avoided when obtaining test

samples. Heavily delaminated panels included a subpanel from one of the replicates treated with PTIP after layup. The extensive delamination in this panel limited the number of samples that could be tested for bondline integrity. Borate postlayup treatment also absorbed extensive moisture and had a high amount of preexisting delamination. The delamination could reflect poor handling and storage or manufacturing error creating too much open assembly time before pressing (Long and Morrell 2011; Ayanleye et al 2022; Lukowsky and Nguyen 2023). Minimal planing was done on the panels to try and limit preservative loss. This also may have limited effective bonding in some of the panels. Although it would be difficult to delineate, it is possible that the treatment of the assembled panels induced stresses along the gluelines that contributed to subsequent delamination. Current APA standards preclude pressure treatment of laminated timbers with water-based systems due to these concerns, although there is evidence that the process does not negatively affect flexural properties (Long and Morrell 2011). Test samples for the delamination test were selected to be free of visible delamination and only two borate-treated samples had any preexisting delamination before they were tested.

Delamination results for all of the different treatments are shown in Table 3. Postlayup treatments had lower levels of delamination than prelayup treatments. Organic and borate postlayup treatments performed similarly to the untreated controls (1.7%) while delamination in PTIB was at 4.5%. Previous studies have also shown that postlayup preservative CLT treatment had less effect on bondline integrity since it eliminated the risk of preservative interference with resin curing (Tascioglu et al 2003; Kuka et al 2022, Taylor et al 2022).

The most extensive delamination was observed in prelayup treatments (Table 3). The greatest delamination was observed in borate and PTIB-based treatments, especially with PUR panels. The panels composed of borate-treated lumber and MF resin were the only other panel to have some prior delamination. PTIP-based treatments were associated with the least delamination for either resin (slightly over 2%) (Faria et al 2020).

Table 3. Effect of pre and postlayup preservative treatment of CLT panels on delamination and block shear. Standard deviations are shown in parentheses.

Test	Control	Postlayup			Prelayup				
Delamination	Control	PTIP	Borate	PTIB	MF-PTIP	MF-Borate	MF-PTIB	PUR-PTIP	PUR-Borate	PUR-PTIB
Total # of specimens	12	9	9	9	12	12	12	12	12	12
Predelamination check	X	X		X	X		X	X	X	X
Avg. sample % delamination	1.7% (2.3)	0.8% (.8)	1.1% (1.5)	4.5% (2.8)	2.5% (2.5)	5.1% (3.3)	5.3% (9.2)	2.2% (2.1)	7.7% (6.2)	14.2% (10.1)
% Specimens failed[a]	(10/12)	(8/9)	(8/9)	(7/9)	(9/12)	(8/12)	(9/12)	(11/12)	(7/12)	(5/12)
	17% (F)	11% (F)	11% (F)	33% (F)	25% (F)	33% (F)	25% (F)	8% (F)	42% (F)	58% (F)
Block shear										
Total # of specimens	12	12	12	12	12	12	12	12	12	12
Avg. WF of all specimens[b]	94.2% (5.1)[a]	98.1% (3.6)[a]	98.0% (3.2)[a]	96.3% (3.2)[a]	97.9% (3.9)[a]	98.2% (2.7)[a]	96.5% (5.3)[a]	93.0% (9.2)[a]	84.2% (23.4)[a]	75.2% (21.6)[b]
Above 60% WF specimens[a]	100%	100%	100%	100%	100%	100%	100%	100%	(11/12)	(9/12)
									8% (F)	25% (F)

[a]F = failure as defined in the PRG-320 standard where if 5% of samples fail the panel does not pass.
**Different lowercase letters indicate statistically significant differences (ANOVA, $\alpha = 0.05$).

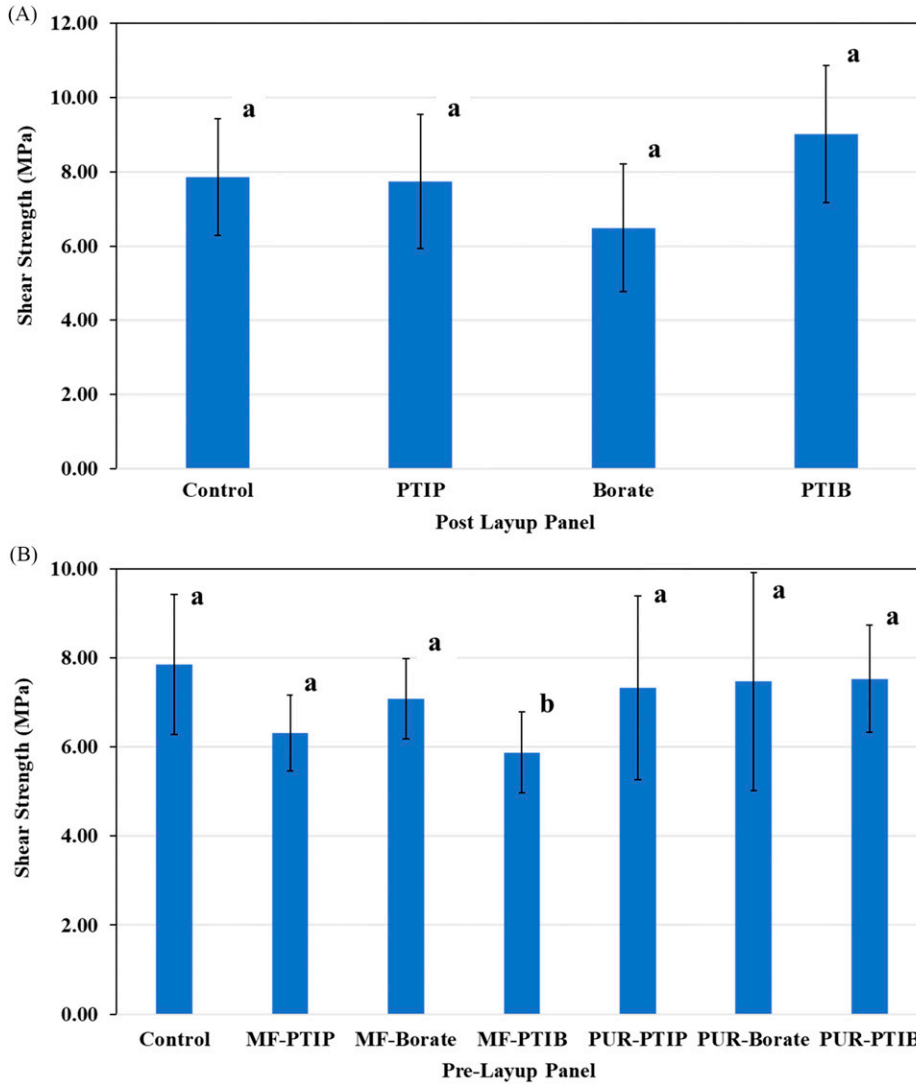

Figure 1. Effects of post layup (A) treatment and pre-layup (B) treatment on maximum shear strength of CLT panels tested. Error bars represent 1 SD while bars with the same letters do not differ significantly from the control at $\alpha = 0.05$.

Mbhamali et al (2022) reported similar negative delamination effects of boron treatments in combination with PUR resins possibly due to the effects of boron on the surface energy of the wood.

Block Shear

Shear strength values were similar among all treatments (Bagheri et al 2022) (Fig 1). The proportion of wood to glueline failure is usually a good indicator of bondline performance (Wang et al 2018). PRG-320 standard requires a minimum of 60% WF in a glueline shear test. WF was above 90% for all treatments except prelayup treatments with borates or PTI. The success of postlayup treatments by this metric could be due to the successful formation of an adhesive bond in the absence of chemical, whereafter chemical interference with the bondline would not be able to interfere with resin curing (Künniger et al 2019;

Kuka et al 2022). Long and Morrell (2011) performed a similar test with nonincised Douglas fir beams and found that post-layup treatment with DOT had the minimum effect on bondline performance and high WF. These findings were consistent with the fact that borates affect resin cure but would be expected to have a negligible effect on cured resin.

PUR was most affected by borate or PTI treatments with WFs of 84.2% and 75.2%, respectively (Table 3). The slightly lower degrees of WF suggest that that adhesive type may play a slight role (Lim et al 2020; Mbhamali et al 2022). Künniger et al (2019) noted that the aromatic backbone of MF resins can form strong crosslinking networks resulting in less ductile failures compared with PUR which may have contributed to less WF.

Increasing boron concentrations in wood composites have been shown to reduce shear strength in PUR- and MF-based composites (Özçifçi 2006; Mbhamali et al 2022). High concentrations of boron have been shown to have negative effects on panel strength (Taylor et al 2022). Organic biocides have been shown to have lower impacts on composite strength than inorganic treatments, although some negative effects have been observed (Antwi-Boasiako and Appiah 2012; Faria et al 2020).

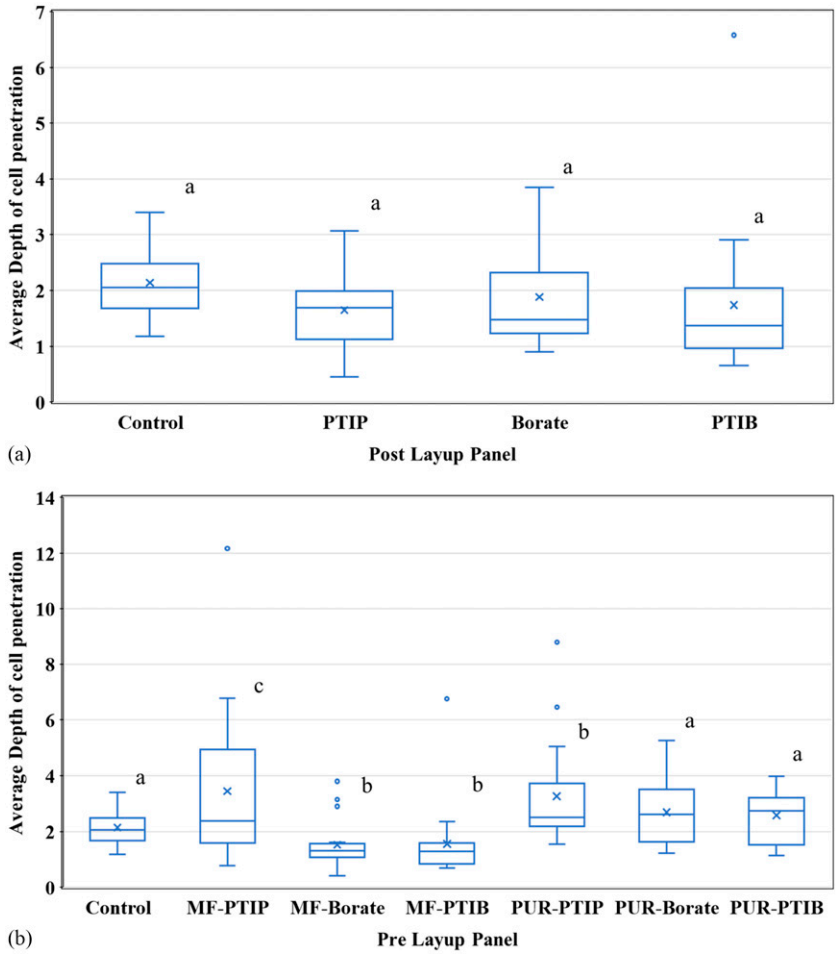

Figure 2. Effect of pre (A) and postlayup (B) preservative treatment of CLT on adhesive penetration represented as the average number of cells containing visible resin from the glueline.

Alipon et al (2018) found comparable results to the current study with deltamethrin + propiconazole and various resins.

Wettability and Adhesive Penetration

Adhesive penetration in CLT panels can be readily visualized by fluorescence microscopy since the resins fluoresce while the wood remains darkened red by safranin staining. Adhesive penetration varied widely between samples even within treatments, which sometimes made it difficult to compare different treatments (Fig 2). Preservative treatments further complicated the analysis.

Adhesive penetration did not differ among the postlayup treatments reflecting the fact that the resin cured before treatment (Fig 2[a]). However, there was evidence of bondline damage with noticeable voids, which could be due to the partial weather cycle during pressure or dip treatment as the water-borne preservative swelled the wood and stressed the bondline (Fig 3[a]).

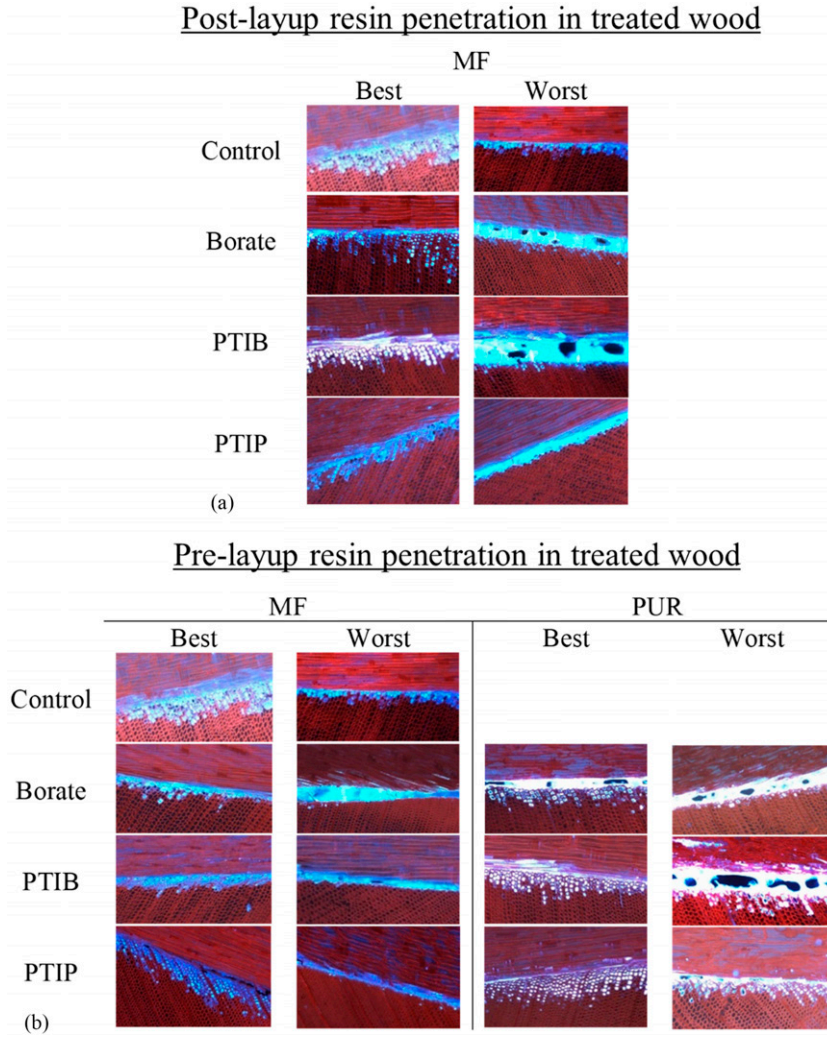

Figure 3. (A) Post layup, melamine formaldehyde (MF) adhesive. (B) examples of safranin-O-stained fluorescence micrographs of CLT bondlines taken from panels made with wood treated with one of three biocides and two adhesives MF or polyurethane (PUR).

Table 4. Contact angle and surface energy for adhesives on treated/nontreated early wood planed boards. Stats compared with control and respective resin treatment combination within the same group.

Sample	CA (θ)	SE (mN/m)
MF-Cont.	82 (14)[a]	69 (12)[a]
MF-PTIP	N/A	N/A
MF-Borate	77 (12)[a]	75 (12)[a]
MF-PTIB	78 (16)[a]	73 (17)[a]
PUR-Cont.	35 (9)[a]	44 (2)[a]
PUR-PTIP	N/A	N/A
PUR-Borate	35 (6)[a]	44 (2)[a]
PUR-PTIB	34 (8)[a]	44 (2)[a]
Water-Cont.	57 (23)[a]	118 (24)[a]
Water-PTIP	N/A	N/A
Water-Borate	7 (2)[b]	152 (1)[b]
Water-PTIB	11 (2)[b]	151 (4)b

Adhesive penetration varied widely in CLT composed of pretreated lamella. Adhesive penetration for MF-Borate and MF-PTI-treated panels trended lower than the controls although there were examples of the opposite trend. This was surprising since contact angle tests using MF adhesive on treated wood used in this study showed that treatments, particularly borates and PTI, were associated with decreased contact angles, indicating greater wettability (Table 4).

Previous studies indicate that boron limits adhesive penetration into the wood surface and increases gelation (Gao et al 2016; Alade et al 2022, 2023). Other studies have shown that lower borate concentrations can have a greater negative effect on bondline quality than higher concentrations by reducing adhesive penetration, creating a thicker bondline, and reducing bond strength (Qin et al 2019; Lim et al 2020).

Borate and PTI treatments were also associated with increased wood surface wettability in CLT constructed with PUR. Microscopic analysis suggested that average PUR penetration was deeper than MF for each treatment type. PUR tends to have lower polarity and a higher viscosity which would limit penetration into the wood cells (Ciglian and Reinprecht 2022). Other preservative systems have been shown to increase wood wettability such as micronized copper azole-treated southern yellow pine using PUR (Cai et al 2022). Composites made with this material had the thinnest bondlines compared with control and the lower retention treatments. Ciglian and Reinprecht (2022) found that treating spruce composites containing PUR with various inorganic treatments reduced surface wettability except with boric acid. Adhesive penetration was also increased over control for all preservatives with boric acid having the highest penetration overall. A similar mechanism could be driving the poorer bondline performance in borate-containing treatments in this study.

Increased resin penetration may occur via several mechanisms. Preservatives can negatively affect resin penetration by physically or chemically blocking resin movement (Lorenz and Frihart 2006; Kamke and Lee 2007; Lim et al 2020). Resin penetration can also be affected by latewood and earlywood differences which can also affect preservative distribution. Earlywood is more permeable and creates a better wettable surface than latewood. Adhesives will follow the path of least resistance during pressing and flow more into earlywood cells than latewood which can cause air pockets to form and create an uneven bondline (Cai et al 2022; Ciglian and Reinprecht 2022). PUR curing is highly dependent on wood moisture and releases carbon dioxide that can create an inner vapor pressure driving more adhesive further into the wood and away from the bondline (Bastani et al 2016). This might explain why PUR panels in our study appeared to have more voids in the bondline than MF (Fig 3[b]). It is also important to note that this study only focused on one commercially relevant wood species used in CLT manufacture, Douglas-fir. The adhesive penetration patterns observed here in combination with treated Douglas-fir may vary with other wood species due to anatomical differences in species that could impact adhesive flow. Chemical distribution can also differ greatly between wood species and these differences may cause changes in how and where adhesives interact with preservative chemicals during the bonding but were not assessed in this study.

The deepest resin penetration was noted with organic treatments for both resin types. In fact, by visual observation, organic treatments had the thinnest bondlines for both the best and worst slide samples (Fig 3[b]). Alipon et al (2018) found that organic treatments such as propiconazole, deltamethrin, and permethrin outperformed inorganic treatments with various adhesives and provided full protection against termite attacks. Cai et al (2022) noted that thin bondlines usually can outperform composites with thicker bondlines as the more highly concentrated treatments accelerated curing reactions and created extensive branching within the wood structure. This could also explain why some authors observed increased shear strength as preservative concentration increased which produced a consequent increase in wettability (Tascioglu et al 2003; Lim et al 2020).

CONCLUSIONS

Prelayup planing of treated wood reduced the active preservative concentrations in MF and PUR CLT panels, average levels were still sufficient to protect pressure-treated materials against Formosan termites on average. This suggests that panels made with pressure-treated laminae (borates and PTIP) would provide good protection against Formosan termites. The presence of preservatives in the wood did impact bondline quality by increasing wettability and starving the bondline. Of the treatments, PTIP, appeared to have less of an effect on the bondline integrity even though the bondline was the thinnest of those in preservative-treated wood. All panels made with treated laminae in this study had significant issues with delamination that would have resulted in them failing quality control according to the PRG-320 standard. This finding indicates there are significant hurdles to manufacturing CLT with currently available preservative-treated wood, although one of the treatments, PTIP had a lower negative effect on panel performance.

REFERENCES

American Wood Protection Association (AWPA) (2021) AWPA book of standards. Birmingham, AL.

APA (2018) ANSI/APA PRG-320 standard for performance-rated cross-laminated timber. APA-The Engineered Wood Association, Tacoma, WA.

Alade AA, Naghizadeh Z, Wessels CB, Stolze H, Militz H (2023) Characterizing surface adhesion-related chemical properties of copper azole and disodium octaborate tetrahydrate-impregnated *Eucalyptus grandis* wood. J Adhes Sci Technol 37(15):2261-2284. https://doi.org/10.1080/01694243.2022.2125208.

Alade AA, Naghizadeh Z, Wessels CB, Tyhoda L (2022) A review of the effects of wood preservative impregnation on adhesive bonding and joint performance. J Adhes Sci Technol 36(15):1593-1617. https://doi.org/10.1080/01694243.2021.1981651.

Alipon MA, Garcia CM, Bondad EO (2018) Glue and preservative effects on the properties and durability of engineered bamboo boards. Philipp J. Sci 147(4):601-616.

Antwi-Boasiako C, Appiah K (2012) Effects of preservative-chemicals on the bonding strength of urea-formaldehyde adhesive in Bambusa vulgaris Schrad. ex J.C. Wendl. var. vulgaris hort. laminates. J Indian Acad Wood Sci 9(1):72-78.

Ayanleye S, Udele K, Nasir V, Zhang X, Militz H (2022) Durability and protection of mass timber structures: A review. J Build Eng 46:103731https://doi.org/10.1016/j.jobe.2021.103731.

Bagheri S, Alinejad M, Ohno K, Hasburgh L, Arango R, Nejad M (2022) Improving durability of cross laminated timber (CLT) with borate treatment. J Wood Sci 68(1)

Bastani A, Adamopoulos S, Koddenberg T, Militz H (2016) Study of adhesive bondlines in modified wood with fluorescence microscopy and X-ray micro-computed tomography. Int J Adhes Adhes 68:351-358. https://doi.org/10.1016/j.ijadhadh.2016.04.006.

Brandner R, Flatscher G, Ringhofer A, Schickhofer G, Thiel A (2016) Cross laminated timber (CLT): Overview and development. Eur J Wood Prod 74(3):331-351. https://doi.org/10.1007/s00107-015-0999-5.

Cai L, Park B-D, Kim M, Jeremic D, Lim H (2022) Adhesion interaction of one-component polyurethane in cross-laminating southern pine wood treated with micronized copper azole—Type C (MCA-C). Eur J Wood Prod 80(2):419-427. https://doi.org/10.1007/s00107-021-01776-1.

Ciglian D, Reinprecht L (2022) The effect of inorganic preservatives in the Norway spruce wood on its wettability and adhesion with PUR glue. Appl Sci 12(11):5642. https://doi.org/10.3390/app12115642.

Crawford RH, Cadorel X (2017) A framework for assessing the environmental benefits of mass timber construction. Procedia Eng 196:838-846. https://doi.org/10.1016/j.proeng.2017.08.015.

Faria DL, Cruz TM, Dias MC, Duarte PJ, Mendes LM, Guimarães Junior JB (2020) Physical and mechanical behavior of glulam beams produced with rubberwood

treated with preservatives. Ciênc Agrotec 44:1-11. https://doi.org/10.1590/1413-7054202044012020.

Forest Products Laboratory (2021) Wood handbook—Wood as an engineering material. General Technical Report FPL-GTR-282. U.S. Department of Agriculture, Forest Service, Forest Products Laboratory, Madison, WI. 543 pp.

França TSFA, Stokes CE, Tang JD, (2018) Durability of cross laminated timber against termite damage. Page 10 *in* Proceedings, 61st international convention of society of wood science and technology and Japan wood research society. Society for Wood Science and Technology, Monona, WI.

Gao W, Du G, Ma H, Li J (2016) Dynamic mechanical analysis of urea formaldehyde resin modified by ammonium pentaborate as wood adhesive. Polym Compos 37(8):2404-2410. https://doi.org/10.1002/pc.23422.

Goodell B, Nielsen G (2023) Wood biodeterioration. *in* P Niemz, A Teischinger, D Sandberg, eds. Springer Handbook of wood science and technology. Springer Handbooks, Springer, Cham. https://doi.org/10.1007/978-3-030-81315-4_4.

Kamke FA, Lee JN (2007) Adhesive penetration in wood-A review. Wood Fiber Sci 39(2):207-220.

Kuka E, Andersone I, Kurnosova N, Cirule D, Andersons B, Danieks M (2022) The potential of improving wood preservative penetration into glued wood products bonded with one-component polyurethane by discontinuous adhesive bondline design. Eur J Wood Prod 80(1): 223-234. https://doi.org/10.1007/s00107-021-01753-8.

Künniger T, Clerc G, Josset S, Niemz P, Pichelin F, van de Kuilen J-WG (2019) Influence of humidity and frequency on the energy dissipation in wood adhesives. Int J Adhes Adhes 92:99-104. https://doi.org/10.1016/j.ijadhadh.2019.05.003.

Lim H, Tripathi S, Tang JD (2020) Bonding performance of adhesive systems for cross-laminated timber treated with micronized copper azole type C (MCA-C). Constr Build Mater 232:117208, https://doi.org/10.1016/j.conbuildmat.2019.117208.

Long B, Morrell JJ (2011) Effects of postlayup borate treatment on appearance and flexural properties of Douglas-fir glued laminated beams. Forest Products J 62(1):46-48. http://meridian.allenpress.com/fpj/article-pdf/62/1/46/1666962/fpj-d-11-00133_1.pdf.

Lorenz LF, Frihart C (2006) Adhesive bonding of wood treated with ACQ and copper azole preservatives. For Prod J. https://www.researchgate.net/publication/237556936.

Lukowsky D, Nguyen H (2023) Analysis of wood bonding failures that initiated before adhesive solidification: Air fingers and cavitation. J Fail Anal and Preven 23(3):1059-1067. https://doi.org/10.1007/s11668-023-01646-3.

Mallo L, Fernanda Laguarda Mallo M, Espinoza O (2014) Outlook for CLT. BioRes.

Mbhamali NQ, Naghizadeh Z, Wessels CB (2022) The influence of preservative treatment on laminated *P. patula* bond performance. Int J Adhes Adhes 117: 103176. https://doi.org/10.1016/j.ijadhadh.2022.103176.

Oliveira GL, De Oliveira FL, Brazolin S (2018) Wood preservation for preventing biodeterioration of cross laminated timber (CLT) panels assembled in tropical locations Procedia Struct Integr 11:242-249. https://doi.org/10.1016/j.prostr.2018.11.032.

Özçifçi A (2006) Effects of boron compounds on the bonding strength of phenol-formaldehyde and melamine-formaldehyde adhesives to impregnate wood materials. J Adhesion Sci Technol 20(10):1147-1153. https://doi.org/10.1163/156856106777890590.

Qin L, Hu L, Yang Z, Duan W (2019) Effect of the ACQ preservative on the bonding strength of aqueous polymer isocyanate bonded Masson pine joints and on the adhesive penetration into wood. BioRes 14(2):2610-2621.

Shahan A, Denavit M, Taylor A, Lloyd J, Mankowski M, Kirker G (2021) Post-fabrication preservative treatment of CLT. Pages 128-131 in Proceedings of the 117th annual meeting of the American Wood Protection Association. Vol. 117. Nashville, TN. July 27-29, 2021, AWPA, Birmingham, AL.

Tascioglu C, Goodell B, Lopez-Anido R (2003) Bond durability characterization of preservative treated wood and E-glass/phenolic composite interfaces. Compos Sci Technol 63(7):979-991. https://doi.org/10.1016/S0266-3538(03)00013-7.

Taylor A, Denavit M, Lloyd J, Kim J, Kirker G, Mankowski M (2022) Borate treatment of CLT panels using vacuum: A proof of concept. Forest Prod J 73(1):24-30. https://www.doi.org/10.13073/FPJ-D-22-00060.

Wang JB, Wei P, Gao Z, Dai C (2018) The evaluation of panel bond quality and durability of hem-fir cross-laminated timber (CLT). Eur J Wood Prod 76(3):833-841. https://doi.org/10.1007/s00107-017-1283-7.

Wang JY, Stirling R, Morris PI, Taylor A, Lloyd J, Kirker G, Lebow S, Mankowski M, Barnes HM, Morrell JJ (2018) Durability of mass timber structures: A review of the biological risks. Wood Fiber Sci 50(Special):110-127. https://doi.org/10.22382/wfs-2018-045.

WOOD MOISTURE CONTENT DETERMINATION BY HANDHELD NEAR-IR REFLECTANCE SPECTROMETER

*Sandesh Thapa**

Graduate student
School of Forest Resources
University of Maine
Orono, ME 04469
E-mail: sandesh.thapa@maine.edu

Ling Li†*

Associate Professor of Sustainable Bioenergy Systems
School of Forest Resources
University of Maine
Orono, ME 04469
E-mail: ling.li@maine.edu

Kennedy Rubert-Nason

Associate Professor of Chemistry
Division of Natural Sciences
University of Maine – Fort Kent
23 University Drive
Fort Kent, ME 04743
E-mail: kennedy.rubertnason@maine.edu

Jinwu Wang

Research Forest Products Technologist
Forest Products Laboratory
U.S. Forest Service
1 Gifford Pinchot Drive
Madison, WI 53726
E-mail: jinwu.wang@usda.gov

Colter Mirtes

Undergraduate Student
Division of Natural Sciences
University of Maine - Fort Kent
23 University Drive
Fort Kent, ME 04743
E-mail: mirtes@maine.edu

Taylor Brown

Laboratory and Field Assistant
Division of Natural Sciences
University of Maine - Fort Kent
23 University Drive
Fort Kent, ME 04743
E-mail: taylor.brown@maine.edu

* Corresponding author.
† SWST member

Wood and Fiber Science, 56(4), 2024, pp. 197-206
https://doi.org/10.22382/wfs-2024-18

Eve Pelletier
Division of Natural Sciences
University of Maine – Fort Kent
23 University Drive
Fort Kent, ME 04743
E-mail: eve.pelletier@maine.edu

Yong-Jiang Zhang
Associate Professor of Plant Physiology
School of Biology and Ecology
University of Maine
Orono, ME 04469
and
Climate Change Institute
University of Maine
Orono, ME 04469
E-mail: yongjiang.zhang@maine.edu

(Received June 14, 2024)

Abstract. Rapid, accurate determination of wood moisture content is paramount for the wood industry, infrastructure maintenance, studies of plant physiology, and forest management. Near-IR reflectance spectroscopy (NIRS) is a widely used nondestructive technique for analyzing the properties of materials, including MC. Small, portable, handheld NIR spectrometers represent an emerging technology with strong potential for rapidly, affordably estimating materials properties. Here, we used a SCiO^{TM} miniature handheld NIR spectrometer and a partial least squares regression model to predict wood MC. The model was developed using spectra (740-1070 nm) collected from increment borer wood samples from 41 representative softwood and hardwood trees, calibrated against gravimetric wood MC determined by oven-drying. The calibration and prediction datasets contained 2/3rd and 1/3rd of all data, respectively. We explored the effects of different spectral preprocessing algorithms (ie first and second-order derivatives and standard normal variate transformations) on model performance. First-order derivative spectra with five latent variables yielded the most robust model (R^2: 0.72, $RMSE_P$: 0.32, the ratio of performance to deviation: 2.2). Broadly, we demonstrated that relatively low-cost miniature handheld NIR spectrometers such as the SCiO^{TM} can rapidly estimate percent MC in the wood of various species.

Keywords: Biometry, moisture content, near-IR spectroscopy, rapid measurement, wood.

INTRODUCTION

Moisture content is an important wood quality variable (Leblon et al 2013), influencing its weight, volume, elasticity, tensile and compression strength, milling properties, and thermal yield during combustion (Mitchell 1961). Determining MC gravimetrically (by weighing a sample before and after oven-drying) is time-consuming. It requires destructive sampling, while passive methods such as Fourier transform IR spectroscopy and X-ray tomography require bulky, costly, and specialized laboratory equipment with limited portability (Leblon et al 2013; Pu et al 2021). Compact, low-cost (~USD 800 in 2024), portable handheld near-IR (NIR) spectrometers represent an emerging technology for affordable, rapid determination of MC in wood in the field, mill, or laboratory.

NIR spectroscopy measures light (400-2500 nm) reflected from a material surface to reveal the chemical bonds associated with various functional groups (eg OH, CH, NH) within the material (Ma et al 2019). The electrons in the O-H bonds of moisture (water) interact specifically with photons corresponding to the following NIR bands: 760, 970, 1190, 1450, and 1940 nm. Broadband or narrow-band spectra can be calibrated against gravimetrically determined MC in reference samples using a multidimensional regression model, which can be used subsequently to predict the MC in samples with similar physicochemical

properties (Kelley et al 2004; Via 2004; Leblon et al 2013; Sundaram et al 2015; Liang et al 2019). In addition to benchtop NIR spectroscopy instruments, many miniature NIR spectrometers have been developed (Li et al 2018; Wiedemair et al 2019; Cazzaniga et al 2022). Compared with the broad spectral range (400-2500 nm) and higher resolution data acquired by benchtop NIR spectrometers, these miniature devices typically acquire narrower band spectra with lower resolution (Pillonel et al 2007; Digman et al 2021; Nkouaya Mbanjo et al 2022; Cazzaniga et al 2022). One example is the handheld SCiO™ spectrometer (Consumer Physics Inc., Tel Aviv, Israel) that can acquire a spectrum ranging from 740 to 1070 nm (wavelength resolution <10 cm^{-1}, sampling frequency: 1 nm). Multiple studies have demonstrated the feasibility of using miniature NIR spectrometers to determine physiochemical properties, such as the proportion of solids, moisture, sugar, and protein in agricultural commodities (eg cheese, hay, corn, apple, kiwifruit, and feijoa [Li et al 2018; Digman et al 2021; Cherney et al 2023]).

Collecting NIR spectral data in the field can be challenging due to variable and suboptimal environmental conditions (eg temperature, humidity), which can potentially decrease measurement precision, accuracy, and resolution. To maximize reliability, the devices should be trained (calibrated) to generate accurate predictions from relatively wide NIR spectral bands acquired under the anticipated range of operating environmental conditions. Because of methodological innovations in machine learning algorithms, increasing affordability and accessibility of computational processing, and affordable data storage, machine learning has become a valuable method to process complex data rapidly and accurately on a large scale, with minimal human intervention. Spectral pretreatments, such as standard normal variates (SNV), first-order derivatives (FD), and second-order derivatives (SD) can increase the reliability of quantitative measurements predicted from NIR spectra and be readily performed on recent versions of personal computing devices such as smartphones. SNV reduces the multiplicative interference present in spectral data (Cazzaniga et al 2022). FD enhances the peaks of the spectral data or reduces the effect of additive baselines, and SD can reduce the effect of multiplicative baseline scattering (Ferrara et al 2022b).

Partial least squares (PLS) regression is a common and effective machine learning algorithm for generating predictive models by calibrating preprocessed NIR spectra against quantitative measurements determined by a secondary method (Li et al 2018; Wiedemair et al 2019; Cazzaniga et al 2022; Ferrara et al 2022a, b; Nkouaya Mbanjo et al 2022). PLS regression utilizes a combination of principal component analysis and multivariate linear regression models involving two sets of data: calibration (training) data and prediction data (Geladi and Kowalski 1986). Calibration model fit and predictive accuracy are iteratively optimized by cross-validation using different subsets of the data (eg 2/3rd of the dataset for calibration and 1/3rd of the dataset for assessing prediction quality). The data quality metrics, namely coefficient of determination (R^2), root mean square error (RMSE), and the ratio of performance to deviation (RPD) are internal validation parameters used to assess calibration model performance (Cazzaniga et al 2022; Ferrara et al 2022a, b; Haruna et al 2022). R^2 (range 0-1) is a variant of the R^2 adapted to n-dimensional space, and as with its 2-dimensional counterpart, a value closer to unity indicates a better calibration model fit. RMSE quantifies the calibration precision, representing the standard deviation of calibration errors. RPD measures the predictive power and accuracy of the calibration model, with higher RPD values (generally >3) being desirable (Rubert-Nason et al 2013; Cazzaniga et al 2022; Ferrara et al 2022a, b; Haruna et al 2022).

In this study, we calibrated and validated a model for predicting the MC of green wood in live forest trees using a low-cost, compact, handheld NIR spectrometer. We hypothesized that a predictive model developed using machine learning would enable the determination of MC in wood from the relatively low-resolution, narrow-band NIR spectra provided by this type of instrument. The influence of various spectral preprocessing combinations on the power of PLS regression for MC

prediction was compared in terms of R^2, RMSE, and RPD.

MATERIAL AND METHODS

Study Site and Data Collection Tools

Wood increment cores (7-10 cm long) for model development and testing were collected from hardwood and softwood trees of merchantable size (41 total, diameter at breast height circa 10-20 cm, core length: 7-10 cm) within the Fournier Biological Park at the University of Maine at Fort Kent (47.246910N, −68.592626W). We developed a single calibration model for estimating MC in wood of the following taxa that are commonly found in northern mixed forests of North America: Poplar (*Populus* spp.), Balsam fir (*Abies balsamea*), Birch (*Betula* spp.), Black ash (*Fraxinus nigra*), Spruce (*Picea* spp.), Cedar (*Thuja occidentalis*), Red pine (*Pinus resinosa*), Pin cherry (*Prunus pensylvanica*), and Maple (*Acer* spp.) (Sibley 2009). The numbers of each species represented in the calibration set represented the approximately uniform abundances of these different species in the sampling site, permitting the development of a single calibration model optimized for determining wood MC in northern mixed forests.

Within 10 min of collection, cores were scanned at a single location near the center along the radial edge with a handheld NIR spectrometer (SCiO™, v 1.2; Consumer Physics Inc.), and the data were stored in the Cloud provided by the vendor. Core samples were promptly placed inside labeled paper envelopes, bundled together, and transported inside plastic bags within a cooler box to prevent moisture loss.

Spectral Data Collection and Mathematical Treatment

Spectral acquisition. Reflectance spectra (six scans per sample spanning 740-1070 nm) were collected for each of the wood cores, by scanning against a white background (Fig 1). The wood samples were weighed when wet, dried in an oven to constant weight at 60°C, and weighed again to determine gravimetric wood MC. Wood MC was calculated and reported as a percentage of dry wood weight.

Spectral preprocessing. We evaluated the effects of using broadband (740-1070 nm) and narrow-band spectra (760 and 950-970 nm) and the following spectral pretreatments on PLS model performance: SNV, FD, and SD. These transformations were tested alone and in combinations to evaluate their impacts on the prediction power and identify the combination with optimal accuracy. For optimizing the selection of preprocessing transformations (Fig 1), we followed a similar approach to Ferrara et al (2022a, b).

PLS Regression Models

We subjected spectral data under various preprocessing combinations to PLS regression to create and select the optimal model for predicting wood MC. The dependent variable was the gravimetric MC (% w/w) of the wood samples and the independent variable was the reflectance of light across the entire 740-1070 nm band. The data set was divided into calibration (training) and validation (test) subsets using the Kennard-Stone sampling method (Kennard and Stone 1969). Calibration data comprised two-thirds of the total samples and prediction data comprised one-third of the total samples.

Spectral preprocessing and PLS regression were computed using Origin Pro (version 2023b; OriginLab Corporation, Northampton, MA). The RPD was calculated using the method of Pillonel et al (2007). The calibration model was cross-validated using 10-fold cross-validation. Following this method, once a calibration model was built based on a subset of the data (calibration dataset), the remaining subset (prediction dataset) was subjected to the model for prediction of MC, and the model was iteratively refined. In this way, the performance of the calibration model was evaluated by the optimal number of latent variables, R^2, RMSE%, and RPD.

RESULTS

Wood spectra varied concerning MC, particularly in the moisture-absorbing bands (760 and

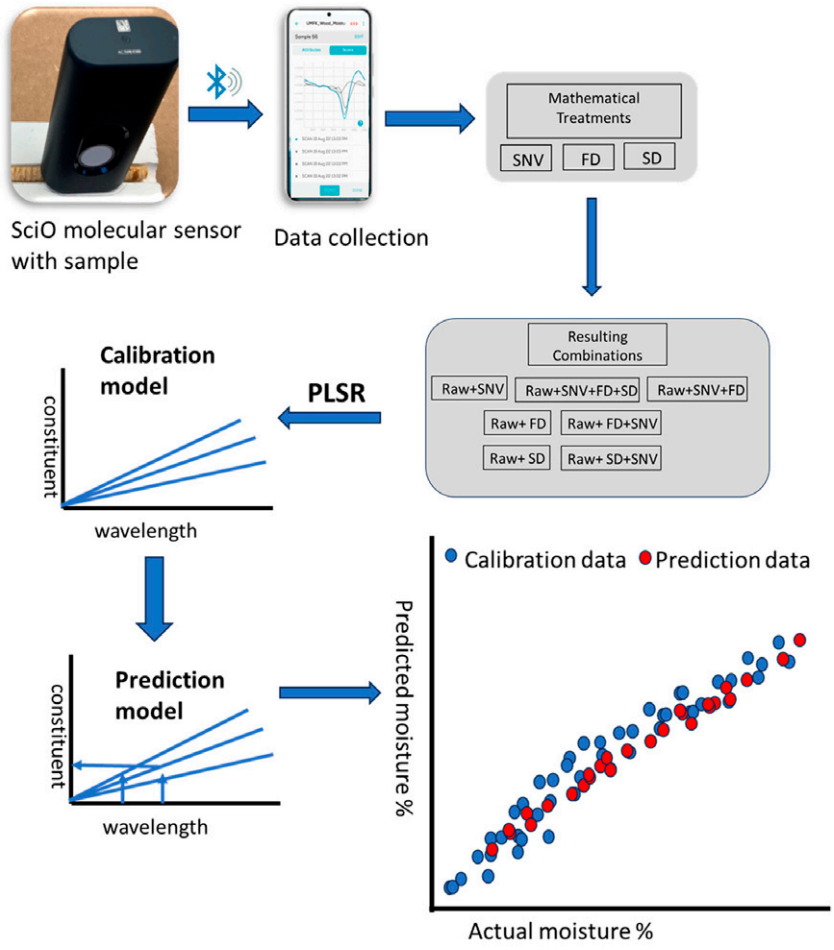

Figure 1. Process flow for data acquisition, calibration model development, and validation for determining wood MC by narrow band near-IR spectrometry showing a theoretical plot of predicted vs actual MC. FD, first-order derivative; SD, second-order derivative; SNV, standard normal variate; PLSR, partial least squares regression.

950-970 nm), and spectral preprocessing influenced the magnitude of features associated with variations in MC (Fig 2). The relative standard deviation (RSD) of the six NIR spectra scanned for each tree sample, averaged across all 41 samples, varied by wavelength from 0.043 to 0.074 (as a proportion of average spectral amplitude at a given wavelength). Within any particular sample, the RSD ranged from 0.0003 to 0.254 (Fig S1). Strategic selection of preprocessing treatments (ie normalization SNV, FD, and SD) was essential to maximizing spectral differences relating to MC (Fig 2) and the predictive power of the resultant calibration (Table 1).

Selection of broadband vs narrow-band spectra (focused on moisture-absorbing wavelengths) had minimal impact on PLSR calibration *model fit* (evidenced by R^2(C) and RMSE(C)); but the *predictive power* of PLSR models based on broadband spectra was superior (evidenced by R^2(P), RMSE(P), and RPD) (Fig 3; Fig S2). The choice of spectral preprocessing methods also substantially influenced the performance of PLSR

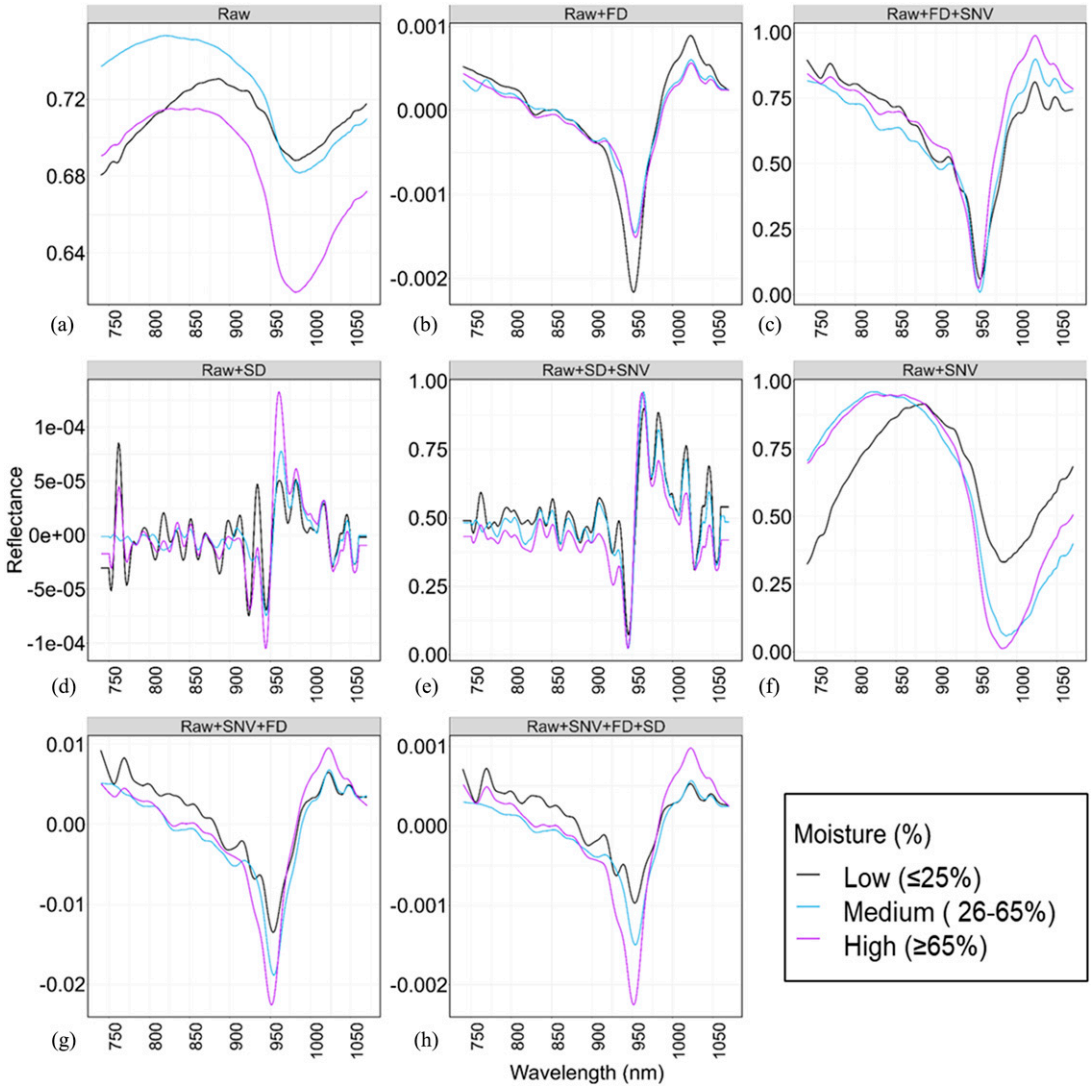

Figure 2. Influence of spectral preprocessing on the visual distinction between low (≤25%), medium (26-65%), and high (≥65%) wood moisture levels. (a) Raw reflectance data for reference; (b-h) effects of different spectral preprocessing method combinations on features associated with differences in wood MC. FD, first-order derivative; SD, second-order derivative; SNV, standard normal variate.

calibration models. Collectively, R^2(C), R^2(P), RMSE(C), RMSE(P), RPD (Table 1), and the correspondence between predicted and actual (secondary) validation measurements of wood MC (Fig 3) revealed that the optimal calibration was obtained with first-derivative pretreatment of broadband spectra (Table 1). Other pretreatment permutations involving first derivative and SNV transformations also produced potentially useable, albeit less accurate calibrations. Some calibration models fit the training dataset well (ie spectra with SNV+FD pretreatment), but predicted MC less reliably (RPD: 2.0).

DISCUSSION

Our study reveals that miniature, narrow bandwidth NIR spectrometers such as the SCiO™ can

Table 1. Quality criteria for partial least squares regression models fitted to reference wood MC and broadband spectra under different spectral pretreatments.

Spectral preprocessing combination	LV	R^2(C)	RMSE(C)	R^2(P)	RMSE(P)	RPD
Raw, FD	5	0.86	0.60	0.72	0.32	2.20
Raw, FD, SNV	7	0.80	0.76	0.72	0.68	1.03
Raw, SD	7	0.97	0.36	0.74	0.39	1.80
Raw, SD, SNV	1	0.48	0.85	0.55	0.32	2.19
Raw, SNV	8	0.80	0.75	0.80	0.48	1.46
Raw, SNV, FD	8	0.88	0.74	0.58	0.35	2.00
Raw, SNV, FD, SD	Calculation was terminated due to model overfitting					

LV, latent variables; R^2, coefficient of determination; RMSE(C), root mean square error of calibration; RMSE(P), root mean square error of prediction; RPD, ratio of performance to deviation; FD, first-order derivative; SD, second-order derivative; SNV, standard normal variate.

provide rapid and cost-effective estimates of MC in the wood of northern temperate forest trees. Our best calibration against gravimetrically determined reference values, obtained by PLS regression with first-derivative broadband spectra as is common in quantitative NIR (Vibhute et al 2018), met validation criteria (R^2_C: 0.86, R^2_P: 0.72, RMSE: 0.32, and RPD: 2.2) that are generally regarded as acceptable for meaningful predictions ($R^2 > 0.70$, RMSE: small [Rubert-Nason et al 2013; Li et al 2018]). Nevertheless, an RPD of 2.2 was less than the preferred threshold of 3.0 and indicated that predictions were of limited precision. Relative to larger, more costly spectrometers such as the Foss NIRSystem 5000 (1100-2498 nm bandwidth) (Yang et al 2024), spectra

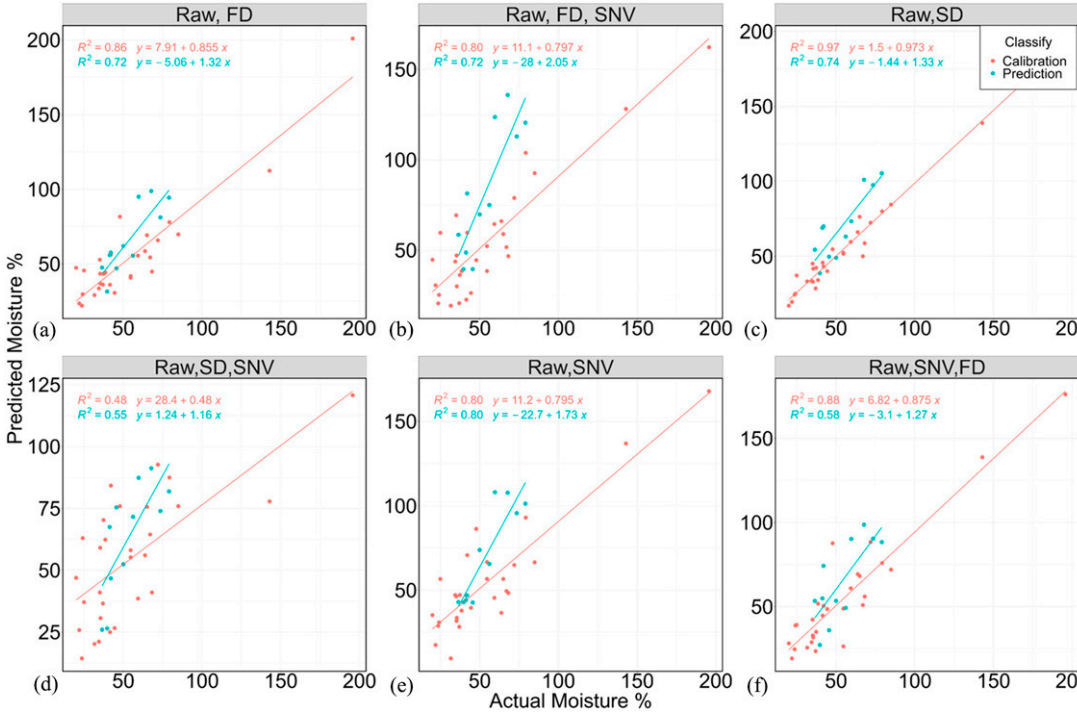

Figure 3. Predicted vs actual wood MC by partial least square regression models fitted with spectra subjected to different preprocessing treatments. (a-f) Effects of different spectral preprocessing method combinations on wood moisture prediction. FD, first-order derivative; SD, second-order derivative; SNV, standard normal variate.

acquired with the SCiO™ were of comparatively lower resolution. The quality of the PLS model fit for moisture determination with the miniature NIR device (R^2: 0.8) was also correspondingly lower than that of the benchtop NIR sensor (R^2: 0.92) (Kaur et al 2017).

The selection of spectral pretreatments is vital to optimizing the predictive power of the PLS model, as evidenced by large variations in the PLS model predictive power in response to the different pretreatment combinations that we explored (Table 1). Selecting a specific preprocessing method is a trial-error process and cannot be addressed prescriptively (Agelet and Hurburgh 2010). Optimizing model fit based on different permutations of common pretreatments (ie SNV, FD, SD) adjusts the baseline and scales the spectra to enhance the weighting of moisture effects (SNV), delineate moisture-related peaks (FD), and reveal more nuanced spectral qualities associated with MC (SD). It is essential to optimize combinations of spectral pretreatments for both model fitting and model predictions because some combinations may produce a strong model fit but less reliable model predictions (as we observed with SD+SNV spectra), and to avoid too many spectral pretreatments as they can lead to model overfitting (ie SNV+FD+SD).

Although the predictive power of miniature NIR spectrometers is limited by hardware characteristics such as narrower bandwidths and lower sensor resolutions compared with larger benchtop devices, it may be possible to increase their predictive power by strategic calibration model selection and diversification of training data sets. While PLS is a common approach to instrument calibration (Li et al 2018; Wiedemair et al 2019; Cazzaniga et al 2022; Ferrara et al 2022b; Nkouaya Mbanjo et al 2022), alternatives such as modified PLS (Rubert-Nason et al 2013), principal component regression (Vigneau et al 1997), and neural network analysis (Wu et al 1996) have occasionally been used and merit further exploration. While developing calibrations for moisture determination using only the two specific, strong spectral maxima for water (760 and 950-970 nm [Kasim et al 2021]) within the SCiO™ spectrometer's operating range (740-1070 nm) would be desirable to increase method specificity and decrease potentially interfering covariances, this action resulted in calibrations with less predictive power. We speculate that the detrimental effect of restricting our spectra to specific narrow bands may be a consequence of insufficient spectral data—attributed to the lower resolution of our instrument.

Multiple authors have examined how the diversity of training sample sets impacts the quality of calibration model fits and predictions. The general trend for PLS calibrations is that prediction power decreases as the diversity of the training sample set increases. For example, the inclusion of a broader range of tree species and ages is associated with lower R^2 values in some calibrations (Schimleck et al 2018). In the case of the SCiO™, Ma et al (2019) compared the effects of various permutations of spectral preprocessing and regression approaches (eg PLS discriminant analysis, interval PLS, and multiple linear regression with forward and backward selection), and found that the use of the instrument's full bandwidth (740-1070 nm) and PLS regression maximized predictive power for casein (R^2: 0.45-0.56, RMSE: 1.28-1.42, RPD: 1.4-1.5) and total protein (R^2: 0.7-0.77, RMSE: 0.53-0.62, RPD: 1.8-2.1), but that predictive power (RPD) was less than the desired 3.0. Because factors such as spectral band selection, preprocessing, plant species, plant age, and sample set size can impact the accuracy of quantitative NIR predictions, it is likely possible to obtain more accurate estimations of wood MC with miniature NIR spectrometers by using a larger training dataset and a calibration routine that statistically accounts for these different factors. Specifically, we suggest that our calibration could be improved by using a larger sample set and a modeling algorithm that incorporates tree taxon and classification of wood samples by age and position within the tree (sapwood/heartwood).

CONCLUSION

Miniature NIR spectrometers with limited bandwidth (ie 740-1040 nm), such as the SCiO™, can provide rapid, cost-effective estimates of wood

MC in field environments when calibrated against gravimetrically determined reference values by PLS regression. However, tools like the SCiO™ appear to be less accurate, presumably due to their lower resolution compared with larger, costlier benchtop and backpack-type NIR spectrometers. Selection of spectral preprocessing routines is key, with our best-performing calibration (R^2: 0.72, $RMSE_P$: 0.32, RPD: 2.2) obtained using first derivatives of spectra. Further studies should aim to improve the predictive power of these miniature instruments, by expansion of training datasets to include a greater diversity of tree species, ages, and sampling locations.

ACKNOWLEDGEMENTS

This project was supported by the USDA National Institute of Food and Agriculture (NIFA), McIntire-Stennis Project Number ME0-42205, Hatch Project Number ME0-22021 through the Maine Agricultural and Forest Experiment Station, U.S. Department of Agriculture's (USDA) Agricultural Research Service (grant number 58-0204-3-008), and the University of Maine Research Reinvestment Fund for Rural Health and Wellbeing Grand Challenge Grant Program (FY21-22, FY22-23).

We would like to acknowledge Associate Professor Dr. Bryan J. Peterson for his guidance and suggestions during the early stage of manuscript writing.

COMPETING INTERESTS

The authors declare that they have no known competing financial interests or personal relationships that could have appeared to influence the work reported in this paper.

REFERENCES

Agelet LE, Hurburgh CR (2010) A tutorial on near infrared spectroscopy and its calibration. Crit Rev Anal Chem 40(4):246-260.

Cazzaniga E, Cavallini N, Giraudo A, Gavoci G, Geobaldo F, Pariani M, Ghirardello D, Zeppa G, Savorani F (2022) Lipids in a Nutshell: Quick determination of lipid content in Hazelnuts with NIR spectroscopy. Foods 12(1):1-11.

Cherney JH, Cherney DJR, Digman MF (2023) Evaluation of a handheld NIRS instrument for determining haylage dry matter. Crop Forage Turfgrass Mgmt 9: e20239.

Digman MF, Cherney JH, Cherney DJ (2021) Dry matter estimation of standing corn with near-infrared reflectance spectroscopy. Appl Eng Agric 37(5):775-781.

Ferrara G, Marcotuli V, Didonna A, Stellacci AM, Palasciano M, Mazzeo A (2022a) Ripeness prediction in table grape cultivars by using a portable NIR device. Horticulturae 8(7):613.

Ferrara G, Melle A, Marcotuli V, Botturi D, Fawole OA, Mazzeo A (2022b) The prediction of ripening parameters in Primitivo wine grape cultivar using a portable NIR device. J Food Compos Anal 114:104836.

Geladi P, Kowalski BR (1986) Partial least squares regression: A tutorial. Anal Chim Acta 185:1-17.

Haruna SA, Li H, Wei W, Geng W, Yao-Say Solomon Adade S, Zareef M, Ivane NMA, Chen Q (2022) Intelligent evaluation of free amino acid and crude protein content in raw peanut seed kernels using NIR spectroscopy paired with multivariable calibration. Anal Methods 14(31):2989-2999.

Kasim NFM, Mishra P, Schouten RE, Woltering EJ, Boer MP (2021) Assessing firmness in mango comparing broadband and miniature spectrophotometers. Infrared Phys Technol 115:103733.

Kaur H, Künnemeyer R, McGlone A (2017) Comparison of hand-held near infrared spectrophotometers for fruit dry matter assessment. J Near Infrared Spectrosc 25(4): 267-277.

Kelley SS, Rials TG, Snell R, Groom LH, Sluiter A (2004) Use of near infrared spectroscopy to measure the chemical and mechanical properties of solid wood. Wood Sci Technol 38(4):257-276.

Kennard RW, Stone LA (1969) Computer aided design of experiments. Technometrics 11(1):137-148.

Leblon B, Adedipe O, Hans G, Haddadi A, Tsuchikawa S, Burger J, Stirling R, Pirouz Z, Groves K, Nader J, LaRocque A (2013) A review of near-infrared spectroscopy for monitoring moisture content and density of solid wood. For Chron 89(05):595-606.

Li M, Qian Z, Shi B, Medlicott J, East A (2018) Evaluating the performance of a consumer scale SCiO™ molecular sensor to predict quality of horticultural products. Postharvest Biol Technol 145:183-192.

Liang L, Fang G, Deng Y, Xiong Z, Wu T (2019) Determination of moisture content and basic density of poplar wood chips under various moisture conditions by near-infrared spectroscopy. For Sci 65(5):548-555.

Ma L, Peng Y, Pei Y, Zeng J, Shen H, Cao J, Qiao Y, Wu Z (2019) Systematic discovery about NIR spectral assignment from chemical structural property to natural chemical compounds. Sci Rep 9(1):9503.

Mitchell HL (1961) A concept of intrinsic wood quality, and nondestructive methods for determining quality in standing timber. USDA Forest Service Forest Products Laboratory: 2233. https://www.fpl.fs.usda.gov/documents/fplr/fplr2233.pdf

Nkouaya Mbanjo EG, Hershberger J, Peteti P, Agbona A, Ikpan A, Ogunpaimo K, Kayondo SI, Abioye RS, Nafiu K, Alamu EO, Adesokan M, Maziya-Dixon B, Parkes E, Kulakow P, Gore MA, Egesi C, Rabbi IY (2022) Predicting starch content in cassava fresh roots using near-infrared spectroscopy. Front Plant Sci 13:990250.

Pillonel L, Dufour E, Schaller E, Bosset J-O, De Baerdemaeker J, Karoui R (2007) Prediction of colour of European Emmental cheeses by using near infrared spectroscopy: A feasibility study. Eur Food Res Technol 226(1-2):63-69.

Pu Y, Pérez-Marín D, O'Shea N, Garrido-Varo A (2021) Recent advances in portable and handheld NIR spectrometers and applications in milk, cheese and dairy powders. Foods 10(10):2377.

Rubert-Nason KF, Holeski LM, Couture JJ, Gusse A, Undersander DJ, Lindroth RL (2013) Rapid phytochemical analysis of birch (Betula) and poplar (Populus) foliage by near-infrared reflectance spectroscopy. Anal Bioanal Chem 405(4):1333-1344.

Schimleck LR, Matos JLM, Trianoski R, Prata JG (2018) Comparison of methods for estimating mechanical properties of wood by NIR spectroscopy. J Spectrosc 2018:1-10.

Sibley DA (2009) The Sibley guide to trees. Alfred A. Knopf. NY, USA.

Sundaram J, Mani S, Kandala CVK, Holser RA (2015) Application of NIR reflectance spectroscopy on rapid determination of moisture content of wood pellets. Am J Anal Chem 06(12):923-932.

Via BK (2004) Modeling Longleaf pine (*Pinus palustris* Mill) wood properties using near infrared spectroscopy. Louisiana State University and Agricultural & Mechanical College. Ann Arbor, MI, USA.

Vibhute AD, Kale KV, Mehrotra SC, Dhumal RK, Nagne AD (2018) Determination of soil physicochemical attributes in farming sites through visible, near-infrared diffuse reflectance spectroscopy and PLSR modeling. Ecol Process 7(1):26.

Vigneau E, Devaux MF, Qannari EM, Robert P (1997) Principal component regression, ridge regression and ridge principal component regression in spectroscopy calibration. J Chemometrics 11(3):239-249.

Wiedemair V, Langore D, Garsleitner R, Dillinger K, Huck C (2019) Investigations into the performance of a novel pocket-sized near-infrared spectrometer for cheese analysis. Molecules 24(3):7-9.

Wu W, Walczak B, Massart DL, Heuerding S, Erni F, Last IR, Prebble KA (1996) Artificial neural networks in classification of NIR spectral data: Design of the training set. Chemom Intell Lab Syst 33(1):35-46.

Yang X, Cerezo AA, Berzaghi P, Magrin L (2024) Comparative near Infrared (NIR) spectroscopy calibrations performance of dried and undried forage on dry and wet matter bases. Spectrochim Acta A Mol Biomol Spectrosc 316(316):124287.

GRAIN ANGLE EFFECTS ON ACOUSTIC EMISSION (AE) CHARACTERISTICS OF SOUTHERN YELLOW PINE (SYP) COLUMNS UNDER COMPRESSION

Rajan Adhikari

Product Engineer
Weyerhaeuser Technology Center,
Federal Way, WA 98001
E-mail: rajan.adhikari@weyerhaeuser.com

Samuel O. Ayanleye

Staff Engineer
APA – The Engineered Wood Association,
Tacoma, WA 98466
E-mail: samuel.ayanleye@apawood.org

*Edward D. Entsminger†**

Extension Associate III
Department of Wildlife, Fisheries and Aquaculture (WFA),
College of Forest Resources (CFR),
Mississippi State University (MSU) Extension,
Mississippi State, MS 39762-9690
E-mail: edward.entsminger@msstate.edu

Franklin Quin†

Assistant Professor
Department of Sustainable Bioproducts (DSB),
Forest and Wildlife Research Center (FWRC),
College of Forest Resources (CFR),
Mississippi State University (MSU),
Mississippi State, MS 39762-9820
E-mail: fq3@msstate.edu

Wengang Hu

Associate Professor
Nanjing Forestry University (NJFU),
Co-Innovation Center of Efficient Processing and Utilization of Forest Resources,
Nanjing, Jiangsu 210037, People's Republic of China
E-mail: hwg@njfu.edu.cn

*Jilei Zhang**

Warren S. Thompson Professor of Wood Science and Technology,
Department of Sustainable Bioproducts (DSB),
Forest and Wildlife Research Center (FWRC),
College of Forest Resources (CFR),
Mississippi State University (MSU),
Mississippi State, MS 39762-9820
E-mail: jz27@msstate.edu

(Received May 1, 2024)

* Corresponding author
† SWST member

Wood and Fiber Science, 56(4), 2024, pp. 207-221
https://doi.org/10.22382/wfs-2024-19

Abstract. This study investigated the influence of wood grain angle (0°, 10°, 20°, 30°, 45°, 60°, 75°, and 90°) on acoustic emission (AE) characteristics of southern yellow pine columns subjected to compressive loading. Four AE parameters considered were counts, cumulative counts, count rate, and amplitude. The main conclusion was that AE cumulative counts vs time curves can be characterized by three distinct stages in terms of AE count rates: initiation, growth, and acceleration. The initiation stage had a constant mean count rate of 0.33 counts/s compared with the growth stage mean count rate of 19.10 counts/s, whereas the acceleration stage had a mean count rate of 608.40 counts/s. Within each stage, count rates increased as the grain angle increased from 0° to 30°, then dropped as the grain angle further increased to 90°. Maximum AE counts and total cumulative AE counts all increased as the grain angle increased from 0° to 30° and decreased as the grain angle further increased to 90°. Higher AE amplitudes were observed in the yield and failing stages of tested wood columns according to their stress–strain curves plotted together with their corresponding amplitude–time curves. Maximum amplitude increased as the grain angle increased from 0° to 20°, then had a decreasing trend as the grain angle increased to 45°, followed by an increasing trend as the grain angle increased to 75°. These differences in AE characteristics suggested that AE "signatures" in terms of AE signals do exist for timber materials when subjected to compressive loading.

Keywords: Grain angle, acoustic emission (AE), southern yellow pine (SYP), compression, stress–strain.

INTRODUCTION

Wood, a natural renewable resource, is a valuable construction material, because of its low energy consumption, workability, high strength properties, and reliability in structural applications (Hindman and Bouldin 2015; Nguyen et al 2017; Ramage et al 2017). Southern yellow pine (*Pinus* spp. L.) (SYP) is a common and widely used group of commercial softwood species in the United States because of its availability, visual appeal, and good strength properties, making it suitable for use in structural applications (Southern Forest Products Association (SFPA) 2018). The SYP species group grows throughout the southeastern United States, from Virginia to Texas (Junaid et al 2018).

Wood is an orthotropic material and has unique mechanical properties in its three principal plane directions: longitudinal (L), radial (R), and tangential (T) (Green et al 1999; Reiterer and Stanzl-Tschegg 2001; Kretschmann 2010). In lumber, tension and shear failure are considered brash failures. However, compression failure is regarded as a ductile failure (André et al 2013; André et al 2014) and must be considered in designing a building structure. The design parameters mostly considered are bending and compression perpendicular to the grain when the wood is used as a construction material (Turkot 2019; Carmona-Uzcategui 2020; Carmona-Uzcategui et al 2020; Irby et al 2020a; Turkot et al 2020). However, wood is extremely strong in both compression and tension parallel to the grain (Turkot 2019; Carmona-Uzcategui 2020; Turkot et al 2020; Carmona-Uzcategui et al 2020; Irby et al 2020a).

One of the most important variables affecting compression properties in wood is grain orientation (Green et al 1999; Kretschmann 2010). The orientation of grain relative to the strength of lumber is critical in understanding the mechanical properties of wood (Green et al 1999; Kretschmann 2010; Ingemi and Yu 2019; Turkot 2019; Carmona-Uzcategui 2020; Carmona-Uzcategui et al 2020; Irby et al 2020b; Turkot et al 2020). Therefore, the evaluation of strength properties including compression parallel or perpendicular to the grain becomes important for structural design purposes (Green 2001).

Koch (1972) reported that southern yellow pine loaded in compression parallel-to-the-grain developed a visibly well-defined pattern of buckling failures. On the tangential faces of failed rectangular wood columns, the lines of failure make a grain angle of 45° to 60° to the column, longitudinal axial direction, whereas on the radial faces, the lines are about perpendicular to the axial direction. Gupta and Sinha (2012) evaluated the compressive properties of Douglas-fir (*Pseudotsuga menziesii* (Mirb.) Franco) columns with grain angles of 0°, 10°, 20°, 30°, 40°, 50°, 60°, 70°, 80°, and 90° (similar to our Fig 1) and found

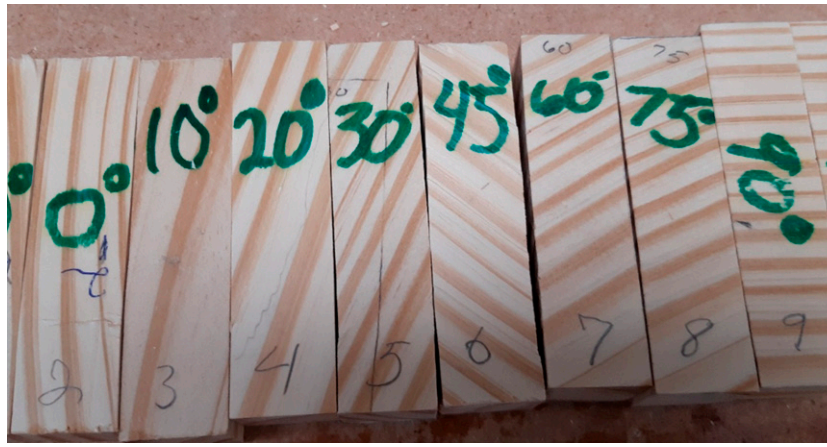

Figure 1. Prepared examples southern yellow pine (*Pinus* spp. L.) wood columns at various cross-grain angles of 0, 10, 20, 30, 45, 60, 75, and 90 degrees, respectively.

that the failure mode changed from shearing parallel to the grain to rolling shear with increasing grain angle orientation. Reiterer and Stanzl-Tschegg (2001) reported that compression failure occurring in columns subjected perpendicular to the grain loading could be attributed to the collapse at the earlywood and latewood sections in the annual rings (the interface section of the wood). Several studies, as reported by Gibson and Ashby (1997) have addressed the complete mechanism responsible for these kinds of failures in softwoods.

Acoustic emission (AE) is defined as the phenomena where transient elastic waves and stresses are generated by the rapid release of energy from a localized source or sources within a material (ASTM 2024). All materials, including wood, contain minute flaws that will initiate microfractures when subjected to stress. These microfractures will enlarge in intermittent step-like bursts as the applied stress increases. During each of these bursts, high-frequency elastic sound waves are produced (Knuffel 1988). These elastic waves released by materials because of fiber breakage, under stress, can be detected and recorded by resonant transducers, such as AE sensors (Sharma 2017; Rescalvo et al 2020). The AE sensing method can allow the detection of destructive changes in materials, like wood, at the moment of being stressed in compression, thereby provide the possibility to follow destructive processes that take place in wood construction beginning with microcracks and ending up in total failure (Reiterer et al 2000; Nasir et al 2022).

The most commonly used parameter for AE signals description is an AE "count." An AE event is "counted" when an AE signal exceeds a preset threshold during any selected portion of the test above any background noises. Derived measurements include the AE cumulative (total) count (Porter et al 1972; Ansell 1982; Sato et al 1984a; Noguchi et al 1992; Raczkowski et al 1999; Ayarkwa et al 2001; Gozdecki and Smardzewski 2005; Ando et al 2006; Chen et al 2006; Ritschel et al 2013) and AE count rate (the number of counts during a given time interval) (Sato et al 1984a; Gozdecki and Smardzewski 2005; Smardzewski and Gozdecki 2007; Du et al 2014). A commonly used frequency domain measurement is the AE amplitude. Hu and Zhang (2022) investigated the peak amplitude of the AE signal. In terms of time-domain vs frequency-domain measurements, AE count rate and cumulative counts are time-domain, whereas the amplitude and peak amplitude are frequency-domain measurements. The time domain refers to analyzing the AE signal as it changes over time, whereas the frequency domain refers to breaking down the AE signal into its constituent frequencies and then analyzing.

Berg and Gradin (2000) investigated the temperature effects on the fracture history of Norway spruce (*Picea abies* (L.) Karst.) under compression in both transverse and longitudinal directions through recording the cumulative AE events. They reported that an ideal temperature level for introducing many failure sites during compression should be well below 120°C and that the longitudinal direction was the most efficient loading direction for introducing flaws in wood during compression (Berg and Gradin 2000). The AE techniques have been effectively used to monitor termite infestation in wood. For instance, AE was used to monitor the activity rhythm and termite feeding of some economically important termites in the United States because microfracturing occurred when wood was attacked by termites that produced AE signals (Mankin et al 2002; Indrayani et al. 2003). The AE techniques have also been used to detect the early stages of wood decay through subjecting wood blocks to compression perpendicular to the grain in the radial (Beall and Wilcox 1987; Raczkowski et al 1999) and tangential directions (Noguchi et al 1992).

However, limited studies have been reported using and assessing AE techniques to monitor the failure progress in wood under a compressive loading (Gong and Smith 2000; Dahlen et al 2018; França et al 2018). Specifically, the AE behavior of SYP wood columns when subjected to external loading with different grain angle orientations has not been fully investigated. The main research investigated the influence of wood grain angles (0°, 10°, 20°, 30°, 45°, 60°, 75°, and 90°) on AE characteristics of SYP columns subjected to compressive loading.

MATERIALS AND METHODS

Materials

One (1) parent SYP (*Pinus* spp. L.) dimensional lumber board with dimensions of 3.810 cm thick × 28.575 cm wide × 3.048 m long was purchased from East Mississippi Lumber Company (Starkville, MS) and planed to a thickness of 2.54 cm.

Experimental Design

A complete one-way factorial experiment with three replicates per experimental combination was conducted to evaluate the effects of grain angle (0°, 10°, 20°, 30°, 45°, 60°, 75°, and 90°), as shown in Fig 1, in reference to the compressive loading direction (that was parallel to the column longitudinal axis). Figure 2 shows a diagram methodology of how each wood column, at various grain angles, was cut from a dimensional lumber board.

AE Apparatus

The AE apparatus consisted of an AE measuring system called Digital Signal Process (μDiSP^{TM}), a laptop computer with Physical Acoustics

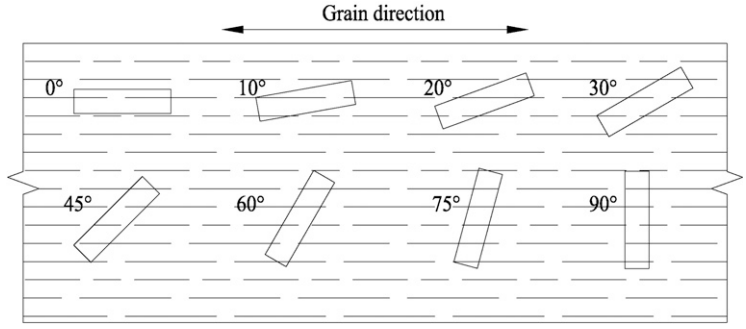

Figure 2. Diagram methodology for cutting wood columns at grain angles of 0°, 10°, 20°, 30°, 45°, 60°, 75°, and 90° from a southern yellow pine (*Pinus* spp. L.) dimensional lumber board.

Corporation (PAC) Acoustic Emission for Windows (AEwin) software installed, and a PAC AE sensor. The AEwin software program collected the AE signal data from the DiSP, recorded it in terms of AE counts and amplitudes vs time, and represented it in a graphical form. The AE sensor operated at a frequency ranging from 50 to 200 kHz. For wood-based materials, the sensor frequency range from 100 to 200 kHz provided sufficient sensitivity to AE emissions of interest (Beall 1985). The AE measuring system had a threshold set to 30 dB, a preamp set to 40 dB, and a filter with the range of 10 to 100 kHz. Gorilla® hot glue sticks (Gorilla Glue Company LLC., Cincinnati, OH) were used in an AdTech® Mini Hi-Temp hot glue gun (Adhesive Technologies, Inc. Hampton, NH) as a couplant between the AE sensor and wood, as the technique to fasten the sensor to the wood sample before testing. The diameter of the AE sensor was 2.71 cm.

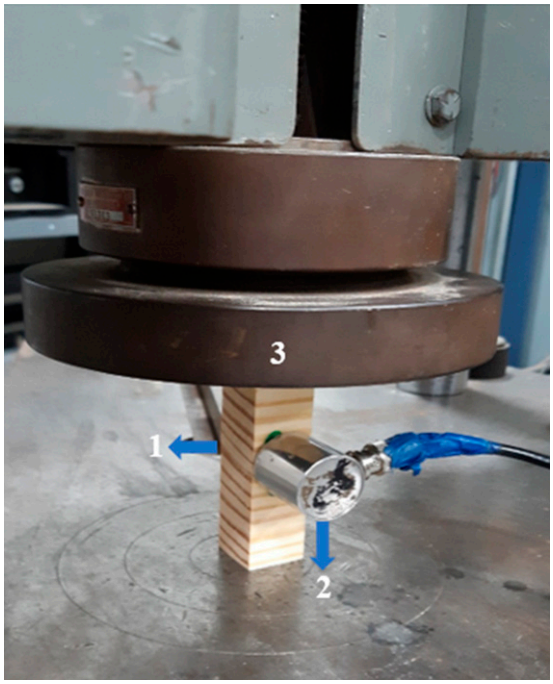

Figure 3. Setup for evaluating acoustic emission (AE) behavior (#2 in image) of southern yellow pine (*Pinus* spp. L.) wood columns (#1 in image) when subjected to a compressive load (#3 in image).

Testing

Twenty-four (24) small clear SYP columns measured 25.40 × 25.40 × 101.60 mm^3 (Fig 1) were cut from the parent board according to American Society for Testing and Materials (ASTM) Standard D143 – 23 (ASTM 2023). Before compression testing, the short columns were conditioned to constant mass in an environmental conditioning chamber for a minimum of three weeks at 22°C and 55.0% RH, and the dimensions were recorded. Figure 3 shows the setup for evaluating AE behavior of SYP wood columns subjected to compressive stress. One AE sensor was hot glued onto the wood column surface at the middle of the column. All columns were mechanically tested on an Instron® Tinius-Olsen Universal Testing Machine at a crosshead speed of 0.30 mm per minute according to the ASTM D143 – 23 standard (ASTM 2023). Load–deformation curves with synchronous AE activities were recorded. Before loading each column at test, physical volume dimensions (width, depth, and length) of each sample were measured using a Mitutoyo Absolute Digital Caliper (Model No. CD-6" CSX, Serial No. 13152425; Kawasaki, Japan, Asia) and recorded. Failure modes for each tested column were evaluated, determined, and recorded. The physical properties such as MC and specific gravity (SG) of the samples were determined by oven-dry mass at 103°C in a Blue M Electric Company Dry Oven (Model B-3005-Q, Blue Island, IL). The coefficient of variation (COV) was determined for all samples.

Statistical Analysis

Data were analyzed using Microsoft Excel 365 software (Microsoft Corporation). SigmaPlot version 14.5 (Inpixon, Palo Alto, CA) software was used for graph plots, scientific graphing, and data analysis.

RESULTS AND DISCUSSION

Physical Properties

The MC values of tested wood columns ranged from 7.70 to 12.80% (oven-dry basis), with an

Table 1. Summary of failure modes recorded for three southern yellow pine (SYP) columns for each of eight different grain angles evaluated under compression.

	Grain angle (°)[a]							
Replicate	0	10	20	30	45	60	75	90
1	B	B	S	S	CO+B	CO+B	CO+B	CO
2	B	B	S	S	CO+B	CO+B	CO+B	CO
3	B	B	S	S	CO+B	CO+B	CO+B	CO

[a]Where B, buckling failure; S, shearing failure; CO, compression failure; and CO+B, compression and buckling failure combination.

average of 10.37% and a COV of 11.43%. The SG values ranged from 0.39 to 0.59, with an average of 0.49 and corresponding COV of 9.61%.

Mechanical Properties

Failure modes. Table 1 summarizes the failure modes recorded for each SYP column evaluated in this study. The columns with 0° and 10° grain angles developed a visibly well-defined pattern of buckling failures. Figure 4 shows the typical failure modes observed in mechanically tested SYP columns. The lines of failure made an angle to the column in a longitudinal direction on the tangential faces of failed columns (Fig 4[a]). The lines were perpendicular to the longitudinal direction on the radial faces and were similar to those described in Koch (1972). This buckling failure was caused mainly by shear failure that occurred at the overlap of the tapered ends of the tracheids, which comprise most of the volume in SYP. This was mainly because under a compressive load parallel to wood cells, the longitudinal direction overlaps the tapered ends of the tracheids as they must induce shear forces between adjacent cells (Koch 1972). Columns with 20° and 30° grain angles all experienced shear parallel to the grain (Fig 4[b]). The grain angles of 20° were observed in shear failure, whereas the 30° was related to the impact of wood density on its mechanical properties, as a change in strength is normally observed within annual rings and at the ring border as described by Jakob et al (1994). The shear failures observed in this study occurred mainly in the earlywood sections of the tested columns because of the collapsing separation of the earlywood regions at the annual growth rings (Reiterer and Stanzl-Tschegg 2001) or wood fiber misalignment (Poulsen et al 1997). Columns with 45° to 75° grain angles failed with earlywood and latewood compression as shown by the "S-wavy" shaped buckling (Fig 4[c]), whereas the 90° samples failed in compression at the earlywood/latewood interface (Fig 4[d]). These compression failures could be attributed to wood tracheid walls bent inward and distorted sideways (Koch 1972) and collapse at the earlywood/latewood interface (Reiterer and Stanzl-Tschegg 2001). In general, the failure modes observed were similar to those observed in other softwood studies (Ayres 1920; Martel 1920; Hankinson 1921; Osgood 1928;

Figure 4. Typical failure modes observed in mechanically tested southern yellow pine (*Pinus* spp. L.) wood columns: (a) buckling (radial face, 0° column); (b) shearing (20° column); (c) compression and "S-wavy shaped" buckling (45° column); and (d) horizontal compression (90° columns).

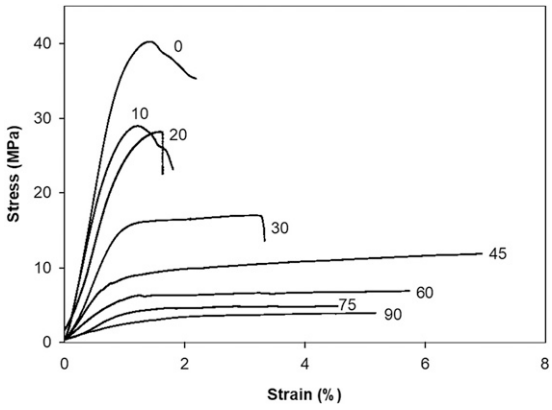

Figure 5. Typical stress–strain curves showing each of the eight-grain angles evaluated on southern yellow pine (SYP) wood columns subjected to compressive loading.

Kojis and Postweilder 1953; Kim 1986; Reiterer and Stanzl-Tschegg 2001).

Stress–strain curves. Typical stress–strain curves of the tested SYP columns are illustrated in Fig 5. These curves indicated that the columns with grain angles between 0° and 20° behaved like brittle materials that had an initial linear stage, a smooth nonlinear curve representing the transition between the proportional limit and ultimate stresses, and then a sharp decrease in stress after reaching the ultimate load (Reiterer and Stanzl-Tschegg 2001; Güntekin and Aydin 2013). Columns with grain angles ranging from 45° to 90° behaved like a ductile or plastic-like material that had poorly deformed ultimate stresses. Columns with a grain angle of 30° behaved like ductile materials with more plastic deformation before failure. The resistance to an external compressive load with grain angles ranging from 0° to 20° decreased sharply after reaching its ultimate value. This could be because of cracking that developed under the compressive stress (Berg and Gradin 2000). These cracks could be related to shear failures of tracheids because of the different separations along the middle lamella, particularly in axial parenchyma cells of certain wood species, but these cells are generally absent in pine. Alternatively, tracheids could separate within the cell wall between the S_1 and S_2 layers (Koch 1972). In the cases of wood columns with grain angles from 45° to 90°, stresses continued increasing with strain beyond their proportional limit; however, at a lower rate of change. Compaction of the wood occurred with increasing deformation after the flattening and failure of the cell walls. This was followed by a continuous rise in the resistance of the compressed columns. Stress at the proportional limit was used to determine allowable stresses in compression perpendicular to the grain because ultimate stresses for this property were not clearly defined (FPL 2021). This recommendation would also be extended for columns with grain angles greater than 30°. Figure 6 plots experimental means of ultimate compressive strength (Fig 6[a]) and stiffness (Fig 6[b]) of the SYP columns together with their corresponding estimated values using Hankinson's formula (FPL 2021) (see Eq 1)

$$N = \frac{\mathrm{PQ}}{P\sin^n\theta + Q\cos^n\theta} \tag{1}$$

where N can be the modulus of elasticity as well as strength properties at angle θ from the fiber direction, Q is the strength perpendicular to the grain, P is the strength parallel to the grain, and n is an empirically determined constant. The calculated ratios (Q/P) based on the experimental mechanical properties were 0.08 (3.28/41.94) and 0.09 (0.37/3.90) for strength and stiffness, respectively. This was close to 0.10, therefore, the empirically determined constant, $n = 2.50$ was considered in Hankinson's formulas for calculating both properties (FPL 2021). Figure 6 indicated that reasonably accurate estimates were obtained using Hankinson's formula for both compression strength and stiffness of SYP wood columns evaluated in this study. The substantial drop in compressive strength starting at the 20° grain angle was attributed to wood fiber misalignment and shearing (Poulsen et al 1997). Reiterer and Stanzl-Tschegg (2001) and Güntekin and Aydin (2013) also indicated that irreversible shear deformation occurred at annual ring borders of softwood species subjected to compressive loads parallel to the grain, causing a steep decrease in strength.

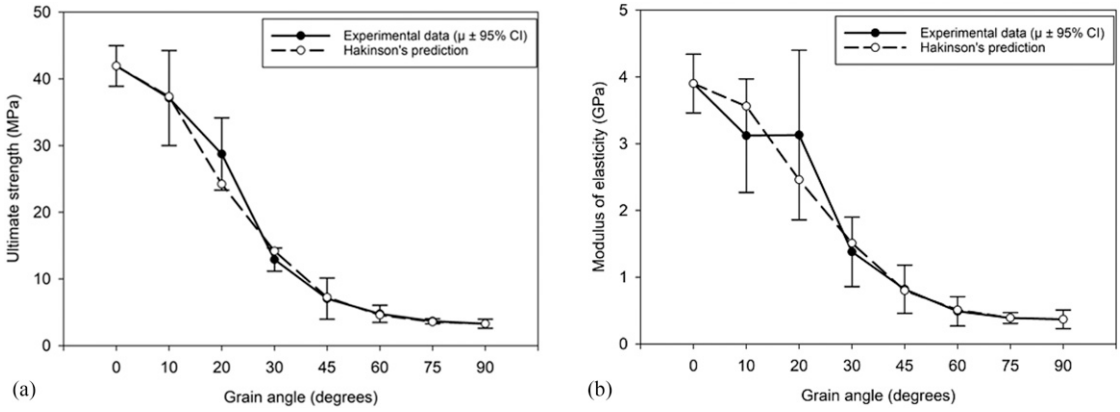

Figure 6. Experimental mean ultimate compressive strength (a) and stiffness (b) values of mechanically tested southern yellow pine (SYP) wood columns at eight different grain angles plotted with their corresponding approximated values using Hankinson's formula.

Cumulative AE Counts–Time Curves

Figure 7 shows a typical cumulative AE counts-time curve plotted with the corresponding stress–strain curve, indicating the damage progression observed in the SYP columns. Three distinct stages were identified in terms of changes in slope (ie, AE cumulative counts) of the cumulative AE counts–time curve: initiation, growth, and acceleration (Raczkowski et al 1994; Du et al 2014). The initiation stage (0 – ~50-100 s) was the first linear portion where the AE count rate was slower (Beall and Wilcox 1987) and constant

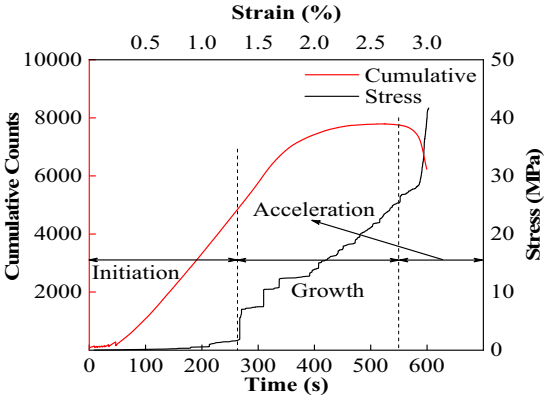

Figure 7. A typical cumulative counts-time curve recorded together with its corresponding stress–strain curve representing acoustic emission (AE) behavior of southern yellow pine (SYP) wood columns subjected to compressive loading.

(Figure 7). Fewer counts were recorded in the initiation stages because microcracks within wood cell walls can occur at stress levels well below the proportional limit (Bodig and Jayne 1982). These microcracks can be detected using AE sensing devices (DeBaise et al 1966) even though these cracks generally do not continue to grow if the load is cyclical, in accordance with the Kaiser Effect (Beall and Wilcox 1987). The growth stage in the second curve portion (~100-300 s) showed a much higher AE count rate relative to the initiation stage (Raczkowski et al 1994) because more cracks developed and propagated as the applied load increased (Bodig and Jayne 1982). Therefore, the growth stage can be considered as a transitional progressive region between the initiation and acceleration stages where the AE count rate changed from relatively low (0.33 counts/s) to higher (608.40 counts/s). The acceleration stage was the third portion (>300 s) where the AE count rate transitioned to an exponential high and constantly increased (Raczkowski et al 1994) because of the collective increase in crack growth. This accelerated crack growth can decrease resistance to stresses and generated more AE activity than the growth stage.

A linear regression method was used to approximate the slope of each of the three stages for each individual AE cumulative counts-time curve for all tested columns. Calculated slope values of all

Table 2. Summary of acoustic emission (AE) count rate values (counts/s) for each of three stages of AE cumulative counts–time curves recorded for mechanically testing southern yellow pine (SYP) columns under compression.

Stages	Mean (counts/s)	Coefficient of variation (COV) (%)	Range (counts/s)
Initiation	0.33	100.0	0.01-1.17
Growth	19.10	149.0	1.07-106.00
Acceleration	608.40	127.0	7.00-2240.00

tested columns at each stage were pooled together. Table 2 summarizes the mean values of the calculated AE count rates together with their corresponding COV values and ranges for each of the three stages. The mean AE count rates were 0.33, 19.10, and 608.40 counts/s for the initiation, growth, and acceleration stages, respectively, indicating that the AE count rate in the initiation stage was much lower than in the growth stage, whereas the count rate in the acceleration stage was much higher than in the growth stage. In addition, larger COV values of count rates ranging from 100.0 to 149.0% were observed in the three stages.

Figure 8 shows mean AE count rates vs grain angle within each stage in AE cumulative counts–time curves of all tested SYP columns. The AE count rate generally increased as the grain angle increased from 0° to 30°, then decreased as the grain angle further increased. The minor changes in the AE count rate within each stage become less important because the differences in magnitude between stages were so large.

Figure 9 plots typical AE counts–time curves of the SYP columns evaluated in this study and shows that some patterns could be identified. There was one peak for columns with grain angles ranging from 0° to 20° (Fig 9[a]–[c]) during the failure process after the stress passed its ultimate value as these columns lost the ability to resist compression loading. This might suggest that the one-peak pattern could be generated by sheared wood cell (like tracheids) walls in compressed SYP columns (Table 1). As the grain angle increased to 30°, the one-peak pattern was still observed in one of the three tested columns (Fig 9[d]), but the other two columns exhibited a different pattern in which two peaks appeared near the point where the stress just exceeded the proportional limit, in addition to the one peak occurring at their failing region (Fig 9[e]). As grain angles further increased above 45°, this pattern of more peaks appearing after the proportional limit (in the yield region) became more common (Fig 9[f] and [g]). The pattern then became one-peak in the yield region right as the stress passed the proportional limit (Fig 9[h] and [i]). The AE count peak patterns observed in SYP columns with grain angles ranging from 45° to 75° suggested that the one-peak pattern could be generated by tracheid wall bending and earlywood and latewood cell wall collapse or flattening. This might suggest that one-peak in counts–time curves could signal the beginning of the cell wall flattening process.

In summary, these different AE patterns that featured count peaks observed in tested SYP columns with different grain angles suggested the existence of some "signatures" in terms of AE signals, and these "signatures" could be related to the different wood fibers or cell failure modes and

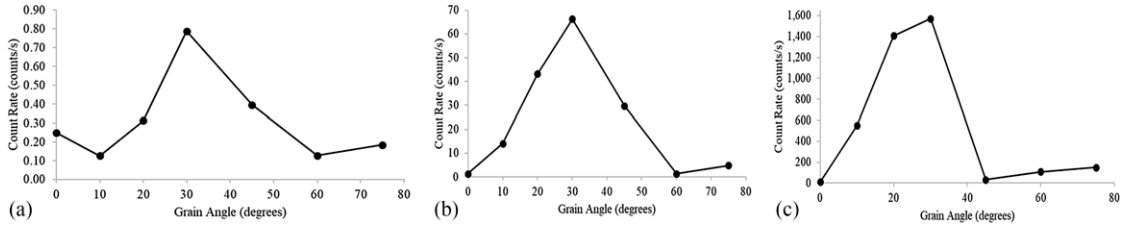

Figure 8. Mean acoustic emission (AE) count rate vs grain angle curves plotted for three stages: (a) initiation, (b) growth, and (c) acceleration as identified in the cumulative AE counts–time curves for the southern yellow pine (SYP) wood columns.

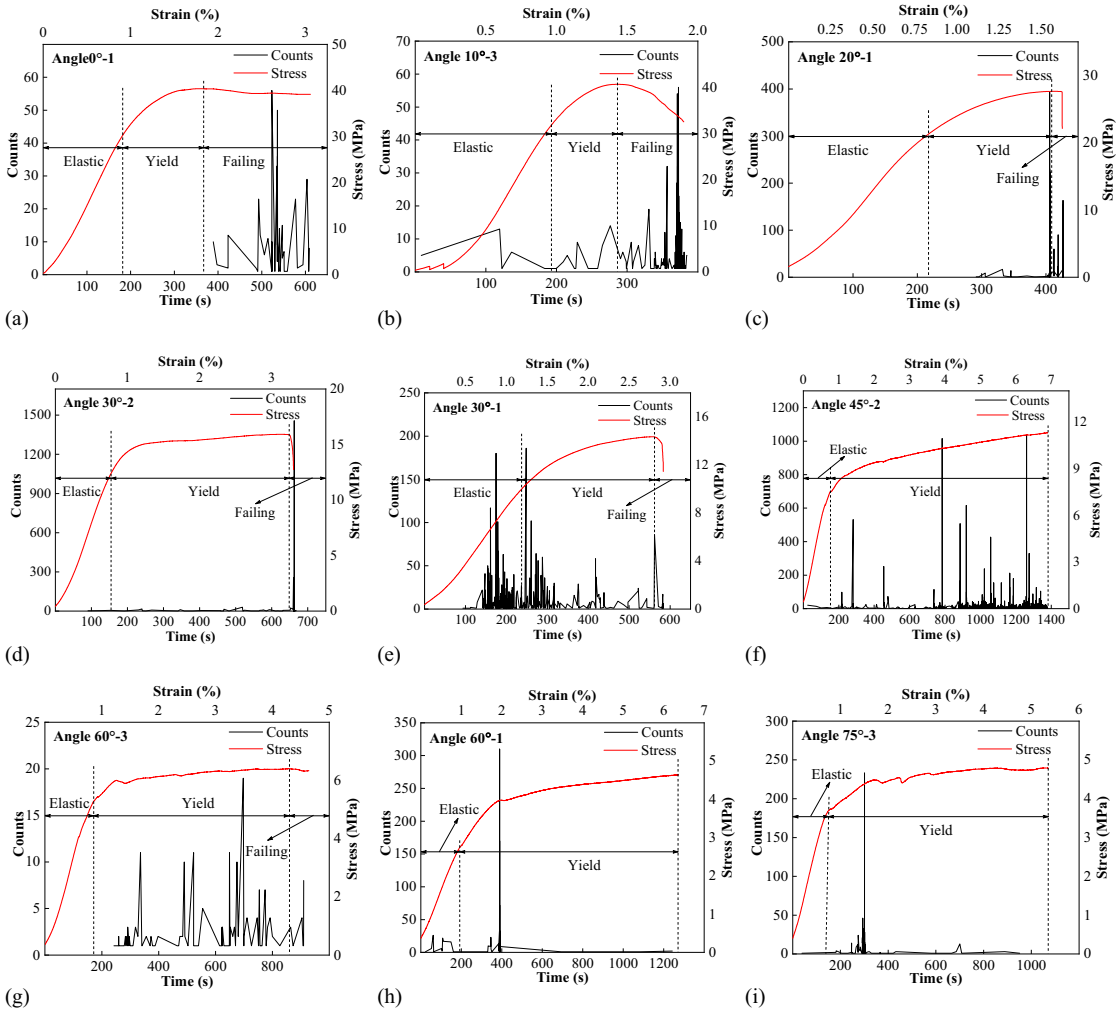

Figure 9. Typical counts–time curves plotted together with their corresponding stress–strain curves for tested southern yellow pine (SYP) wood columns with grain angles: 0° (a), 10° (b), 20° (c), 30° (d), 30° (e), 45° (f), 60° (g), 60° (h), and 75° (i), representing acoustic emission (AE) behavior of these columns in terms of different peak patterns.

processes when subjected to compressive stresses. These "signatures" could be used for nondestructive evaluation (NDE) of wood structures. Table 3 summarizes and Fig 10 plots the mean values of maximum AE counts (Fig 10[a]) and total cumulative AE count emissions (Fig 10[b]) of tested SYP columns, and these values vs grain angle. Maximum AE counts had large COV's ranging from 17.0 to 162.0%, whereas the total cumulative AE counts COV values ranged from 31.0 to 170.0%. The general trend was that as the grain angle increased from 0° to 30°, maximum AE counts and total cumulative AE counts all increased, then decreased as the grain angle further increased from 30° to 90°. Less than 36 counts were recorded for the SYP columns with a 90° grain angle. Fewer AE events recorded in this study could be because of micro cracking produced by cell wall deformation and flattening that generated fewer AEs or lower dB signals.

Table 3. Mean values of maximum acoustic emission (AE) counts and total cumulative counts of mechanically tested southern yellow pine (SYP) columns with different grain angles.[a]

Angle (°)	Maximum counts	Total cumulative counts
0	37 (17)	266 (59)
10	329 (111)	3303 (61)
20	3112 (104)	6092 (31)
30	4299 (141)	12,646 (123)
45	360 (162)	6929 (170)
60	208 (79)	693 (59)
75	779 (117)	6897 (145)
90	30 (119)	36 (125)

[a]Values represent means of three replicates per treatment. The numbers within parentheses indicate the coefficient of variation (COV).

This suggests that an adjustment reducing the threshold setting or increasing the preamp value might be needed for future studies.

AE Amplitude

Figure 11 shows typical AE amplitude–time curves plotted together with the corresponding stress–strain curves for the SYP columns tested in this study. In general, the AE signals with higher AE amplitudes were observed in the yield and failing stages (Fig 11[a]–[d]) and yield stages (Fig 11[e]–[g]). These values ranged from 60 to 100 dB. The mean values of maximum AE peak amplitude are summarized in Table 4 and plotted

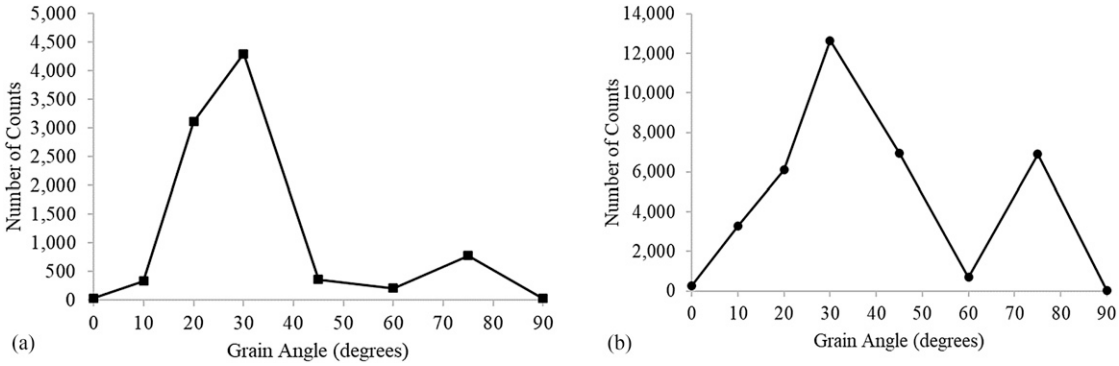

Figure 10. Mean values of maximum acoustic emission (AE) counts (a) and total cumulative acoustic emission counts (b) as a function of grain angle of mechanically tested southern yellow pine (SYP) wood columns in this study.

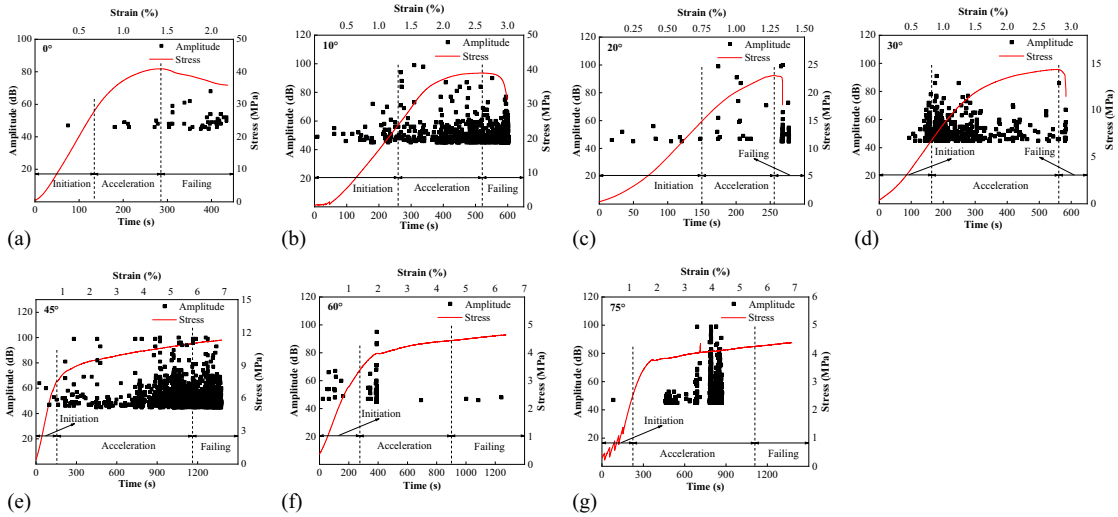

Figure 11. Typical acoustic emission (AE) amplitude vs time curves plotted together with their corresponding stress–strain curves for southern yellow pine (SYP) columns mechanically tested at grain angles of: (a) 0°, (b) 10°, (c) 20°, (d) 30°, (e) 45°, (f) 60°, and (g) 75°.

Table 4. Mean values of maximum acoustic emission (AE) amplitude (dB) on southern yellow pine (SYP) columns that were mechanically tested at the indicated grain angles.[a]

Grain angle (°)						
0	10	20	30	45	60	75
69.3 (12)	89.7 (15)	99.7 (1)	96.7 (5)	76.7 (28)	84.7 (25)	94.0 (8)

[a]Values represent means of three replicates per treatment. The numbers within parentheses indicate the coefficient of variation (COV).

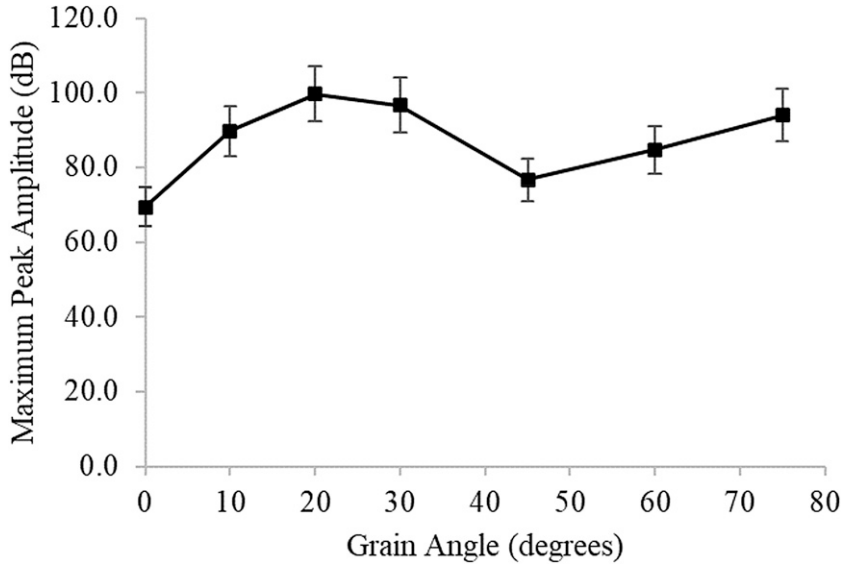

Figure 12. Mean values of maximum acoustic emission (AE) peak amplitude with standard error (SE) bars of the mean vs grain angle plot for southern yellow pine (SYP) wood columns assessed in this study.

in Fig 12. These results indicated that the maximum amplitude increased as the grain angle increased from 0° to 20° grain angles, then decreased as the grain angle decreased to 45°, followed by an increasing trend as the grain angle increased further to 75°. This pattern could be related to different micro-cracking failures occurring in SYP columns as the grain angle changed from 0 to 75°. In particular, the transition point of the failure mode of cells can be identified at 45°, where there was a change from shearing to bending and flattening.

CONCLUSIONS

1. Three distinct stages were identified in the cumulative AE counts–time curve in terms of AE count rate which included initiation, growth, and acceleration. The lowest count rate was observed at the initiation stage (0.33 counts/s) whereas the highest rate was observed at the acceleration stage (608.40 counts/s).
2. The AE count rate increased as the grain angle increased from 0° to 30° and then decreased as the grain angle further increased beyond 30°. We observed the same trend for maximum AE counts and total cumulative AE counts.
3. The maximum AE amplitude increased as the grain angle increased from 0° to 20°, then began a decreasing trend as the grain angle decreased to 45°, followed by an increasing trend as the grain angle increased to 75°. The AE signals with a higher

amplitude were observed in the yield and failing stages.

4. Some "signatures" in terms of AE signals do exist and could be related to different responses in wood fibers or cell failure modes such as shearing, bending, and compression and their corresponding development processes.
5. The combination of these "signatures" could be used to develop an NDE device algorithm to detect the progression of mechanical damage in structures constructed using SYP columns.

ACKNOWLEDGMENTS

The authors acknowledge Mississippi State University (MSU), College of Forest Resources (CFR), Department of Sustainable Bioproducts (DSB), and the Forest and Wildlife Research Center (FWRC) for providing financial support for this novel research. This publication is a contribution of the Forest and Wildlife Research Center (FWRC) at Mississippi State University (MSU).

REFERENCES

Ando K, Hirashima Y, Sugihara M, Hirao S, Sasaki Y (2006) Microscopic processes of shearing fracture of old wood, examined using the acoustic emission technique. J Wood Sci 52(6):483-489. https://doi.org/10.1007/s10086-005-0795-7.

André A, Kliger R, Asp LE (2014) Compression failure mechanism in small-scale timber specimens. Constr Build Mater 50(15 January 2014):130-139. https://doi.org/10.1016/j.conbuildmat.2013.09.018.

André A, Kliger R, Olsson R (2013) Compression failure mechanism in small-scale wood specimens reinforced with CFRP: An experimental study. Constr Build Mater 41(April 2013):790-800. https://doi.org/10.1016/j.conbuildmat.2012.12.038.

Ansell MP (1982) Acoustic emission from softwood in tension. Wood Sci Technol 16(1):35-57. https://doi.org/10.1007/BF00351373.

ASTM (2023) D 143-23. Standard test methods for small clear specimens of timber. American Society for Testing and Materials, West Conshohocken PA. https://www.astm.org/d0143-23.html.

ASTM (2024) E 1316-24b Standard terminology for nondestructive examinations. American Society for Testing and Materials, West Conshohocken, PA. https://www.astm.org/e1316-24.html.

Ayarkwa J, Hirashima Y, Ando K, Sasaki Y (2001) Monitoring acoustic emission to predict modulus of rupture of finger-joints from tropical African hardwoods. Wood Fiber Sci 33(3):450-464. https://wfs.swst.org/index.php/wfs/article/view/130/130.

Ayres QC (1920) Crushing strength of southern pine at angles to grain. Eng News-Record 85(14):653-654. https://archive.org/details/engineeringnewsr85newy/page/653/mode/1up. (30 August 2024).

Beall FC (1985) Relationship of acoustic emission to internal bond strength of wood-based composite panel materials. J Acoustic Emission 4(1):19-29. http://www.aewg.org/jae/JAE-Vol_04-1985.pdf. (30 August 2024).

Beall FC, Wilcox WW (1987) Relationship of acoustic emission during radial compression to mass loss from decay. Forest Prod J 37(4):38-42. http://kb.forestprod.org/Main/ind/?id=66433.

Berg JE, Gradin PA (2000) Effect of temperature on fracture of spruce in compression, investigated by use of acoustic emission monitoring. J Pulp Paper Sci 26(8):294-299. https://www.researchgate.net/publication/274256796_Effect_of_Temperature_on_Fracture_of_Spruce_in_Compression_Investigated_by_Use_of_Acoustic_Emission_Monitoring. (30 August 2024).

Bodig J, Jayne BA, (1982) Mechanics of wood and wood composites. Van Nostrand Reinhold Company Inc., New York. 712 pp. ISBN-10: 0442008228. https://archive.org/details/mechanicsofwoodw0000bodi/page/n5/mode/2up. (30 August 2024).

Carmona-Uzcategui MG (2020) Properties of four domestic hardwood species. MS thesis, Mississippi State, MS: Mississippi State University. 54 pp. https://scholarsjunction.msstate.edu/td/3662. (30 August 2024).

Carmona-Uzcategui MG, Seale RD, França FJN (2020) Physical and mechanical properties of clear wood from red oak and white oak. BioRes 15(3):4960-4971. https://bioresources.cnr.ncsu.edu/resources/physical-and-mechanical-properties-of-clear-wood-from-red-oak-and-white-oak/.

Chen Z, Gabbitas B, Hunt D (2006) Monitoring the fracture of wood in torsion using acoustic emission. J Mater Sci 41(12):3645-3655. https://doi.org/10.1007/s10853-006-6292-6.

Dahlen J, Auty D, Eberhardt TL (2018) Models for predicting specific gravity and ring width for loblolly pine from intensively managed plantations, and implications for wood utilization. Forests 9(6):292-312. https://doi.org/10.3390/f9060292.

DeBaise G, Porter A, Pentoney R (1966) Morphology and mechanics of wood fracture. Mat Res Stand 6(10):493-499. https://www.cabidigitallibrary.org/doi/full/10.5555/19660602840. (30 August 2024).

Du Y, Zhang J, Shi S (2014) Acoustic emission of bolt-bearing testing on structural composite lumbers. Wood Fiber Sci 46(1):118-126. https://wfs.swst.org/index.php/wfs/article/view/637.

FPL (2021) Wood handbook: Wood as an engineering material. Gen Tech Rep FPL-GTR-282. USDA For

Serv Forest Products Laboratory, Madison, WI. 546 pp. https://www.fpl.fs.usda.gov/documnts/fplgtr/fplgtr282/fpl_gtr282.pdf. (30 August 2024).

França TSA, França FJN, Seale RD, Shmulsky R (2018) Bending strength and stiffness of No. 2 grade southern pine lumber. W&Fs 50(2):205-219. https://wfs.swst.org/index.php/wfs/article/view/2698.

Gibson LJ, Ashby MF, (1997) Cellular solids: Structure and properties, 2nd edition. Cambridge University Press, Cambridge, England, United Kingdom. 510 pp. ISBN: 9781139878326. https://doi.org/10.1017/CBO9781139878326.

Gong M, Smith I (2000) Failure of softwood under static compression parallel to grain. J Institute Wood Sci 15(4): 204-210. https://www.researchgate.net/publication/287178221_Failure_of_softwood_under_static_compression_parallel_to_grain. (30 August 2024).

Gozdecki C, Smardzewski J (2005) Detection of failures of adhesively bonded joints using the acoustic emission method. Holzfor 59(2):219-229. https://doi.org/10.1515/HF.2005.035.

Green DW, (2001) Wood: Strength and stiffness. Pages 9732-9736 *in* KH Jürgen Buschow, RW Cahn, MC Flemings, B Ilschner, EJ Kramer, S Mahajan, and P Veyssière, eds. Encyclopedia of materials: Science and technology, 2nd edition. Elsevier, Amsterdam and New York. ISBN: 9780080431529. https://doi.org/10.1016/B0-08-043152-6/01766-6.

Green DW, Winandy JE, Kretschmann DE (1999) Chapter 4: Mechanical properties of wood. Pages 4-1 to 4-45 in Wood handbook: Wood as an engineering material. Gen Tech Rep FPL-GTR-113. USDA For Serv Forest Products Laboratory, Madison, WI. 463 pp. https://doi.org/10.2737/FPL-GTR-113.

Güntekin E, Aydin TY (2013) Effects of moisture content on some mechanical properties of Turkish red pine (*Pinus brutia* Ten.). Pages 878-883 *in* Proceedings, International Caucasia Forestry Symposium, 24-26 October 2013, Artvin, Turkey. https://www.researchgate.net/publication/281236918_Effects_of_Moisture_Content_on_Some_Mechanical_Properties_of_Turkish_Red_Pine_Pinus_brutia_Ten. (30 August 2024).

Gupta R, Sinha A (2012) Effect of grain angle on shear strength of Douglas-fir wood. Holzforschung 66(5):655-658. https://doi.org/10.1515/hf-2011-0031.

Hankinson RL (1921) Investigation of crushing strength of spruce at varying angles of grain. United States Army, Engineering Division, Washington D.C. McCook Field Report, Serial No. 1570. Air Service Information Circular No. 259, Volume 3, 16 pp. https://content.lib.auburn.edu/digital/collection/asic/id/382/rec/18. (30 August 2024).

Hindman DP, Bouldin JC (2015) Mechanical properties of southern pine cross-laminated timber. J Mater Civ Eng 27(9):04014251. https://doi.org/10.1061/(ASCE)MT.1943-5533.0001203.

Hu W, Zhang J (2022) Effect of growth rings on acoustic emission characteristic signals of southern yellow pine wood cracked in mode I. Constr Build Mater 329(25 April 2022):127092. https://doi.org/10.1016/j.conbuildmat.2022.127092.

Indrayani Y, Nakayama T, Yanase Y, Fujii Y, Yoshimura T, Imamura Y (2003) Feeding activities of the drywood termite *Cryptotermes domesticus* (Haviland) under various relative humidity and temperature conditions using acoustic emission monitoring. Jpn J Environ Entomol Zoo 14(4):205-212. https://www.jstage.jst.go.jp/article/jjeez/14/4/14_205/_pdf. (30 August 2024).

Ingemi CM, Yu T (2019) Detection of grain angle in wood specimens using synthetic aperture radar imaging. Proceedings, Society of Photo-Optical Instrumentation Engineers (SPIE), Volume 10971, Nondestructive Characterization and Monitoring of Advanced Materials, Aerospace, Civil Infrastructure, and Transportation XIII, 109710U. SPIE Smart Structures and Nondestructive Evaluation Conference, April 1, 2019, Denver, Colorado. https://doi.org/10.1117/12.2513972.

Irby NE, França FJN, Barnes HM, Seale RD, Shmulsky R (2020a) Effect of growth rings per inch and density on compression parallel to grain in southern pine lumber. BioRes 15(2):2310-2325. https://bioresources.cnr.ncsu.edu/resources/effect-of-growth-rings-per-inch-and-density-on-compression-parallel-to-grain-in-southern-pine-lumber/.

Irby NE, França FJN, Barnes HM, Seale RD, Shmulsky R (2020b) Effect of growth rings per inch and specific gravity on compression perpendicular to grain in No. 2: 2 by 8 and 2 by 10 southern pine lumber. For Prod J 70(2):213-220. https://doi.org/10.13073/FPJ-D-19-00043.

Jakob HF, Fratzl P, Tschegg SE (1994) Size and arrangement of elementary cellulose fibrils in wood cells: A small-angle X-ray scattering study of *Picea abies*. J Struct Biol 113(1):13-22. https://doi.org/10.1006/jsbi.1994.1028.

Junaid O, Owens FC, Entsminger ED, Seale RD, Shmulsky R (2018) Strength and stiffness properties of small clear specimens taken from commercially procured No. 2 2×8 and 2×10 southern pine dimension lumber. Wood Fiber Sci 50(3):363-369. https://wfs.swst.org/index.php/wfs/article/view/2732.

Kim KY (1986) A note on the Hankinson formula. Wood Fiber Sci 18(2):345-348. https://wfs.swst.org/index.php/wfs/article/view/698.

Knuffel WE (1988) Acoustic emission as strength predictor in structural timber. Holzfor 42(3):195-198. https://doi.org/10.1515/hfsg.1988.42.3.195.

Koch P, (1972) Utilization of the southern pines. Agriculture Handbook No. 420. Volume 1 – The raw material. USDA U.S. Forest Service, Southern Forest Experiment Station. https://www.srs.fs.usda.gov/pubs/ah/ah420_vol1.pdf. (30 August 2024).

Kojis DD, Postweilder RS (1953) Allowable loads for common bolts at various angles to the grain for southern yellow pine. For Prod J 3(3):21-26. http://kb.forestprod.org/Main/ind/?id=70289.

Kretschmann DE (2010) Chapter 5: Mechanical properties of wood. Pages 5-1 to 5-44 *in* Wood handbook – Wood as an engineering material. Gen Tech Rep FPL-GTR-190. USDA For Serv Forest Products Laboratory, Madison, WI. 509 pp. https://doi.org/10.2737/FPL-GTR-190.

Mankin RW, Osbrink WL, Oi FM, Anderson JB (2002) Acoustic detection of termite infestations in urban trees. J Econ Entomol 95(5):981-988. https://doi.org/10.1093/jee/95.5.981.

Martel RR (1920) Tests of bearing strength of redwood agree with Howe's Formula. Eng News-Record 85(20): 959. https://archive.org/details/engineeringnewsr85newy/page/958/mode/2up. (30 August 2024).

Nasir V, Ayanleye S, Kazemirad S, Sassani F, Adamopoulos S (2022) Acoustic emission monitoring of wood materials and timber structures: A critical review. Constr Build Mater 350(3 October 2022):128877. https://doi.org/10.1016/j.conbuildmat.2022.128877.

Nguyen TT, Ji X, Van Nguyen TH, Guo M (2017) Wettability modification of heat-treated wood (HTW) via cold atmospheric-pressure nitrogen plasma jet (APPJ). Holzfor 72(1):37-43. https://doi.org/10.1515/hf-2017-0004.

Noguchi M, Ishii R, Fujii Y, Imamura Y (1992) Acoustic emission monitoring during partial compression to detect early stages of decay. Wood Scitechnol 26(4): 279-287. https://doi.org/10.1007/BF00200163.

Osgood WR (1928) Compressive stress on wood surfaces inclined to the grain. Eng News-Record 100(6):243-244. https://archive.org/details/sim_enr_1928-02-09_100_6/page/242/mode/2up. (30 August 2024).

Porter AW, El-Osta ML, Kusec DJ (1972) Prediction of failure of finger joints using acoustic emissions. Forest Prod J 22(9):74-82. http://kb.forestprod.org/Main/ind/?id=70090.

Poulsen JS, Moran PM, Shih CF, Byskov E (1997) Kink band initiation and band broadening in clear wood under compressive loading. Mech Mater 25(1):67-77. https://doi.org/10.1016/S0167-6636(96)00043-9.

Raczkowski J, Lutomski K, Moliński W, Woś R (1999) Detection of early stages of wood decay by acoustic emission technique. Wood Sci Technol 33(5):353-358. https://doi.org/10.1007/s002260050121.

Raczkowski J, Moliński W, Ranachowski Z (1994) Acoustic emission in fracture mechanics of wood. J Theor Appl Mech 32(2):299-322. http://www.ptmts.org.pl/jtam/index.php/jtam/article/viewFile/v32n2p299/1082. (30 August 2024).

Ramage MH, Burridge H, Busse-Wicher M, Fereday G, Reynolds T, Shah DU, Wu G, Yu L, Fleming P, Densley-Tingley D, Allwood J, Dupree P, Linden PF, Scherman O (2017) The wood from the trees: The use of timber in construction. Renew Sust Energ Rev 68(1): 333-359. https://doi.org/10.1016/j.rser.2016.09.107.

Reiterer A, Stanzl-Tschegg SE (2001) Compressive behaviour of softwood under uniaxial loading at different orientations to the grain. Mech Mater 33(12):705-715. https://doi.org/10.1016/S0167-6636(01)00086-2.

Reiterer A, Stanzl-Tschegg SE, Tschegg EK (2000) Mode I fracture and acoustic emission of softwood and hardwood. Wood Sci Tech 34(5):417-430. https://doi.org/10.1007/s002260000056.

Rescalvo FJ, Morillas L, Valverde-Palacios I, Gallego A (2020) Acoustic emission in I-214 poplar wood under compressive loading. Eur J Wood Prod 78(4):723-732. https://doi.org/10.1007/s00107-020-01536-7.

Ritschel F, Brunner AJ, Niemz P (2013) Nondestructive evaluation of damage accumulation in tensile test specimens made from solid wood and layered wood materials. Compos Struct 95(January 2013):44-52. https://doi.org/10.1016/j.compstruct.2012.06.020.

Sato K, Fushitani M, Noguchi M (1984a) Discussion of tensile fracture of wood using acoustic emissions. Estimation of tensile strength and consideration of AE generation based on fracture mechanics. Mokuzai Gakkaishi. J Japan Wood Res Soc 30(2):117-123. https://www.jwrs.org/english/journals/mkz-toce/mkze-30/. (30 August 2024).

Sato K, Kamei N, Fushitani M, Noguchi M (1984b) Discussion of tensile fracture of wood using acoustic emissions: A statistical analysis of the relationships between the characteristics of AE and fracture stress. J Japan Wood Res Soc 30(8):653-659. https://www.jwrs.org/english/journals/mkz-toce/mkze-30/. (30 August 2024).

Sharma K (2017) Investigation of failure in different materials using acoustic emission technique. ME thesis, Thapar University, Patiala, India. 89 pp. https://tudr.thapar.edu:8443/jspui/bitstream/10266/4845/5/4845.pdf. (30 August 2024).

Smardzewski J, Gozdecki C (2007) Decohesion of glue bond in wood connections. Holzfor 61(3):291-293. https://doi.org/10.1515/HF.2007.061.

Southern Forest Products Association (SFPA (2018) Southern pine use guide: Strength, treatability, and beauty. 2018 Edition. Metairie, LA. https://www.southernpine.com/wp-content/uploads/2023/09/SP_USEguide_METRIC_10-18L.pdf. (30 August 2024).

Turkot CG (2019) Preliminary characterization of physical and mechanical properties of species used in staircase manufactures. MS thesis, Mississippi State University, Mississippi State, MS. 45 pp. https://scholarsjunction.msstate.edu/td/3619. (30 August 2024).

Turkot CG, Seale RD, Entsminger ED, França FJN, Shmulsky R (2020) Nondestructive evaluation of red oak and white oak species. Forest Prod J 70(3):370-377. https://doi.org/10.13073/FPJ-D-20-00015.

SUSTAINABILITY REPORTING AND PERFORMANCE: A COMPARATIVE STUDY OF LEADING PAPER AND PAPER-BASED PACKAGING COMPANIES

*Arzu Meriç**

Assistant Professor
Department of Finance, Banking and Insurance,
Malatya Vocational School, Inonu University,
Inonu Street No: 192, Yesilyurt, Malatya, Turkey
E-mail: arzu.meric@inonu.edu.tr

Hayrettin Meriç

Lecturer
Department of Forestry and Forest Products,
Banaz Vocational School, Usak University,
Dilek Mah. Değirmenler Street No. 9, Banaz, Uşak, Turkey
E-mail: hayrettin.meric@usak.edu.tr

(Received June 26, 2024)

Abstract. This research presents a comparative analysis of the sustainability performance of four prominent companies within the paper and paper-based packaging industry. Utilizing established sustainability indicators encompassing environmental, social, and economic dimensions, the study evaluated company performance based on publicly available data from their sustainability reports and disclosures. The findings revealed a diverse landscape of sustainability commitments and achievements, highlighting both shared industry-wide trends and company-specific approaches to sustainability management. All four companies demonstrated a strong commitment to waste management and circular economy principles, while also exhibiting varying degrees of progress in areas, such as renewable energy adoption, carbon emissions reductions, employee well-being, and social responsibility initiatives. The analysis further identified opportunities for improvement and highlighted the need for greater transparency, data disclosure, and industry collaboration to enhance overall sustainability performance and contribute to a more sustainable future for the paper and paper-based packaging sector. By examining the similarities and differences in the sustainability journeys of these four companies, this study provides valuable insights for industry stakeholders, policymakers, and researchers interested in promoting sustainable development within the paper and packaging industry and beyond.

Keywords: Economic sustainability, environmental performance, social responsibility, sustainability reporting, paper and paper-based packaging industry

INTRODUCTION

The amount of paper and paperboard a country uses is a reliable indicator of its development. Having access to paper is essential to our daily life, supporting communication, commerce, and countless aspects of modern society. As global demand for paper products continues to rise, the paper and packaging industry faces the critical challenge of ensuring a sustainable supply of raw materials (Pydimalla et al 2023). This challenge is further compounded by concerns regarding deforestation, high resource consumption, and waste generation associated with traditional paper production methods.

In response to these challenges, the industry is actively investigating alternative fiber sources and more sustainable production practices. This research paper focuses on a comparative analysis of the sustainability performance of four prominent companies within the paper and paper-based packaging industry. The companies considered were Duran Dogan, Kartonsan, Mondi Group, and Viking Kağıt.

* Corresponding author

Duran Dogan: A leading Turkish packaging manufacturer specializing in cardboard and paperboard packaging solutions for a diverse range of industries, including food, cosmetics, and pharmaceuticals. The company places great emphasis on innovation and sustainability, as evidenced by its development of the "Gloss&Green" technology and its commitment to responsible sourcing and waste reduction.

Kartonsan: A prominent Turkish producer of coated cardboard, recognized for its high utilization of waste paper in production and its commitment to circular economy principles. The company operates a self-sufficient energy generation system and actively invests in environmental protection measures.

Mondi Group: A global leader in sustainable packaging and paper solutions, operating across the entire value chain, from responsible sourcing of raw materials to production and distribution of a wide range of packaging products. The company is known for its comprehensive sustainability strategy, including ambitious climate action goals and a strong focus on employee well-being and social responsibility.

Viking Kağıt: A leading Turkish tissue paper manufacturer, recognized for its pioneering Recyfiber® technology, which utilizes recycled beverage cartons to produce eco-friendly tissue paper products. The company demonstrates a strong commitment to sustainability, focusing on resource recovery, waste reduction, and responsible sourcing practices.

The sustainability strategies, initiatives, and performance data of the four companies across environmental, social, and economic dimensions were used, to provide insights into the diverse pathways toward sustainability within the sector and contribute to the ongoing discussion on responsible business practices in the paper and packaging industry.

The Size and Importance of the Global Paper Industry

Recent events, such as the Ukraine war and the COVID-19 pandemic, have demonstrated the significant impact that global disruptions can have on industries, including the paper and packaging sector. This can lead to challenges in the supply chain and shifts in consumer behavior (Vivas et al 2024). The global paper and paper-based packaging industry is a significant force, underpinning communication, commerce, and numerous aspects of modern life. In 2020 alone, the industry produced over 401 million tons of paper and paperboard, solidifying its position as the 15th largest industry globally (Deshwal et al 2019; Worku et al 2023). The industry's reach extends across four major submarkets: board and packaging paper, writing and printing paper, newsprint, and specialty papers (Deshwal et al 2019). Each of these submarkets caters to diverse needs and applications. Paper and paper-based packaging are ubiquitous, interwoven into the very fabric of our daily routines. They are used in the books we read and the documents we write, in the boxes that protect our goods, and in the tissues, used for hygiene.

The significance of the industry extends beyond its size. Paper remains a vital medium for information dissemination and cultural preservation, even in our increasingly digital world (Aithal and Shenoy 2016). Furthermore, paper-based packaging plays a critical role in the global supply chain, ensuring the safe and efficient transport of goods, while also offering sustainable and recyclable solutions compared with other packaging materials (Zhang and Sablani 2021; Le Quyen 2023).

However, the industry faces significant sustainability challenges. Deforestation, high resource consumption, and waste generation have led to concerns about the environmental footprint of the industry (Skene and Vinyard 2019; Vinyard 2021). Furthermore, the shift toward digital communication has the potential to threaten the availability of recovered paper, a key raw material for sustainable paper production (Ucelay 2020; Zambrano et al 2021). These challenges necessitate a transition toward more sustainable practices, including the use of alternative fiber sources such as agricultural waste and by-products (Baetge and Martin 2018; Otieno et al 2021), along with the

development of innovative recycling and waste management solutions (Méndez et al 2009).

In response to these challenges, the industry is investigating a range of potential avenues for enhancing its sustainability performance. The utilization of agro-based paper production, which employs agricultural residues in place of wood fibers, presents a promising avenue for addressing environmental concerns and facilitating accelerated growth (Jiang et al 2019; Neis et al 2019). Moreover, ongoing research into bio-derived materials, such as lignin and cellulose derived from agricultural waste, offers promising avenues for creating sustainable and functional packaging materials (Li et al 2012; Tajeddin 2014; Fadeyibi et al 2017; Shaghaleh et al 2018; Fitch-Vargas et al 2019; Travalini et al 2019; Karlovits 2020; Liyanage et al 2021; Nanda et al 2022).

By embracing innovation and adopting a more circular approach, the global paper and paper-based packaging industry can continue to fulfill its vital societal role while minimizing its environmental footprint and ensuring a sustainable future.

The Paper Industry: A Comprehensive Look at Its Environmental and Social Impacts

The paper and paper-based packaging industry, while essential to modern society, faces a complex interplay of environmental and social impacts. On the environmental front, concerns regarding resource consumption, and waste generation pose significant challenges (Skene and Vinyard 2019; Vinyard 2021). Additionally, the production process is resource-intensive, requiring substantial amounts of water and energy (Skene and Vinyard 2019; Vinyard and Skene 2020). Furthermore, the disposal of paper-based products, particularly single-use items, contributes to a number of problems that necessitate robust waste management solutions (Méndez et al 2009).

Nevertheless, the industry has certain environmental benefits compared with alternative materials. Paper is inherently recyclable, allowing for the recovery and reuse of fibers to create new products. Furthermore, the transition toward agro-based paper production can utilize agricultural residues as an alternative to wood fibers. Indeed, studies have demonstrated that the manufacture of agro-based paper utilizes up to 90% less water and 60% less energy than traditional wood-based paper production, thereby underscoring its potential for resource conservation (Pydimalla et al 2023). Moreover, ongoing research into bio-derived materials derived from agricultural waste presents promising avenues for the development of environmentally friendly packaging solutions.

The social impacts of the industry are complex and multifaceted. On the one hand, the industry provides employment opportunities and contributes to economic development, particularly in rural communities where agro-based paper production thrives (Otieno et al 2021). Moreover, the industry plays a pivotal role in supporting education, communication, and cultural preservation through the production of paper-based materials (Aithal and Shenoy 2016). Nevertheless, concerns regarding fair labor practices, human rights, and the impact of globalized production on local communities necessitate careful consideration (Mattila et al 2018). Furthermore, the industry's environmental practices can influence consumer perceptions and purchasing decisions, emphasizing the importance of transparency and responsible sourcing (Parguel et al 2011; Lewandowska et al 2017).

To ensure a sustainable future, the paper and paper-based packaging industry must navigate the complex environmental and social impacts it currently faces. To do so, it is crucial that the industry embraces sustainable practices, such as responsible forestry management, increased use of recycled content, and the development of innovative bio-based materials. Simultaneously, it is essential that the industry prioritizes fair labor practices, engages with local communities, and fosters transparency, to mitigate negative social impacts and build a more equitable and sustainable industry. By addressing both its environmental and social responsibilities, the paper and paper-based packaging industry can continue to

meet the needs of society while contributing to a more sustainable and just future.

The Purpose and Significance of Sustainability Reporting for Companies

The practice of sustainability reporting has emerged as a crucial aspect of business operations for companies across various industries, including the paper and pulp sectors. Reporting provides a framework for transparently communicating their environmental, social, and economic performance to stakeholders. The primary objective of sustainability reporting is to disclose a company's impacts on the environment and society. This enables stakeholders to assess the company's sustainability performance and hold it accountable for its actions. Such transparency fosters trust and credibility with stakeholders, including investors, customers, employees, and communities, who increasingly demand information about environmental and social responsibility.

Sustainability reports represent a valuable instrument for companies to monitor their advancement toward sustainability objectives, identify areas for enhancement, and benchmark their performance against industry counterparts. By meticulously collating and analyzing data on their environmental and social impacts, companies can gain invaluable insights into their operations and make well-informed decisions to enhance their sustainability performance. This data-driven approach enables companies to assess the efficacy of their sustainability initiatives, identify potential risks and opportunities, and develop strategies for continuous improvement.

Public disclosure of sustainability goals and performance incentivizes companies to develop and implement innovative solutions that address environmental and social challenges. This can result in the adoption of cleaner technologies, more efficient resource management, and the development of new products and services with reduced environmental footprints. Furthermore, sustainability reporting can facilitate collaboration among companies, industry associations, and other stakeholders to collectively address sustainability issues and promote industry-wide best practices.

The Role of Transparency and Accountability in Driving Sustainable Practices

Transparency and accountability are fundamental pillars for driving sustainable practices within companies and across industries. Transparency, characterized by open and honest communication about environmental, social, and economic performance, enables stakeholders to make informed decisions and hold companies accountable for their actions. Companies that openly disclose their sustainability goals, strategies, and performance data, create a culture of accountability that builds trust and credibility with stakeholders. This, in turn, incentivizes companies to prioritize sustainability and continuously improve their practices to meet stakeholder expectations.

Transparency plays a crucial role in promoting responsible environmental management. Companies that disclose their environmental impacts, such as greenhouse gas emissions, water usage, and waste generation provide stakeholders with the necessary information to assess their environmental performance. This transparency encourages companies to adopt cleaner technologies, reduce their environmental footprint, and invest in sustainable solutions to mitigate their impacts.

It is similarly important for companies to be held to account to encourage them to embrace social responsibility. Companies disclosing their social impacts, including labor practices, human rights, and community engagement demonstrate their commitment to ethical conduct and social well-being. Such accountability encourages companies to uphold high social standards, promote fair labor practices, and contribute positively to the communities in which they operate. Moreover, accountability mechanisms, such as external audits and stakeholder engagement processes, provide further assurance that companies are meeting their social responsibilities.

Together, transparency and accountability constitute a potent force for driving sustainable practices. The adoption of these principles by companies engenders a culture of continuous improvement, innovation, and responsible business conduct, thereby contributing to a more sustainable and equitable future.

Purpose of the Research and Contributions to Scientific Literature

This research involves a comprehensive, comparative analysis of the sustainability performance of four prominent companies within the Turkish paper and paper-based packaging industry. Sustainability strategies, initiatives, and performance data were used to illuminate the diverse sustainability pathways and to demonstrate a deeper understanding of the complexities and opportunities within the sector.

Firstly, the research offers a unique comparative assessment of sustainability practices across industry segments within the paper and paper-based packaging sector. This comparative approach transcends the limitations of single-case studies by providing valuable insights into the diverse challenges and opportunities faced by companies operating in varying contexts, from regulatory landscapes to resource availability and cultural nuances. By showcasing best practices and identifying areas for improvement across different companies, the research facilitates cross-learning and knowledge transfer within the industry, paving the way for a more collaborative and informed approach to sustainability.

The study also examines the ongoing discourse surrounding the measurement and evaluation of corporate sustainability performance. By utilizing established sustainability indicators and meticulously evaluating company performance across environmental, social, and economic dimensions, the research constructs a holistic framework for assessing sustainability progress and identifying areas necessitating further development. This comprehensive framework transcends the limitations of siloed approaches to sustainability by considering the interconnectedness of environmental, social, and economic factors, providing a more nuanced and integrated understanding of corporate sustainability performance.

Thirdly, the research underscores the paramount importance of transparency and data disclosure to foster corporate accountability and propelling sustainability performance. The study examines the level of transparency exhibited by each company to identify best practices in sustainability reporting and underscores the indispensable need for standardized and comprehensive disclosure of environmental, social, and economic data. Increased transparency not only empowers stakeholders with information for making informed decisions but also provides an incentive for companies to continuously improve their sustainability performance and contribute to a more sustainable and equitable future.

Finally, this research contributes to the growing body of knowledge on sustainable development within the paper and paper-based packaging industry. Identifying key challenges and opportunities across different geographic regions and industry segments can help create a deeper understanding of sustainability trends within the paper and packaging sector and inform future research directions. While the findings offer potential insights for industry stakeholders, policymakers, and researchers, it is important to acknowledge that the analysis is based on company-reported data that may present inherent limitations and potential biases. Further research, employing diverse methodologies and data sources, is encouraged to corroborate these findings and strengthen their implications for stakeholders across the industry. This includes exploring innovative solutions for mitigating environmental impacts, promoting responsible sourcing practices, fostering social equity and well-being within the workforce, and ensuring economic viability and the creation of shared value for all stakeholders.

METHODOLOGICAL PROCEDURES

Definition of the Case Report

A total of 13 companies are currently listed on the Borsa Istanbul (BIST), operating in the paper and

paper product printing sector in Turkey. This study employed a comparative case study approach focusing on four companies within the Turkish paper and packaging industry: Duran Dogan, Kartonsan, Mondi Group, and Viking Kağıt. These companies were selected based on a purposeful sampling strategy designed to 1) represent a diverse cross-section of the industry, 2) provide insights into both local and global sustainability practices, and 3) facilitate a comparative analysis of the influence of global trends on local operations. The companies were used to examine the following questions:

1. How do the sustainability approaches and performance of domestic Turkish paper and packaging companies compare to those of a multinational company operating within the same national context?
2. What are the key similarities and differences in their sustainability strategies, initiatives, and performance, and what factors might contribute to these variations?
3. To what extent do global sustainability trends and standards influence the practices of local companies operating in Turkey?

The inclusion of Mondi Group, a multinational company with a well-established global sustainability strategy provided a valuable benchmark for assessing the extent to which global sustainability trends and standards have been adopted by domestic Turkish companies. By analyzing the similarities and differences in their approaches, this study offers insights into the unique challenges and opportunities faced by companies operating at different scales and the potential influence of global sustainability frameworks on local practices within the Turkish paper and packaging industry.

Analysis of Mondi Group's sustainability performance in this study was specifically limited to their Turkish operations. This approach ensured a more direct and meaningful comparison with the domestic companies, focusing on their performance within the same national context and regulatory environment.

By employing this purposeful sampling strategy and providing a clear and transparent rationale, this study aimed to contribute to a deeper understanding of the multifaceted sustainability landscape within the paper and packaging industry and offer insights for both local and global stakeholders.

Identification of Indicators and Sustainability Index Structure

This study employed a set of established sustainability indicators encompassing environmental, social, and economic dimensions. These indicators were selected based on their relevance to the paper and packaging industry and their alignment with widely recognized sustainability frameworks, such as the Global Reporting Initiative (GRI) Standards and the Sustainability Accounting Standards Board (SASB) industry standards. The indicators were organized into three distinct categories, each representing a key dimension of sustainability (Feil et al 2015; Feil et al 2017; Feil et al 2022):

1. Environmental Indicators: This category focused on the company' environmental impact and their efforts to minimize their ecological footprint. The specific scoring considerations for each indicator are detailed below:

Hazardous Waste Generation (0-0.3: high generation with limited mitigation; 0.4-0.7: moderate generation with some mitigation efforts; 0.8-1.0: minimal generation with comprehensive mitigation and transparency): Assesses the volume of hazardous waste generated, the implementation of reduction and mitigation strategies, and the transparency of reporting.

Waste Disposal Practices (0-0.3: high reliance on landfill with limited recycling; 0.4-0.7: moderate landfill use with some recycling efforts; 0.8-1.0: minimal landfill use with comprehensive waste diversion and circularity strategies): Evaluates the company's approach to waste disposal, including landfill use, recycling rates, and implementation of circular economy initiatives.

Treatment of Effluents (0-0.3: inadequate treatment with noncompliance issues; 0.4-0.7: basic treatment with some compliance challenges; 0.8-1.0: advanced treatment with full compliance and monitoring of key parameters): Assesses the quality of effluent treatment, adherence to discharge regulations, and monitoring of key water quality parameters.

Recycling of Waste (0-0.3: limited recycling with low rates; 0.4-0.7: moderate recycling with some innovative approaches; 0.8-1.0: extensive recycling with industry-leading innovation and closed-loop systems): Evaluates the extent of recycling efforts, the use of innovative technologies, and the implementation of closed-loop systems for material recovery and reuse.

Atmospheric Emissions (0-0.3: high emissions with limited mitigation; 0.4-0.7: moderate emissions with some reduction efforts; 0.8-1.0: minimal emissions with science-based targets and comprehensive strategies): Assesses the volume of greenhouse gas emissions, the implementation of reduction strategies, and the setting of science-based targets aligned with global climate goals.

Recycling and Reuse of Products (0-0.3: limited product recyclability; 0.4-0.7: moderate recyclability with some design for circularity; 0.8-1.0: high product recyclability with a comprehensive focus on circular economy principles): Evaluates the recyclability of the company's products, the incorporation of design for circularity principles, and the company's commitment to a circular economy.

Renewable Energy Utilization (0-0.3: minimal or no use of renewable energy; 0.4-0.7: moderate use of renewable energy with plans for expansion; 0.8-1.0: extensive use of renewable energy with ambitious targets and investments): Assesses the percentage of energy sourced from renewable sources, investments in renewable energy infrastructure, and the setting of targets for renewable energy adoption.

Energy Efficiency (0-0.3: low energy efficiency with limited improvement; 0.4-0.7: moderate energy efficiency with some initiatives; 0.8-1.0: high energy efficiency with industry-leading performance and continuous improvement): Evaluates the company's energy efficiency performance, the implementation of energy-saving measures, and its progress toward improving energy efficiency.

Use of Renewable Materials (0-0.3: minimal use of renewable materials; 0.4-0.7: moderate use of renewable materials with some sourcing challenges; 0.8-1.0: extensive use of renewable materials with responsible sourcing practices): Assesses the percentage of raw materials sourced from renewable sources, the implementation of responsible sourcing policies, and efforts to diversify the sourcing of renewable materials.

Environmental Compliance (0-0.3: significant noncompliance issues; 0.4-0.7: some compliance challenges; 0.8-1.0: full compliance with environmental regulations and implementation of robust management systems): Evaluates the company's compliance with environmental regulations and permits, the implementation of environmental management systems, and the effectiveness of monitoring and auditing procedures.

Water Consumption (0-0.3: high water consumption with limited reduction efforts; 0.4-0.7: moderate water consumption with some water-saving initiatives; 0.8-1.0: minimal water consumption with comprehensive water stewardship programs): Assesses the volume of water withdrawal, the implementation of water-saving measures, and the company's participation in water stewardship initiatives.

2. Social Indicators: This category assesses the company' social responsibility and its impact on employees, communities, and other stakeholders. The scoring considerations for each social indicator are as follows:

Employee Satisfaction (0-0.3: low satisfaction with limited engagement; 0.4-0.7: moderate satisfaction with some initiatives to improve well-being; 0.8-1.0: high satisfaction with comprehensive programs and a focus on work–life balance): Evaluates the level of employee satisfaction, the existence and effectiveness of employee

engagement programs, and the company's efforts to promote work–life balance and well-being.

Employee Training and Development (0-0.3: limited training opportunities; 0.4-0.7: moderate training programs with some focus on skills development; 0.8-1.0: extensive training opportunities covering a wide range of topics, including sustainability and leadership): Assesses the availability and scope of employee training programs, covering technical and soft skills development, leadership training, and sustainability awareness.

Serious and Fatal Accidents (0-0.3: high incidence of accidents and fatalities; 0.4-0.7: moderate accident rate with some safety programs in place; 0.8-1.0: very low accident rate with a strong safety culture and commitment to zero harm): Evaluates the company's safety performance based on the frequency and severity of accidents and fatalities, the existence and effectiveness of safety programs, and the company's commitment to achieving a zero-harm workplace.

Employee Health and Well-being (0-0.3: limited or no health and well-being programs; 0.4-0.7: Basic health and safety programs with some focus on well-being; 0.8-1.0: Comprehensive health and well-being programs with a focus on mental and physical health): Assesses the availability and comprehensiveness of health and well-being programs, including mental health support, health screenings, and initiatives promoting healthy lifestyles.

Child Labor Policies (0-0.3: evidence of child labor practices; 0.4-0.7: limited or ineffective policies; 0.8-1.0: zero-tolerance policy for child labor with comprehensive monitoring and enforcement mechanisms): Evaluates the company's policies on child labor, its adherence to international standards, and the effectiveness of monitoring and enforcement mechanisms within the company and its supply chain.

Management of Community Impacts (eg noise, dust) (0-0.3: significant negative community impacts; 0.4-0.7: moderate community impacts with some mitigation efforts; 0.8-1.0: minimal community impacts with proactive engagement and effective mitigation measures): Assesses the company's impact on surrounding communities, particularly relating to noise, dust, and other potential environmental disturbances, and its efforts to mitigate those impacts and engage with communities.

Business Ethics and Transparency (0-0.3: evidence of unethical or corrupt practices; 0.4-0.7: limited or ineffective policies; 0.8-1.0: strong ethical principles and transparent reporting on business practices and governance): Evaluates the company's commitment to ethical business practices, the existence and implementation of anticorruption policies, and the level of transparency in reporting on business conduct and governance structures.

3. Economic Indicators: This category evaluates the company' economic performance and their contributions to sustainable economic development. The scoring considerations are:

Sales Revenue (N/A): Evaluating sales revenue as a sustainability indicator necessitates a detailed contextual analysis, including industry specifics and economic conditions, making a direct score assignment challenging.

Operating Profit (N/A): Similar to sales revenue, assessing operating profit as a sustainability indicator requires a nuanced understanding of the business environment and industry benchmarks.

Net Profit (N/A): Evaluating net profit within a sustainability context requires a holistic analysis of the company's financial performance and its alignment with sustainable business practices.

Tax Payments (0-0.3: tax avoidance or evasion practices; 0.4-0.7: basic compliance with tax regulations; 0.8-1.0: transparent reporting on tax payments and contributions to local economies): Assesses the company's tax practices, including transparency in reporting, compliance with regulations, and contributions to local economies through tax payments.

Operational Costs and Expenses (N/A): Evaluating operational costs and expenses requires a detailed understanding of the business model, industry specifics, and cost structures, making a standardized score assignment challenging.

Wages and Market Standards (0-0.3: evidence of unfair labor practices or below-standard wages; 0.4-0.7: basic compliance with wage regulations; 0.8-1.0: fair compensation exceeding legal and industry standards, promoting employee well-being): Assesses the company's compensation practices, adherence to wage regulations, and efforts to promote employee well-being through fair and competitive wages and benefits.

Local Suppliers (0-0.3: minimal or no engagement with local suppliers; 0.4-0.7: moderate engagement with some local sourcing; 0.8-1.0: high engagement with local suppliers, fostering local economic development and resilient supply chains): Evaluates the company's engagement with local suppliers, the percentage of procurement from local sources, and the impact of sourcing practices on local economic development and supply chain resilience.

Data Collection and Analysis

This study employed a mixed-methods approach, combining qualitative analysis with a quantitative scoring system to facilitate a comparative assessment of sustainability performance across the four selected companies.

The data collection process involved a comprehensive review of publicly available data from multiple sources for each company. These sources included:

2022 Sustainability Reports: Integrated reports, standalone sustainability reports, and other relevant company disclosures.

Corporate Websites: Sustainability sections and related information on company websites.

Third-Party Platforms: Independently verified data submitted to platforms such as Carbon Disclosure Project (CDP).

This triangulation approach utilized multiple sources of data to mitigate potential biases and enhance the reliability of the assessment.

The analysis focused on identifying key sustainability initiatives, strategies, and performance data related to the established environmental, social, and economic indicators. For each indicator, the researchers conducted a thorough qualitative assessment of the company's performance, considering various factors, including:

Scope and Scale of Initiatives: The breadth and depth of the company's sustainability initiatives and programs.

Transparency and Data Disclosure: The level of detail and comprehensiveness of the information provided in company disclosures.

Progress Toward Stated Goals: Company' progress in achieving its stated sustainability targets and commitments.

Alignment with Industry Trends and Best Practices: The extent to which company' activities aligned with broader industry trends and international best practices in sustainability.

Performance for each indicator was then assigned a score on a scale of 0 to 1, with 0 representing the lowest possible performance and 1 representing the highest possible performance. This scoring system, while acknowledging its inherent limitations, facilitated a standardized comparison of company performance across different indicators and enabled the identification of areas of strength and weakness within each company' sustainability profile.

The analysis also involved a comparative assessment of the four companies, examining similarities and differences in their sustainability approaches, challenges faced, and opportunities identified. This comparative perspective, informed by both the qualitative assessment and the quantitative scoring system, allowed for a deeper understanding of the diverse sustainability landscape within the paper and packaging industry, highlighting best practices that can be adopted or adapted by other companies within the sector.

FINDINGS

Environmental Sustainability

The paper and packaging industry has significant environmental impacts throughout its value chain,

from raw material sourcing to production processes and waste management (Jones and Comfort 2017).

The commitment of Mondi Group to environmental sustainability was evident across multiple facets of its operations. The company demonstrated exemplary performance in waste management, achieving a score of 0.8 for waste disposal practices. This is due to a 44% reduction in waste sent to landfills since 2020. This was further evidenced by their 0.9 score for recycling waste, which reflected a 74% recycling/reuse rate for production waste and ongoing efforts to identify innovative solutions for remaining waste streams. Furthermore, Mondi's commitment to transitioning toward renewable energy sources was evidenced by its score of 0.8, which reflected its utilization of 78% renewable energy sources and its continued investments in energy self-sufficiency. Nevertheless, the analysis also indicates the necessity for further attention in certain areas. A score of 0.6 for effluent treatment indicated the need to implement of enhanced strategies to manage effluent load, particularly in light of the recent increases in chemical oxygen demand levels. Similarly, while the company was engaged in reducing air emissions and has made progress in mitigating NOx emissions, a score of 0.7 for atmospheric emissions indicated that further efforts are necessary to minimize the overall air quality impacts. Despite these challenges, Mondi's proactive approach to environmental management, including adherence to ISO 14001 standards and ongoing water stewardship initiatives, indicated a commitment to minimizing its environmental footprint and progressing toward a more sustainable future (Table 1).

Kartonsan's environmental performance presented a multifaceted picture, showcasing notable strengths alongside areas necessitating further development. The company demonstrated exceptional performance in waste management, achieving a score of 0.9 for waste recycling. This was due to the 91% utilization of waste paper in coated cardboard production. This achievement, which exceeded European averages, positioned Kartonsan as a leader in circular economy practices within the industry. Furthermore, company' commitment to responsible waste disposal was reflected in a score of 0.8, driven by its "Zero Waste Certificate" and a comprehensive waste management system that prioritized waste reduction, recycling, and responsible disposal of remaining waste streams. Similarly, Kartonsan's focus on water resource management was commendable, achieving a score of 0.8 through the utilization of modern wastewater treatment techniques and the successful implementation of water recovery and reuse initiatives, which have led to a 24% reduction in freshwater consumption. Nevertheless, the analysis also revealed areas that required additional focus and improvement. Although the report acknowledged the importance of controlling greenhouse gas emissions and mentioned measurement and reporting of Scope 1 emissions, the lack of specific reduction targets

Table 1. Environmental indicators used to assess the four Turkish paper and packaging companies.[a]

Environmental indicator	Mondi Group	Kartonsan	Duran Dogan	Viking Kağıt
A1 - Hazardous Waste Generation	0.7	0.7	0.7	0.7
A2 - Waste Disposal	0.8	0.8	0.9	0.9
A3 - Treatment of Effluents	0.6	0.8	0.8	0.7
A4 - Recycling of Waste	0.9	0.9	0.9	0.9
A5 - Atmospheric Emissions	0.7	0.6	0.9	0.7
A6 - Recycling and Reuse of Products	0.9	0.9	0.8	0.9
A7 - Renewable Energy	0.8	0.4	0.5	0.4
A8 - Energy Efficiency	0.7	0.7	0.7	0.7
A9 - Renewable Materials	0.8	0.9	0.7	0.8
A10 - Environmental Compliance	0.8	0.8	0.9	0.9
A11 - Water Consumption	0.7	0.7	0.7	0.7

[a]Values range from 0 (poor) to 1.0 (high) for each parameter.

and strategies resulted in a score of 0.6 for atmospheric emissions. Furthermore, company' current reliance on conventional energy sources, primarily natural gas, for its operations resulted in a score of 0.4 for renewable energy. The planned establishment of a biomass energy plant in 2024 represented a positive step toward the transition to more sustainable energy sources in the future (Table 1).

Duran Dogan's commitment to environmental sustainability was evident across multiple facets of its operations, showcasing a promising trajectory toward a more sustainable future. The company excelled in waste management and circular economy practices, achieving scores of 0.9 for both waste disposal and recycling of waste. Similar to the observations of Jones and Comfort (2017) regarding leading global companies, the four companies examined in this study demonstrated a pronounced focus on waste management and circular economy principles. For instance, Duran Dogan's "Gloss&Green" technology, which eliminated plastic film lamination and promoted recyclability, aligned with the industry-wide trend toward developing sustainable packaging solutions. This technology eliminates the need for plastic film lamination in packaging, resulting in fully recyclable cardboard products, and facilitates the recycling of PET film waste into valuable raw materials for the plastic industry, contributing significantly to circularity and resource conservation. Duran Dogan also demonstrated a strong commitment to responsible water management, achieving a score of 0.8 for effluent treatment through investments in advanced water treatment plants and ongoing efforts to improve water efficiency. Duran Doğan, the inaugural packaging company in Turkey to pledge adherence to international standards for greenhouse gas emissions reporting, was the sole Turkish packaging company to be included in the CDP (Carbon Disclosure Project) 2013 Global 500 report and was bestowed with the CDP Turkey 1st place award. Carbon footprint calculations were conducted annually, encompassing Scope 1, Scope 2, and Scope 3, and were subjected to verification and subsequent reporting to CDP. However, the analysis also revealed areas where further progress was needed to fully realize company' sustainability ambitions. While Duran Dogan is taking positive steps toward renewable energy adoption through investments in solar panels and plans for future renewable energy procurement, its current reliance on conventional energy sources reduced the score for renewable energy to 0.5. While Duran Dogan has established a solid foundation for environmental sustainability, continued efforts and strategic investments are necessary to achieve its ambitious climate goals and fully transition to a low-carbon and circular economy model (Table 1).

Viking Kağıt demonstrated a strong commitment to environmental sustainability, particularly excelling in the areas of waste management and resource recovery. Company' dedication to circular economy principles was evidenced by scores of 0.9 for both waste disposal and recycling of waste. These achievements highlighted Viking Kağıt's leadership in minimizing waste and maximizing resource utilization within its operations. The implementation of a comprehensive waste management system, culminating in the "Zero Waste Certificate," underscored the proactive approach to waste reduction, recycling, and responsible disposal of remaining waste streams. Furthermore, Viking Kağıt's innovative Recyfiber® technology exemplified its commitment to circularity by utilizing recycled beverage cartons to produce eco-friendly tissue paper products, thereby closing the loop and creating value from waste materials. The company also demonstrated responsible water management practices, earning a score of 0.7 for the treatment of effluents. This score reflects adherence to discharge regulations and a significant 30% reduction in its water footprint since the base year 2014; indicating ongoing efforts to conserve water resources. In terms of climate action, Viking Kağıt achieved a score of 0.7 for atmospheric emissions by actively monitoring and reporting its Scope 1 and 2 greenhouse gas emissions, achieving a notable 33% reduction compared with the base year 2010. Although these achievements are commendable, the analysis also

identified opportunities for further enhancing environmental performance. A score of 0.4 for renewable energy underscores the need for increased integration of renewable energy sources within company' operations to further reduce reliance on conventional energy and minimize its carbon footprint. Additionally, expanding the scope of emissions reporting to encompass Scope 3 emissions and developing comprehensive strategies for emissions reductions across the entire value chain are crucial next steps toward achieving greater environmental sustainability and contributing to global climate action goals (Table 1).

While Jones and Comfort (2017) observed variations in company' commitment to climate action, the companies in this study collectively demonstrated a degree of progress toward renewable energy adoption and emissions reductions. This suggested a potential shift within the Turkish paper and packaging industry toward greater emphasis on addressing climate change.

Furthermore, as highlighted by Vivas et al (2024), the global trend toward digitalization is leading to a decline in the availability of recycled paper, posing a significant challenge for the paper industry. This is particularly relevant for the Turkish context, where securing a sustainable supply of raw materials is crucial for the long-term viability of the paper and packaging sector. Moreover, the exploration of alternative fibers, such as agricultural residues or fast-growing plants, as proposed by Pydimalla et al (2023), becomes imperative to mitigate the risk of supply chain disruptions and ensure the continued growth of the industry while minimizing its environmental impact.

Social Sustainability

Mondi Group's approach to social responsibility demonstrates a multifaceted commitment to its employees, communities, and ethical business practices, as revealed through a comprehensive assessment using established social sustainability indicators. Company' efforts to cultivate a positive and enriching work environment for its employees were reflected in a score of 0.75 for employee satisfaction. This score acknowledged the generally positive feedback regarding opportunities for development, a sense of purpose, and overall work–life balance, while also recognizing the need for continued improvement in areas such as inclusivity and psychological safety. Mondi's dedication to fostering employee growth and development was further evidenced by a score of 0.8, highlighting significant investments in upskilling programs, leadership development initiatives, and specialized training on sustainability and safety. Commitment to ethical business practices was also noteworthy, earning a score of 0.9 due to its robust Code of Business Ethics, comprehensive anticorruption policies, and the implementation of the SpeakOut platform, a confidential grievance mechanism accessible to both employees and external stakeholders, ensuring a safe and secure environment for raising concerns. Despite these commendable efforts, the analysis identified areas requiring further attention and improvement. A score of 0.5 for serious and fatal accidents underscored the critical need for continued efforts to enhance safety performance and strive toward the company's zero-harm target. While Mondi actively promotes health and well-being initiatives and provides access to health services and Employee Assistance Programs, a score of 0.7 suggests that further development and expansion of these programs will be essential to ensure comprehensive and accessible support for employee well-being, both physically and mentally (Table 2).

Kartonsan's approach to social responsibility presented a complex picture, with notable strengths in employee development and ethical business practices alongside challenges in employee relations and safety performance. The company demonstrated a commendable dedication to fostering employee growth and expertise, achieving a score of 0.8 for employee training and development. This score reflected Kartonsan's investment in comprehensive training programs covering diverse areas such as technical skills development, occupational health and safety, sustainability awareness, and leadership training, highlighting a commitment to employee upskilling and long-term employability. Furthermore, the company

Table 2. Social indicators used to assess the four Turkish paper and packaging companies.[a]

Social indicator	Mondi Group	Kartonsan	Duran Dogan	Viking Kağıt
S1 - Employee Satisfaction	0.7	0.6	0.7	0.7
S2 - Employee Training and Development	0.8	0.8	0.8	0.8
S3 - Serious and Fatal Accidents	0.5	0.6	0.7	0.8
S4 - Employee Health Evaluation	0.7	0.7	0.7	0.7
S5 - Child Labor	1.0	1.0	1.0	1.0
S6 - Dust Complaints	0.8	0.7	0.7	0.8
S7 - Business Ethics	0.9	0.8	0.8	0.8

[a]Values range from 0 (poor) to 1.0 (high) for each parameter.

reported a strong commitment to ethical business practices, earning a score of 0.8 due to adherence to legal requirements, transparency in reporting, and implementation of ethical guidelines and policies. Kartonsan's proactive approach to uphold human rights and ensure fair labor practices was further evidenced by its perfect score of 1.0 for its zero-tolerance policy against child labor. The analysis also revealed challenges that require attention and improvement. A score of 0.6 for employee satisfaction pointed to potential concerns regarding employee relations and overall satisfaction with working conditions or compensation, particularly considering an ongoing strike initiated by the labor union representing a significant portion of the workforce. Additionally, while Kartonsan prioritized occupational health and safety and operated under the ISO 45001 standard, a score of 0.6 for serious and fatal accidents highlighted the need for continued efforts to enhance safety performance and strive toward the zero-harm target (Table 2).

Duran Dogan's approach to social responsibility revealed a multifaceted commitment to its employees, ethical business practices, and fostering a safe and healthy work environment. Dedication to employee development and upskilling was reflected in a score of 0.8 for employee training and development, highlighting its investment in comprehensive training programs that covered diverse areas such as technical skills, sustainability awareness, leadership development, and responsible supply chain practices. This focus on continuous learning and development not only enhances employee expertise but also contributes to long-term employability and career advancement opportunities within the organization. Furthermore, Duran Dogan demonstrated a strong commitment to ethical business practices, earning a score of 0.8 due to its adherence to ethical labor principles, implementation of a "ethical policy" system for reporting violations, and its proactive approach to upholding human rights across its operations and supply chain. This commitment was further evidenced by its perfect score of 1.0 for its zero-tolerance policy against child labor, ensuring the protection of vulnerable individuals and adherence to responsible labor practices. The focus on occupational health and safety was also noteworthy, achieving a score of 0.7 due to its ISO 45001 certification and implementation of comprehensive safety measures and training programs. Despite these commendable efforts, the analysis identified limitations in available data, particularly concerning employee satisfaction. Although the company' focus on employee engagement and well-being initiatives suggested a positive work environment, the lack of detailed data on employee satisfaction surveys limited a more thorough assessment of employee morale, engagement, and overall satisfaction with working conditions and compensation. Addressing this data gap and actively engaging with employees to understand their needs and concerns will be crucial for Duran Dogan to further enhance its social performance and create a truly inclusive and supportive work environment (Table 2).

Viking Kağıt's approach to social responsibility revealed a strong commitment to its employees, fostering a safe and healthy work environment, and upholding ethical business practices. Company' dedication to employee development and

upskilling was reflected in a score of 0.8 for employee training and development. This score highlighted investment in comprehensive training programs spanning various areas, including technical skills, sustainability awareness, leadership development, and responsible supply chain practices. This emphasis on continuous learning not only enhanced employee expertise and adaptability but also contributed to long-term employability and created opportunities for career advancement within the organization. Furthermore, Viking Kağıt demonstrated a commitment to occupational health and safety, achieving a score of 0.8. This score reflected the proactive approach to managing workplace safety through risk assessments, implementation of preventive measures, and comprehensive safety training programs for both employees and contractors. The absence of reported significant incidents or accidents further suggested a strong safety culture embedded within operations. Additionally, adherence to ethical business practices, including a zero-tolerance policy for child labor, contributes to a score of 0.8 in this category. This commitment aligned with Yaşar Holding's broader dedication to responsible business conduct and respect for human rights throughout its subsidiaries and supply chains. Despite these positive findings, the analysis also identified a need for increased transparency and data disclosure to facilitate a more comprehensive assessment of social performance. While the focus on employee engagement and well-being initiatives suggested a positive work environment, the limited availability of specific data on employee satisfaction surveys prevented a more thorough evaluation of employee morale, engagement levels, and overall satisfaction with working conditions and compensation. Similarly, while the company's alignment with Yaşar Holding's commitment to diversity and inclusion indicated a positive direction, the lack of specific data on diversity and inclusion initiatives limited a comprehensive assessment of its progress and effectiveness in promoting a diverse and inclusive workplace. Addressing these data gaps and actively engaging with employees to understand and respond to their needs and concerns will be crucial for Viking Kağıt to further enhance its social performance and build a truly inclusive and equitable work environment for all (Table 2).

Our study found that the participating companies demonstrated a consistent commitment to fair compensation and positive employee relations. All four companies adhered to collective bargaining agreements with relevant labor unions, ensuring that employee wages and benefits were negotiated fairly and transparently. This emphasis on equitable labor practices was crucial, as working conditions within the forest, paper, and packaging industry could significantly impact employee satisfaction and overall organizational performance. Research indicated that conducive working conditions, including fair remuneration and opportunities for professional development, were essential for fostering job satisfaction (Arokiasamy 2019; Mo & Borbon 2022). Conversely, inadequate support from management, limited opportunities for intellectual growth, or generally poor working conditions could contribute to employee dissatisfaction and increased turnover intentions (Herliana et al 2021). This was particularly relevant in labor-intensive industries like forest, paper, and packaging, where employee morale directly influenced productivity and, ultimately, the quality of products and services delivered (Heimerl et al 2020; Bañuls et al 2018).

Economic Sustainability

Mondi Group's approach to economic sustainability demonstrated a commitment to responsible practices that contributed to the well-being of local communities and upheld fair labor standards, as revealed through the analysis of key economic sustainability indicators. Dedication to transparency and accountability in its tax practices was reflected in a score of 0.8 for tax payments, highlighting its significant contributions to local economies through responsible tax contributions. Furthermore, Mondi's commitment to fair compensation was evidenced by a score of 0.8 for wages and market standards, underscoring its adherence to legal and industry benchmarks for wages and benefits, ensuring fair and equitable treatment of its employees. Mondi's prioritization

of local sourcing further strengthened its economic sustainability performance, earning a score of 0.8 for its emphasis on procuring goods and services from local suppliers. This focus on local procurement not only contributed to local economic development but also fostered community resilience and promoted sustainable supply chains. However, the analysis acknowledged limitations in available data, particularly concerning metrics such as sales revenue, operating profit, and net profit. Assessing the sustainability implications of these indicators will require a more nuanced understanding of industry-specific benchmarks, economic contexts, and overall financial performance about its sustainable business practices (Table 3).

Kartonsan's approach to economic sustainability also revealed a commitment to responsible practices that contributed to the economic well-being of local communities and upheld fair labor standards. Dedication to transparency and accountability in its tax contributions was reflected in a score of 0.8 for tax payments, highlighting its significant role as a contributor to the Turkish economy and its support for public services and infrastructure through responsible tax practices. Furthermore, Kartonsan demonstrated a commitment to fair compensation, earning a score of 0.7 for wages and market standards. Adherence to legal and industry benchmarks for wages and benefits, ensuring equitable treatment of its employees while also recognizing potential areas for improvement, particularly in light of the ongoing labor strike related to negotiations for a new collective bargaining agreement. Kartonsan's prioritization of local sourcing further strengthened its economic sustainability performance, achieving a score of 0.8 for its emphasis on procuring goods and services from local suppliers. This focus on local procurement not only stimulates local economic development and job creation but also fosters community resilience and promotes sustainable supply chain practices by reducing transportation distances and associated environmental impacts. However, the analysis acknowledged limitations in available data, particularly concerning metrics such as sales revenue, operating profit, and net profit. A more comprehensive evaluation of Kartonsan's overall economic sustainability performance would require a deeper understanding of these financial indicators within the context of industry-specific benchmarks, economic fluctuations, and the strategic alignment of financial performance with sustainable business practices (Table 3).

Duran Dogan's approach to economic sustainability also revealed a multifaceted commitment to responsible financial practices, fair labor standards, and contributions to local economic development. The company demonstrated transparency and accountability in its tax contributions, receiving a score of 0.8 for tax payments, highlighting its role as a responsible corporate citizen and its support for public services and infrastructure development within the Turkish economy. Furthermore, Duran Dogan's commitment to local sourcing was evident in its score of 0.8 for prioritizing procurement from local suppliers. This practice not only stimulates local economic growth and job creation but also fosters resilient supply chains by reducing dependence on long-distance transportation, thereby minimizing

Table 3. Economic indicators used to assess the four Turkish paper and packaging companies.[a]

Economic indicator	Mondi Group	Kartonsan	Duran Dogan	Viking Kağıt
E1 - Sales Revenue	N/A	N/A	N/A	N/A
E2 - Operating Profit	N/A	N/A	N/A	N/A
E3 - Net Profit	N/A	N/A	N/A	N/A
E4 - Tax Payments	0.8	0.8	0.8	0.8
E5 - Operational Costs and Expenses	N/A	N/A	N/A	N/A
E6 - Wages and Market Standards	0.8	0.7	0.7	0.7
E7 - Local Suppliers	0.8	0.8	0.8	0.7

[a]Values range from 0 (poor) to 1.0 (high) for each parameter.

associated environmental impacts and promoting regional economic development. Although the focus on employee well-being and ethical labor practices suggested an inherent commitment to fair compensation, the lack of specific data on wages and benefits limited a comprehensive assessment in this area. A score of 0.7 was assigned for wages and market standards, acknowledging the potential need for increased transparency and disclosure regarding employee compensation practices. Additionally, the analysis recognized limitations in the available data concerning metrics such as sales revenue, operating profit, and net profit. Evaluating these financial indicators within the context of sustainable business practices necessitates a more nuanced understanding of industry-specific benchmarks, economic fluctuations, and strategic alignment of financial performance with long-term sustainability goals. Future research and reporting should focus on providing a more comprehensive and contextualized analysis of these economic indicators to fully assess Duran Dogan's overall contribution to sustainable economic development (Table 3).

Viking Kağıt's approach to economic sustainability demonstrated a commitment to responsible financial practices, fostering local economic development, and upholding fair labor standards. Dedication to transparency and accountability in its tax contributions is reflected in a score of 0.8 for tax payments, signifying its role as a responsible corporate citizen and its contribution to supporting public services and infrastructure development within the Turkish economy. Furthermore, Viking Kağıt's emphasis on local sourcing, particularly for materials and services other than virgin pulp, which is primarily imported due to limited domestic availability, contributed to a score of 0.7 for supporting local economies and fostering resilient supply chains. This preference for local procurement not only stimulates regional economic growth and job creation but also reduces the environmental impacts associated with long-distance transportation, thereby promoting both economic and environmental sustainability. Although specific data on wages and benefits was limited, Viking Kağıt's adherence to a collective bargaining agreement with the Selüloz-İş union and its alignment with Yaşar Holding's commitment to ethical labor practices suggested fair compensation for its employees. However, a score of 0.7 was assigned for wages and market standards to acknowledge the potential need for increased transparency and disclosure regarding specific wage structures and benefits provided to employees. The analysis further recognized limitations in the available data concerning overall financial performance. Evaluating metrics such as sales revenue, operating profit, and net profit within the context of sustainable business practices necessitates a more nuanced understanding of industry-specific benchmarks, economic fluctuations, and the company's strategic alignment of financial performance with long-term sustainability goals. Providing greater transparency and disclosure regarding these financial indicators and demonstrating how financial success translates into positive social and environmental impacts would enable a more holistic assessment of Viking Kağıt's contribution to sustainable economic development and its overall commitment to creating shared value for all stakeholders (Table 3).

CONCLUSIONS

Comparative analysis of the sustainability performance of the four companies revealed a diverse approach to sustainability within the Turkish paper and packaging industry. While the companies all demonstrated a commitment to environmental and social responsibility, their performance and areas of emphasis varied, likely influenced by factors such as company size, access to resources, and specific product lines.

All four companies exhibited a strong commitment to waste management and circular economy principles. This shared focus was evident in Mondi Group's achievement of a 44% reduction in waste to landfill since 2020; Kartonsan's 91% utilization of wastepaper in its coated cardboard production, Duran Dogan's development of "Gloss&Green" technology, and Viking Kağıt's innovative Recyfiber® technology, which utilizes

recycled beverage cartons. These initiatives align with the industry's growing recognition of the environmental and economic benefits of minimizing waste and maximizing resource recovery.

However, company approaches to energy management and carbon emissions reduction varied. While Mondi Group and Duran Dogan have established ambitious science-based targets for emissions reduction, Kartonsan and Viking Kağıt primarily focused on energy efficiency and responsible sourcing. This difference highlighted a potential challenge for the Turkish paper and packaging industry: balancing the cost-competitiveness of conventional energy sources with the need to transition to renewables to achieve more significant emissions reductions.

The analysis also revealed variations in social performance. Mondi Group stood out with its comprehensive approach to employee well-being, actively measuring employee satisfaction, promoting diversity and inclusion, and implementing a robust grievance mechanism. Although the other companies demonstrated commitment to fair labor practices and employee training, the limited data on employee satisfaction and diversity initiatives made it difficult to comprehensively assess their social performance.

Furthermore, this study highlighted industry progress toward adopting circular bioeconomy principles, as evidenced by initiatives such as using recycled content, developing biodegradable materials, and investing in waste reduction strategies. However, the decline in the availability of recycled paper, presents a challenge, particularly in the Turkish context. Exploring alternative fibers, such as agricultural residues or fast-growing plants may be necessary to mitigate supply chain risks and ensure the industry's long-term sustainability.

This research underscored the importance of transparency and data disclosure in driving sustainable practices within the paper and packaging industry. Although Mondi Group provided comprehensive data, the other companies offered limited information on how their economic performance translated into positive social and environmental impacts. Adopting integrated reporting frameworks that connect financial performance with environmental and social outcomes can enhance transparency and demonstrate the value of a holistic approach to sustainability.

While the results are based on company-reported data, they offer valuable insights into the current state of sustainability in the Turkish paper and packaging industry and illuminate key areas for future research. Further investigation into the economic feasibility and scalability of circular economy solutions, the social implications of a circular bioeconomy, and the role of policy in driving industry-wide sustainability improvements is warranted. Moreover, exploring emerging technologies to enhance transparency and traceability within the supply chain can contribute to a more responsible and sustainable paper and packaging industry.

Future Research Directions

Building upon the findings of this comparative analysis, several avenues for future research emerge. Investigating the economic feasibility and scalability of circular economy solutions within the Turkish paper and packaging industry is crucial, exploring factors, such as investment costs, technological advancements, and consumer acceptance. Further research could also delve deeper into the social implications of the transition to a circular bioeconomy, examining its impact on employment, community development, and social equity within the sector. Additionally, exploring the role of policy interventions in incentivizing sustainable practices and promoting industry-wide collaboration on resource efficiency and emissions reduction presents a significant research opportunity. Moreover, investigating the potential of emerging technologies, such as blockchain and artificial intelligence, to enhance transparency and traceability within the paper and packaging supply chain could provide valuable insights for promoting responsible sourcing and ethical production practices. Finally, comparative studies expanding the scope to encompass other emerging economies could shed light on the broader challenges and opportunities associated with

sustainable development within the global paper and packaging industry.

REFERENCES

Aithal S, Shenoy P (2016) A study on history of paper and possible paper free world. https://doi.org/10.5281/ZENODO.161141.

Arokiasamy ARA (2019) Exploring the internal factors affecting job satisfaction in the fast-food industry in Malaysia. International Journal of Advanced and Applied Sciences 6(11): 11-20. https://doi.org/10.21833/ijaas.2019.11.003.

Baetge S, Martin K (2018) Rice straw and rice husks as energy sources—Comparison of direct combustion and biogas production. Biomass Conv Bioref 8(3):719-737. https://doi.org/10.1007/s13399-018-0321-y.

Bañuls AL, Casado-Díaz JM, Simón H (2018) Examining the determinants of job satisfaction among tourism workers. Tourism Economics 24(8): 980-997. https://doi.org/10.1177/1354816618785541.

Deshwal GK, Panjagari NR, Alam T (2019) An overview of paper and paper based food packaging materials: Health safety and environmental concerns. J Food Sci Technol 56(10):4391-4403. https://doi.org/10.1007/s13197-019-03950-z.

Fadeyibi A, Osunde ZD, Egwim EC, Idah PA (2017) Performance evaluation of cassava starch-zinc nanocomposite film for tomatoes packaging. J Agricult Engineer 48. https://doi.org/10.4081/jae.2017.565.

Feil AA, Muller de QD, Schreiber D (2015) Selection and identification of the indicators for quickly measuring sustainability in micro and small furniture industries. Sustainable Production and Consumption 3: 34-44. ISSN 2352-5509, https://doi.org/10.1016/j.spc.2015.08.006.

Feil AA, Muller de QD, Schreiber D (2017) An analysis of the sustainability index of micro- and small-sized furniture industries. Clean Techn Environ Policy 19: 1883-1896. https://doi.org/10.1007/s10098-017-1372-7.

Feil, A.A., De Brito RI, Oberherr R, et al. (2022) Analysis and measurement of the sustainability level in the furniture industry. Environ Dev Sustain 24:13657-13682. https://doi.org/10.1007/s10668-021-02005-8.

Fitch-Vargas PR, Camacho-Hernández IL, Martínez-Bustos F, Islas-Rubio AR, Carrillo-Cañedo KI, Calderón-Castro A, Jacobo-Valenzuela N, Carrillo-López A, Delgado-Nieblas CI, Aguilar-Palazuelos E (2019) Mechanical, physical and microstructural properties of acetylated starch-based biocomposites reinforced with acetylated sugarcane fiber. Carbohydr Polym 219:378-386. https://doi.org/10.1016/j.carbpol.2019.05.043.

Heimerl P, Haid M, Benedikt L, Scholl-Grissemann U (2020) Factors influencing job satisfaction in hospitality industry. SAGE Open 10(4): 215824402098299. https://doi.org/10.1177/2158244020982998.

Herliana NF, Handaru AW, Parimita W (2021) The effect of job satisfaction and work-life balance on employee turnover intention in real estate industry. Jurnal Dinamika Manajemen Dan Bisnis, 4(2): 45-68. https://doi.org/10.21009/jdmb.04.2.3.

Jiang Y, Wu Q, Wei Z, Wang J, Fan Z, Pang Z, Zhu Z, Zheng S, Lin X, Chen Y (2019) Papermaking potential of *Pennisetum hybridum* fiber after fertilizing treatment with municipal sewage sludge. J Clean Prod 208:889-896. https://doi.org/10.1016/j.jclepro.2018.10.14.

Jones P, Comfort D (2017) The forest, paper and packaging industry and sustainability. Int J Sale Retail Mark 6 (1):3-21.

Karlovits I (2020) Lignocellulosic bio-refinery downstream products in future packaging applications. Int Symp Graph Eng Des:39-53. https://doi.org/10.24867/GRID-2020-p2.

Le Quyen TT (2023) The impact of COVID-19 on packaging design and production: A case study. KnE Soc Sic 8(20):453-467. https://doi.org/10.18502/kss.v8i20.14620.

Lewandowska A, Witczak J, Kurczewski P (2017) Green marketing today: A mix of trust, consumer participation and life cycle thinking. Management 21(2):28-48. https://doi.org/10.1515/manment-2017-0003.

Li M-C, Lee JK, Cho UR (2012) Synthesis, characterization, and enzymatic degradation of starch-grafted poly(methyl methacrylate) copolymer films. J Appl Polym Sci 125(1): 405-414. https://doi.org/10.1002/app.35620.

Liyanage S, Acharya S, Parajuli P, Shamshina JL, Abidi N (2021) Production and surface modification of cellulose bioproducts. Polymers (Basel) 13(19):3433. https://doi.org/10.3390/polym13193433.

Pydimalla P, Chirravuri HV, Uttaravalli AN (2023) An overview on non-wood fiber characteristics for paper production: Sustainable management approach. Mater Today Proc https://doi.org/10.1016/j.matpr.2023.08.278.

Mattila TJ, Judl J, Macombe C, Leskinen P (2018) Evaluating social sustainability of bioeconomy value chains through integrated use of local and global methods. Biomass Bioenergy 109:276-283. https://doi.org/10.1016/j.biombioe.2017.12.019.

Méndez A, Fidalgo JM, Guerrero F, Gasćo G (2009) Characterization and pyrolysis behaviour of different paper mill waste materials. J Anal Appl Pyrolysis 86(1): 66-73. https://doi.org/10.1016/j.jaap.2009.04.004.

Mo Y, Borbon NMD (2022) Interrelationship of total quality management (tqm), job satisfaction and organizational commitment among hotel employees in zhejiang and hainan provinces in china towards a sustainable development framework. International Journal of Research Studies in Management, 10(3). https://doi.org/10.5861/ijrsm.2022.31.

Nanda S, Patra BR, Patel R, Bakos J, Dalai AK (2022) Innovations in applications and prospects of bioplastics and biopolymers: A review. Environ Chem Lett 20(1): 379-395. https://doi.org/10.1007/s10311-021-01334-4.

Neis FA, de Costa F, de Araújo AT, Fett JP, Fett-Neto AG (2019) Multiple industrial uses of non-wood pine products. Ind Crop Prod 130:248-258. https://doi.org/10.1016/j.indcrop.2018.12.088.

Otieno JO, Okumu TN, Adalla M, Ogutu F, Oure B (2021) Agricultural residues as an alternative source of fibre for the production of paper in Kenya: A review. Asian J Chem Sci 10(1):22-37. https://doi.org/10.9734/ajocs/2021/v10i119084.

Parguel B, Benoît-Moreau F, Larceneux F (2011) How sustainability ratings might deter 'greenwashing': A closer look at ethical corporate communication. J Bus Ethics 102(1):15-28. https://doi.org/10.1007/s10551-011-0901-2.

Shaghaleh H, Xu X, Wang S (2018) Current progress in production of biopolymeric materials based on cellulose, cellulose nanofibers, and cellulose derivatives. RSC Adv 8(2):825-842. https://doi.org/10.1039/C7RA11157F.

Skene J, Vinyard S (2019) The issue with tissue: How Americans are flushing forests down the toilet. NRDC, pp. 1-30. www.stand.earth. (4 March 2024).

Tajeddin B, (2014) Cellulose-based polymers for packaging applications. In Lignocellulosic polymer composites: Processing, characterization, and properties; Scrivener Publishing LLC: Beverly, MA, USA, pp. 477-498. ISBN 978-1-118-77357-4.

Travalini AP, Lamsal B, Magalhães WLE, Demiate IM (2019) Cassava starch films reinforced with lignocellulose nanofibers from cassava bagasse. Int J Biol Macromol 139:1151-1161. https://doi.org/10.1016/j.ijbiomac.2019.08.115.

Ucelay AR (2020) Europe paper industry–statistics & facts. The European Paper Industry. Statista Research Department, pp. 1-30. https://www.statista.com/topics/7737/paperindustry-in-europe/#topicOverview. (27 February 2024).

Vinyard S (2021) Charmin's toilet paper—Thin sustainability claims. NRDC: New York, NY, 23 pp.

Vinyard S, Skene J (2020) The issue with Tissue 2.0: How the tree-to-toilet pipeline fuels our climate crisis. NRDC. pp: 1-28. https://www.nrdc.org/sites/default/files/issue-with-tissue-2-report.pdf. (14 March 2024).

Vivas KA, Vera RE, Dasmohapatra S, Marquez R, Van Schoubroeck S, Forfora N, Azuaje AJ, Phillips RB, Jameel H, Delborne JA, Saloni D, Venditti RA, Gonzalez R (2024) A multi-criteria approach for quantifying the impact of global megatrends on the pulp and paper industry: Insights into digitalization, social behavior change, and sustainability. Logistics 8(2):36. https://doi.org/10.3390/logistics8020036.

Worku LA, Bachheti A, Bachheti RK, Rodrigues Reis CE, Chandel AK (2023) Agricultural residues as raw materials for pulp and paper production: Overview and applications on membrane fabrication. Membranes 13(2):228. https://doi.org/10.3390/membranes13020228.

Zambrano F, Wang Y, Zwilling JD, Venditti R, Jameel H, Rojas O, Gonzalez R (2021) Micro- and nanofibrillated cellulose from virgin and recycled fibers: A comparative study of its effects on the properties of hygiene tissue paper. Carbohydr Polym 254:117430. https://doi.org/10.1016/j.carbpol.2020.11743.

Zhang H, Sablani S (2021) Biodegradable packaging reinforced with plant-based foodwaste and by-products. Curr Opin Food Sci 42:61-68. https://doi.org/10.1016/j.cofs.2021.05.003.

DEFLECTION PERFORMANCE OF MEDIUM DENSITY FIBERBOARD AND PARTICLEBOARD SHELVES JOINED ABS, PLA, AND WOOD-PLA FILAMENT PINS

*E. S. Erdinler**†*

E-mail: seda@iuc.edu.tr

S. Seker†

Faculty of Forestry, Department of Forest Industry Engineering,
Istanbul University–Cerrahpasa, Istanbul, Turkey
E-mail: sedanur.seker@iuc.edu.tr

(Received May 2023)

Abstract. This study determined the deflection performance of melamine-faced medium-density fiberboard and particleboard shelves supported by acrylonitrile butadiene styrene, polylactic acid (PLA), or WOOD-PLA pins. The study was based on the BS EN 16122 standard and TS EN 9215 to assess deformation subjected to increasing loads. Material type, filament fill, and filament material type significantly affected deflection with R^2 and adjusted R^2 values of 96.1% and 94.2%, respectively.

Keywords: Shelves, 3D printer, joints, deflection, wood.

INTRODUCTION

Wall and floor cabinets serve as storage units in various spaces, such as kitchens, bathrooms, and offices. These cabinets are typically constructed in the form of box furniture. Owing to their versatile nature, furniture units can be subjected to various loads with varying sizes and qualities, depending on the intended purpose of the furniture (İmirzli 2008). Shelves can deflect to varying degrees depending on the material composition and load. Understanding these effects is an important aspect of proper design. Shelves are normally supported by pins of varying materials including wood, metal, or plastic. Metal or wood pins are normally fabricated from larger pieces, whereas plastic pins are extruded or cast.

The evolution of three-dimensional (3D) printing has created an exciting new opportunity to create pins with more specific properties tailored to the specific application. Three-dimensional printing provides greater flexibility in controlling the microarchitecture to fabricate cellular structures than conventional manufacturing methods (Compton and Lewis 2014). There are many 3D printing methods, including stereolithography, inkjet printing, fused deposition modeling (FDM), selective laser sintering, and laminated object manufacturing.

Objects that are already fabricated include functional parts, such as toys, tools, household items, and customized scientific instruments (Perce 2017). Three-dimensional fused filament fabrication (FFF) printers have the potential to be used not only for conventional prototyping but also for small-scale manufacturing (Pearce et al 2010; Perce 2017).

Polylactic acid (PLA), a bio-based polymer, is one of the most widely used thermoplastics to fabricate objects with 3D FFF printers. PLA develops strong bonds between successive layers of melt materials during printing because the glass transition temperature is low enough to facilitate effective bonding between layers, yet high enough to ensure that the printed parts maintain their shape when subjected to moderate operating temperatures. PLA is already used in disposable packaging applications and is currently being investigated for more durable applications (Harris and Lee 2010; Mannoor et al 2013; Wertz et al 2014; Notta-Cuvier et al 2014, 2015; Bouzouita et al 2016; Nagarajan et al 2016).

* Corresponding author

Layer height, printing orientation, density and infill type, and number of outline perimeters strongly influence the mechanical properties of finished parts in additive manufacturing printing. Pandzic et al (2019) examined the influence of density and infill type on the tensile properties of PLA specimens and showed that an increase in infill density PLA-improved mechanical properties.

PLA has the potential to either replace conventional petrochemical-based polymers for industrial applications or as a leading biomaterial for numerous medical applications (Drumright et al 2000; Lopes et al 2012). Economic, environmental, and safety challenges have encouraged packaging producers and scientists to partially substitute petrochemical-based polymers with biodegradable ones. PLA is a high-strength, thermoplastic, high-modulus polymer that can be made from annually renewable resources. It is easily processable on standard plastic equipment to yield molded film, fibers, or parts (Garlotta 2002; Czuba 2014).

Blend materials can be applied in many industrial applications due to their higher strength-to-weight ratios than base materials. Applications requiring high tensile strength can include these filament materials among thermoplastics (Blok et al 2018).

Yildirim et al (2019) studied the properties of dowels produced in 3D printers for fixed construction furniture corner joints using a diagonal pressure test. They produced two different acrylonitrile butadiene styrene (ABS) and PLA 8 mm diameter dowels using a 3D printer using the FDM method. The long side of the dowels was produced parallel (tangent) and perpendicular (radial) to the ground plane. The main construction material was medium-density fiberboard (MDF Lam) coated with synthetic resin paper (melamine). The dowel was produced in the 3D printer as the joining element and L-type construction was prepared using polyurethane glue as the adhesive.

The most common printing filaments used in FDM are PLA and ABS, as they have shown impressive results against various stresses. ABS has high strength, whereas PLA (Garric et al 2008; Zhang et al 2019) is flexible. Blending them together can produce a product with improved strength and mechanical properties (Dizon et al 2018).

Wood is an organic material, and its powder can be used for printing in combination with different materials. The thermoplastic composite industry uses wood owing to its affordability, renewability, high modulus, and excellent machinability (Ayrilmis 2018; Deb and Jafferson 2021). Adding wood to PLA decreases filament costs, but further investigation into the mechanical characterization of 3D-printed PLA-wood composites is required.

Previous studies have primarily focused on optimizing and characterizing fully dense material parts (Lanzotti et al 2015; Song et al 2017).

Recent studies have characterized the effects of build orientation (flat, on-edge, or upright), layer thickness (0.06 to 0.24 mm), and feed rate (20-80 mm/s) on the mechanical performance of PLA samples manufactured with a low-cost 3D printer using tensile and three-point bending tests. Upright samples exhibited interlayer failure with lower strength and stiffness performance for built orientations. Upright samples also exhibited increased tensile and flexural strengths as layer thickness increased. On the other hand, iTensile and flexural strengths decreased as the feed rate used to produce these samples increased (Chacón et al 2017).

Afrose et al (2014) investigated the tensile properties of dog-bone-sized PLA thermoplastic material printed in different build orientations processed by a Cube-2 3D Printer. The ultimate tensile stress of PLA samples built in the X-direction (PLA-X) was highest at 38.7 MPa and ranged from 60% to 64% of the raw PLA material, whereas values were lower at 31.1 and 33.6 MPa for PLA-Y and PLA-45, respectively. The study suggested that although different build orientations have varying effects on the strength and toughness of printed parts, a balance can be achieved by considering the specific application requirements.

Tymrak et al (2014) quantified the basic tensile strength and elastic modulus of printed components

using realistic environmental conditions for standard users of a selection of open-source 3D printers. They found average tensile strengths of 28.5 MPa for ABS and 56.6 MPa for PLA with average elastic moduli of 1807 and 3368 MPa, respectively.

Tensile strength, flexural properties, fracture toughness, and compressive properties, as well as impact strength, have also been investigated (Guntekin 2003; Imirzi 2008; Wang et al 2017). Mechanical properties of fully dense parts fabricated with an optimal selection of process parameters are comparable to parts fabricated with conventional methods such as injection molding.

Eckelman (2003) stated that shelf deflections between 1/200 and 1/500 of the shelf length were within acceptable limits. He stated that deflections up to 1/180 of the shelf length were pleasing to the eye, but ratios at or below 1/165 were aesthetically pleasing (Eckelman 2003).

Jivkov et al (2010) examined the deflection properties of shelves made of melamine-coated particleboard (PB) and fiberboard under distributed load by placing two to three slats of plywood in channels drilled on the lower surfaces of the shelves. The incorporation of three slats beneath the shelf structure resulted in a 20% improvement in deflection properties compared with standard PB. Moreover, they also found that fiberboard exhibited a 30% increase in deflection properties with the same support (Jivkov et al 2010).

Tankut et al (2008) reported a 33% improvement in deflection when screws were placed behind the shelves to improve the deflection properties of fiberboard and PB (Tankut et al 2008). Joining elements of in-cabin shelves used as cargo racks were produced with three different filaments in a 3D printer.

The furniture industry employs various joint assembly methods, including those that involve plastics, metals, and other materials. The goal of this study was to determine the deflection of PB and MDF shelves supported by pins composed of different material types.

MATERIALS AND METHODS

Materials

Wood cabinet and shelves. Typical wooden cabinets of MDF and PB (1800 mm (height) × 450 mm (width) × 450 mm (thickness)) were chosen randomly. The shelves in these cabinets were made of 18-mm thick MDF and PB materials (Fig 1).

A total of 36 shelves manufactured with two different materials were tested. Density, MC, MOR, and MOE values of the shelves were 0.716 g/cm^3, 6.98%, 28.48 N/mm^2, 6028.72 N/mm^2, respectively, for MDF and 0.63 g/cm^3, 9.02%, 12.86 N/mm^2, 5821.2 N/mm^2, respectively, for PB.

Fasteners. The cabinets featured MDF and PB shelves secured in place by shelf pins. The load-bearing capacity of the shelf pins is often more important than the overall durability of the shelf itself. The shelf pin design used in this study (Fig 2[a] and [b]) is a widely adopted product utilized by numerous companies.

In-fill percentages of the printer shelf fastener were 30% or 40%. Various pins were produced using different fill levels to determine the most suitable fill rate for the desired conditions. The filaments used for 3D printing included PLA, ABS, and PLA-Wood materials from a filament manufacturing company in Turkey (Porima Polymer Technologies Inc., Yalova, Turkey).

Forty-eight PLA filament pins were (1.75 mm in diameter) used to mount MDF and PB shelves at 30% and 40% fill to the cabinet. Figure 3 shows pins made of PLA filament with 30% or 40% fill (Nikon SMZ-445).

ABS, a commonly used thermoplastic, is used in a broad range of products from television remote controls to the automotive industry. ABS has high flexural strength and elongation before breaking. In the study, 48 ABS shelf pins were used to mount MDF and PB shelves at 30% and 40% fill to the cabinet. Figure 4 shows pins made of ABS filament with 30% or 40% fill.

PLA/wood filaments incorporate 30% wood reinforcement materials into their composition,

Figure 1. Examples of the test shelves along with side views of the MDF and PB shelves.

enabling the printing of products with greater resolution, reduced mass, superior thermal properties, and a realistic wood texture than standard PLA filaments (Chacón et al 2017).

Forty-eight 3D-printed PLA/wood shelf pins were used to mount MDF and PB shelves with 30% or 40% fill to the cabinet (Fig 5).

Test Method

Test method for shelves. The study was based on BS Standard EN 16122 (2012) while TS EN 9215 (2005) was followed to measure shelf deformation with increasing loads. Eighty kilogram square meter of test load was added for every 40 mm of shelf length and held for 7 d resulting

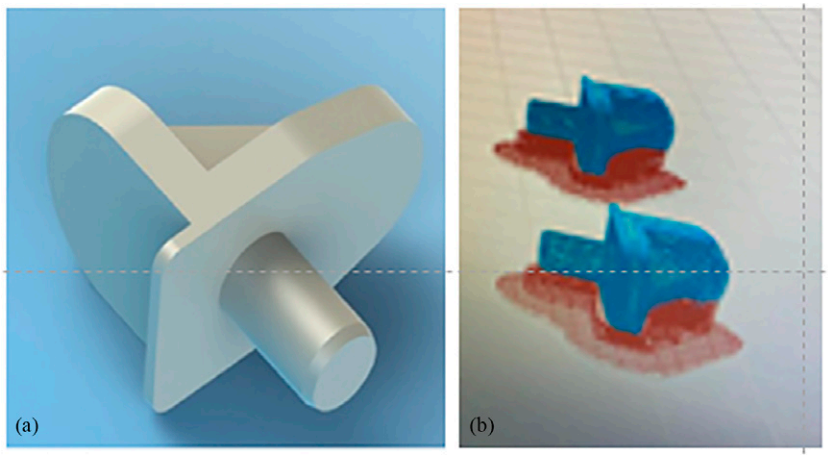

Figure 2. Example of (a) the model pin and (b) the pin as modeled using 3D printer software.

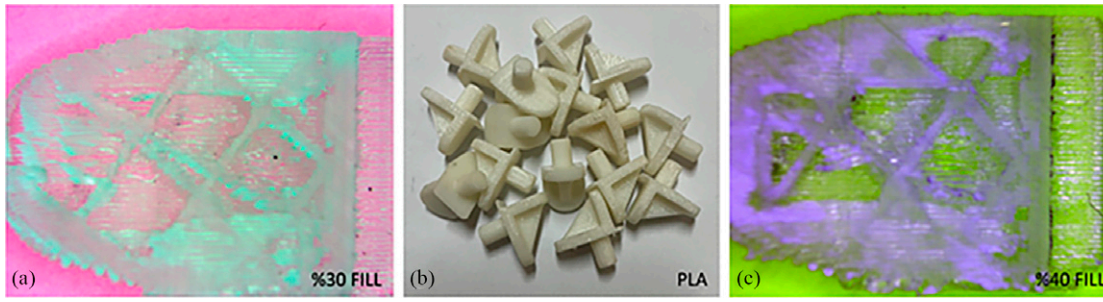

Figure 3. Examples of (b) PLA filament pins along with microscopic images of pins with 30% or 40% fill ratios (a and c, respectively).

Figure 4. Examples of (b) ABS filament pins along with microscopic images of pins with 30% or 40% fill ratios (a and c, respectively).

in a total load of 12.8 kg. However, the test was repeated two times since the material used was new and not of the type of glass, metal, or plastic specified in the standard. Total deflection was recorded at the end of 7 d.

The first deflection measurements were made at midspan (shelves) on unloaded racks, then again after applying the uniform load using a deflection yoke equipped with a comparator (Devotrans digital indicator) to measure center deflection to the nearest 0.001 mm. Measurements were taken at the midpoint along the shelf length where maximum deflection occurred (Fig 6).

Wood and wood-based materials tend to deform when under long-term loading. Deflection takes place as a result of the changes in molecular structure. In this study, deflection tests were conducted on shelves that were subjected to a distributed and fixed loading for 7 d. Deflection at the time of initial loading is fast (primary deflection), and then declines to a slower steady rate (secondary deflection) (Guntekin 2003).

Figure 5. Examples of (b) PLA-WOOD filament pins along with microscopic images of pins with 30% or 40% fill ratios (a and c, respectively).

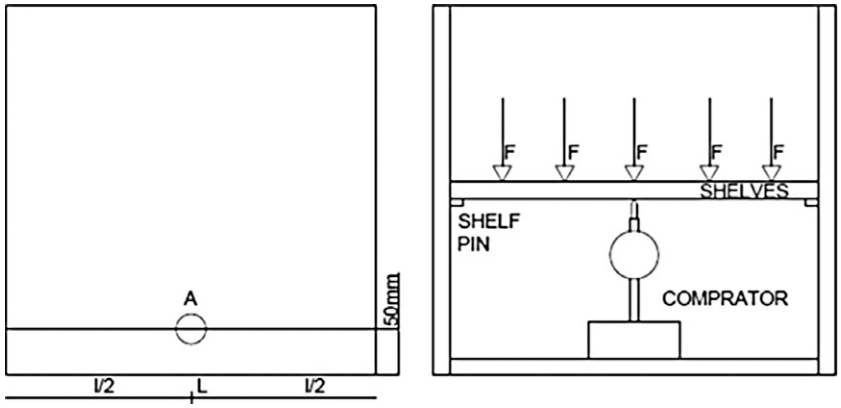

Figure 6. Diagram showing the load pattern for the shelves along with the comparator used to measure the deflection.

The data were subjected to multivariate analysis of variance (ANOVA). When the difference between groups was significant, univariate analysis was used to determine the difference between means at $\alpha = 0.05$ using SPSS software.

SolidWorks finite element analyses. The availability of computer-based finite element methods (FEM) allows even complex structures such as furniture construction to be analyzed without destroying the furniture. This method also helps to accelerate the engineering design of furniture. In this study, the FEM software SolidWorks (Dassault Systèmes SOLIDWORKS Corp, Waltham, MA) was used to analyze the shelf models. Geometry, loading, and the meshing process for the shelves are displayed in Fig 7 Triangular meshing structure, as maximum mesh, was used to evaluate several intervals. MOR, MOE, density, and MC values of MDF and PB shelves were determined by laboratory tests and for the filaments. Technical values from the supplier were used to determine the deflection values of both shelf types.

RESULTS AND DISCUSSION

Damage Symptoms and Deflection Values

The midpoint of the shelves and the connection pins in both PB and MDF were the most frequently observed damage locations. Standard loads, combined with pins made of ABS, PLA, and PLA-WOOD (Fig 8), were applied during the testing process, and deflection was measured using a comparator.

As part of the standard (BS 16122-2012) testing protocol, shelves were left under load for 7 d, and varying degrees of deflection was observed in the MDF and PB materials. The results demonstrated that the deflection of pins used as joining elements varied across different ranges (Fig 9) and were further impacted by the saturation point.

Statistical Analyses Results

According to the ANOVA, shelf material type, fill, and filament material type factors had statistically significant effects on deflection. Two-factor ANOVA statistics were performed for shelf material, filament type, and saturation unrelated sample groups, and the mean and standard deviations of edge and fill (Table 1).

The average filament type deflections used in the tests and the fill ratios of these filaments were 1.3261 mm for MDF shelves and 1.6029 mm for PB.

The statistical results for the average deflection results according to shelf material, filament material, and fill variables are shown in Table 2.

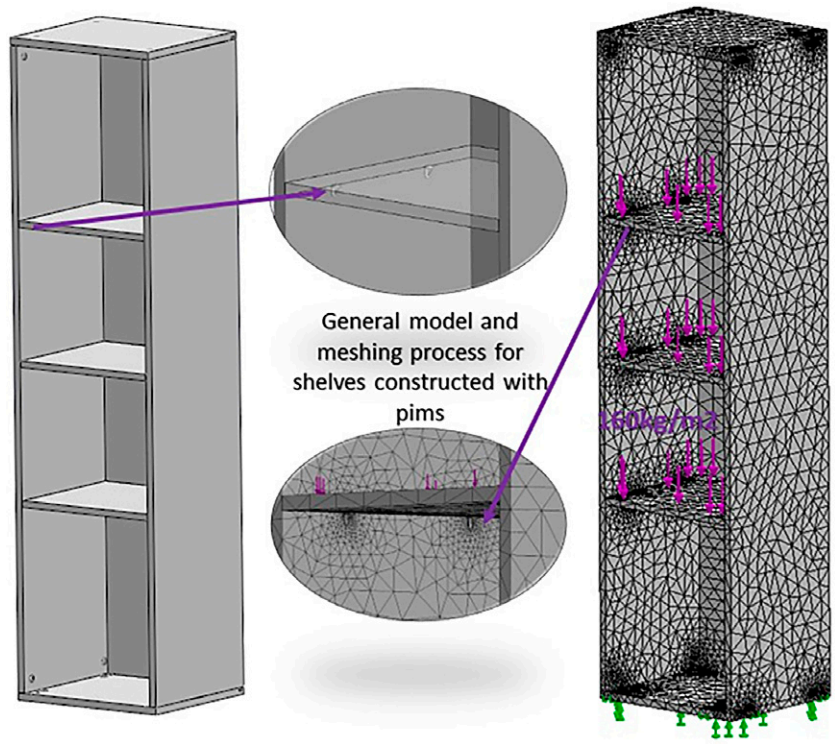

Figure 7. Diagram showing the shelving unit along with the meshing used for the model.

Figure 8. Photos showing the loads applied to a shelf unit as well as examples of shelves with the three-pin materials.

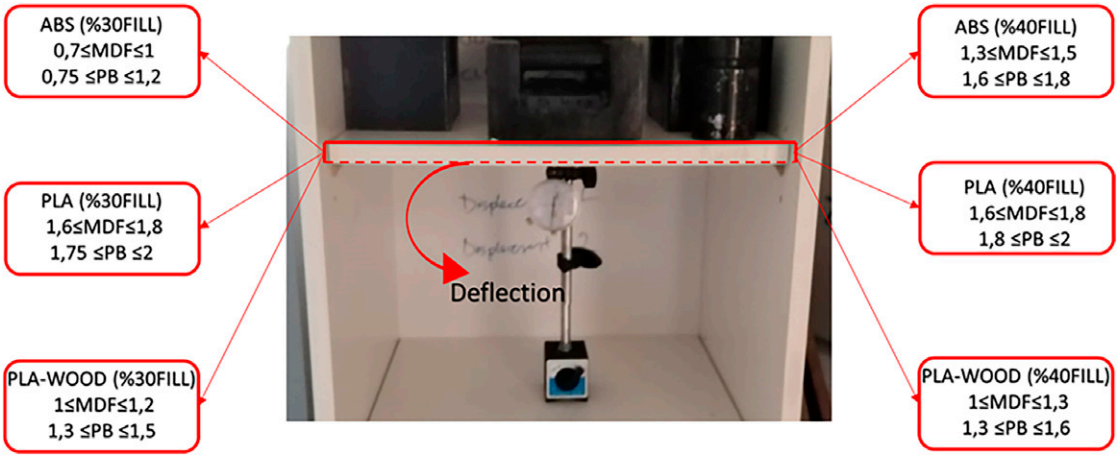

Figure 9. Data groups were obtained from test results of loads applied to shelves supported with PLA, ABS, or PLA-WOOD pins.

Table 1. Results of two-factor statistical analysis.

MDF				PB				Total			
		Mean	SD			Mean	SD			Mean	SD
ABS	%30	0.71	0.15	ABS	30%	0.88	0.13	ABS	30%	0.80	0.15
	%40	1.43	0.08		40%	1.71	0.08		40%	1.57	0.17
PLA	%30	1.66	0.08	PLA	30%	1.83	0.13	PLA	30%	1.75	0.13
	%40	1.85	0.05		40%	2.36	0.15		40%	2.10	0.30
PLA-WOOD	%30	1.19	0.15	PLA-WOOD	30%	1.35	0.04	PLA-WOOD	30%	1.27	0.13
	%40	1.10	0.10		40%	1.40	0.14		40%	1.22	0.19
Total	%30	1.19	0.43	Total	30%	1.35	0.42	Total	30%	1.27	0.42
	%40	1.46	0.33		40%	1.88	0.44		40%	1.65	0.43
Total		1.32	0.40	Total	1.60	0.50	Total	1.46	.462	1.32	0.40

Table 2. Table of average statistics.

Source	Type III sum of squares	*df*	Mean square	*F*	Sig.	Partial eta squared
Corrected Model	6.975[a]	11	0634	51.375	0.00	0.96
Intercept	73.556	1	73.556	5959.799	0.00	1.00
Shelf_Material	0.609	1	0609	49.367	0.00	0.68
Filament_Material	3958	2	1979	160.333	0.00	0.93
Fill	1190	1	1190	96.413	0.00	0.81
Shelf_Material * Filament_Material	0.026	2	0013	1040	0.37	0.08
Shelf_Material * Fill	0.088	1	0088	7157	0014	0.24
Filament_Material * Fill	0.896	2	0448	36.292	0.00	0.76
Shelf_Material * Filament_Material * Fill	0.024	2	0012	0.990	0.39	0.08
Error	0.284	23	0.012			
Total	81.923	35				
Corrected Total	7259	34				

[a] $R^2 = 0.961$ (adjusted $R^2 = 0.942$).

Solid Finite Element Analysis

Samples tested for 7 d were modeled in the SolidWorks finite element analysis (FEA) program and subjected to the same load. Deformation ranges were similar to the actual tests. Pins made of ABS filament deflected 0.959 mm in MDF shelves at 30% fill, 0.959 mm in PB shelves, 1.03 mm in MDF shelves at 40% fill, and 1.35 mm in PB shelves, 1.72 mm in Fig 10.

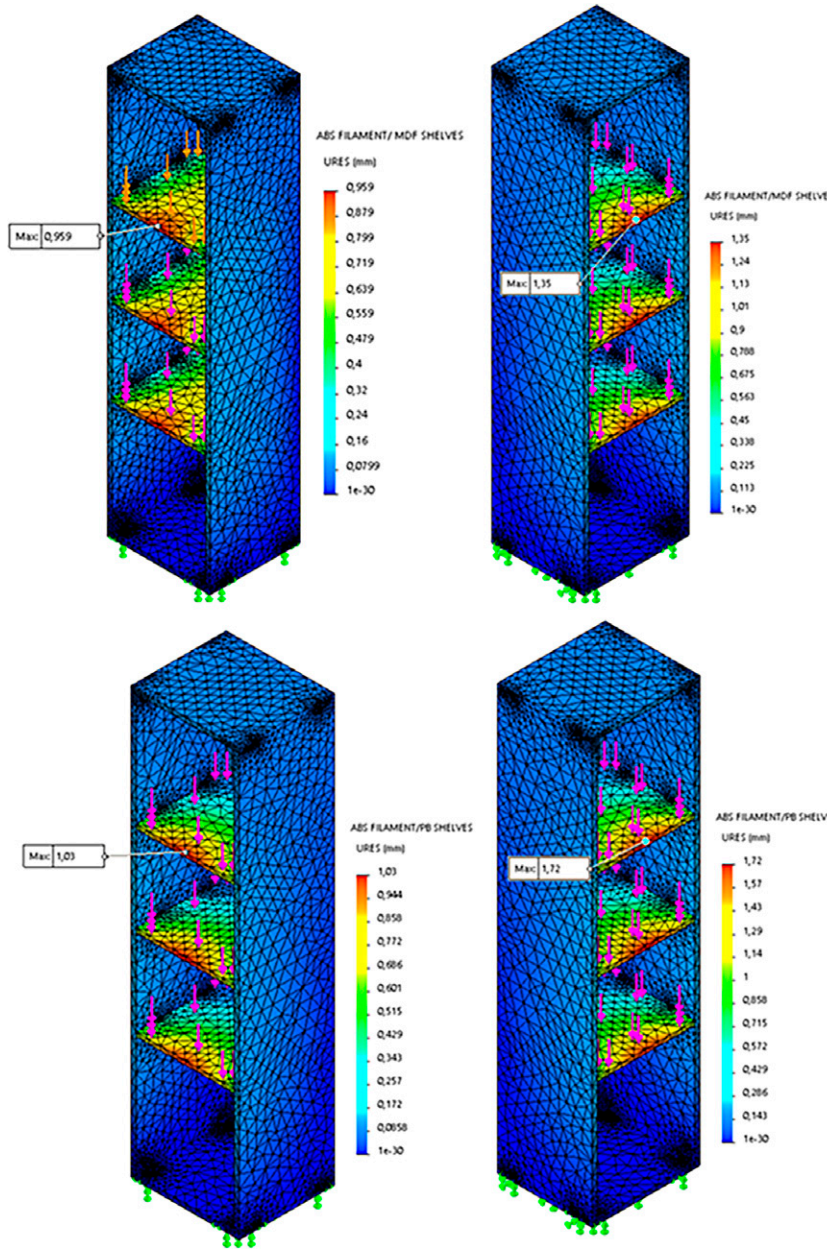

Figure 10. FEM analysis results show load–deflection of shelves with ABS pins.

Pins made of PLA filament gave a deflection of 1.65 mm in MDF shelves at 30% fill, 1.65 mm in PB shelves, 1.83 mm in MDF shelves at 40% fill, and 1.78 mm in PB shelves; 1.94 mm in Fig 11.

Pins made of PLA-WOOD filament deflected 1.40 mm in MDF shelves at 30% fill compared with 1.10 mm in PB shelves, whereas those at 40% fill deflected 1.37 mm in MDF shelves and 1.14 mm in PB shelves (Fig 12).

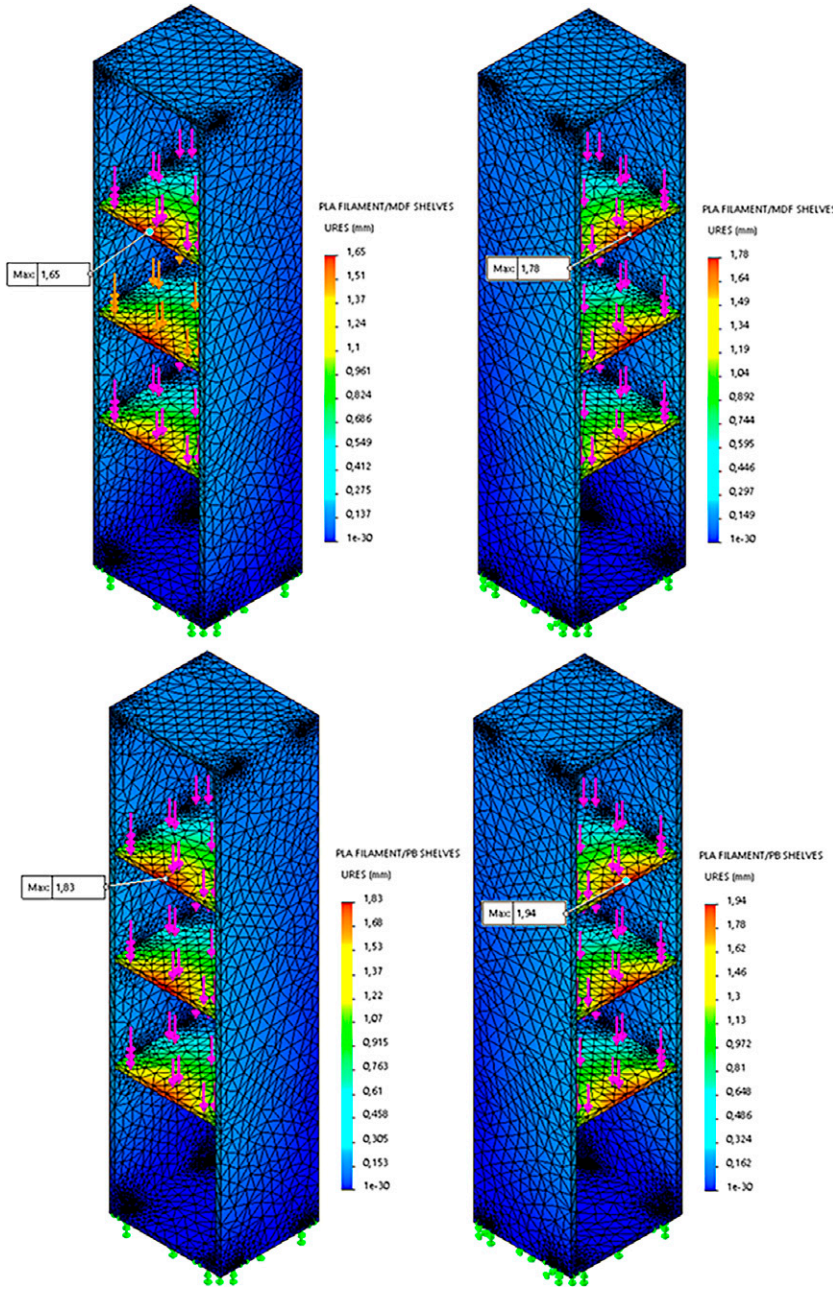

Figure 11. FEM analysis results show load–deflection of shelves with PLA pins.

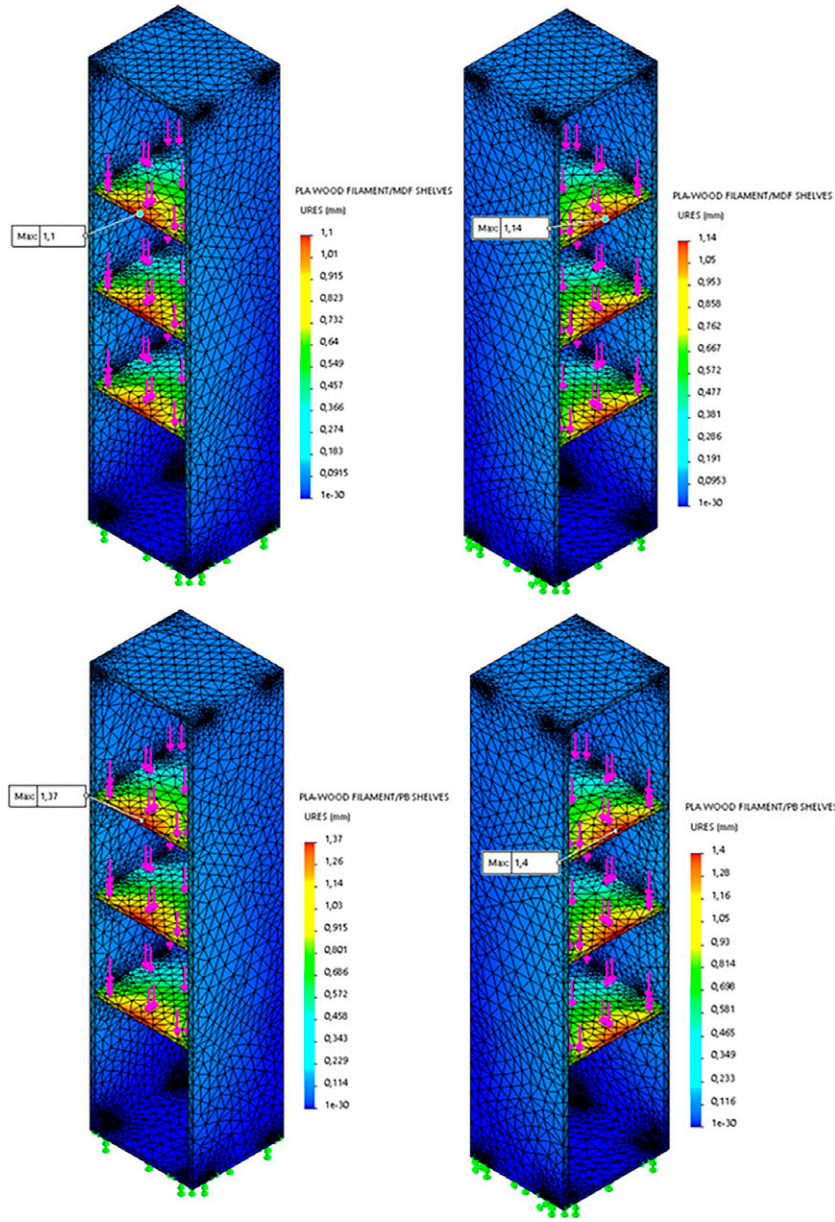

Figure 12. FEM analysis results show load–deflection of shelves with PLA-WOOD pins.

Emerging technology allows pins to be reverse-engineered to optimize properties for specific applications. For example, Koprnicky et al (2017) evaluated an upper extremity prosthesis made with 3D printing technology including bionic hands. Yildirim et al (2019) determined the effect of biscuit-type joining elements produced in 3D printers on the bending moment. Strength is targeted in "L" type corner joints. For this purpose, 18-mm thick MDF-lam, wood-based biscuits of ABS, or PLA were produced with a 3D printer.

The least amount of deflection in the current study was observed with ABS filament, followed by

PLA-WOOD and PLA. Zhang et al (2019) reported that ABS filament was more durable, while Ayrilmis (2018) noted that WOOD PLA was more durable than PLA. Assembly pins of ABS, PLA, and PLA-WOOD materials were produced with 30% and 40% saturation levels. Saturation level directly affected pin mechanics, which is consistent with the findings of Pandzick et al (2019). Finite element method (FEM) has been used in many fields, such as healthcare, construction, and automotive applications to optimize materials before actual production. The numerical modeling of 3D-printed natural fiber-reinforced plastic composites is still in its infancy, which underlines the need for further research. For example, Nagib et al (2023) evaluated a personalized polymeric 3D-printed, digitally planned surgical guide designed to achieve precision and predictability in nonstandard mini-implant orthodontic cases. The analysis was used to design a surgical guide for the placement of mini-implants as temporary crown supports. A FEM simulation was performed using Abaqus numerical analysis software. Finite element simulation revealed the maximum displacements and stresses in the surgical guide. Kuşkun et al. (2023) optimized the cross-sectional geometry for dowels created by 3D printing, and optimization supported by FEM analysis. Tankut et al (2008) determined the effects of various construction practices on the flexural properties of bookcases made of composite materials. They performed a deflection test on MDF and PB racks in 18 bookshelves using different fasteners. Each of the three cases was made for 1) determining the actual deflection of the leading edge of a shelf as a function of the reinforcement of the trailing edge; 2) evaluating the contribution of installing an intermediate shelf on the side walls to the bending of the walls; and 3) examining the effect of bezels on cheek deflection. The remaining six cases were used to investigate the effect of rack-to-sidewall joint stiffness on midspan rack deflection. The results of the study showed that the performance of existing designs could be improved by attaching the racks to the back of the chassis with screws, securely attaching the racks to the chassis edges, and increasing the chassis thickness, or MOE. The results showed that the PB material exhibited greater aberration, consistent with similar findings obtained using ANSYS software. These results are consistent with the findings of the present study.

CONCLUSIONS

In the current study, the deflection values were directly proportional to the shelf and filament materials. Furthermore, deflection values were proportional to the filament material's fill content. MDF shelves were more durable under load than PB shelves. ABS pins experienced less deflection than those composed of PLA or PLA-Wood and would be recommended for shelves subjected to longer-term, heavier loads. Despite the presence of variables, the results indicated that shelves made of MDF were more durable under load than PB. Therefore, considering the typical loads encountered by shelves within cabinets during daily use, such as books, plates, detergents, etc., it is recommended to utilize MDF materials for enhanced durability. In the conducted study, the same load was uniformly applied for the same duration. Deflection values were recorded under conditions where ABS filament was utilized for both shelf materials, and it was found that deflection values were lower compared with those obtained using other filaments. ABS material pin fitting would be recommended for shelf construction for a longer duration of use. According to the experimental data, the deflection value of shelves supported by pins from ABS filaments was less than that of PLA and PLA-WOOD filaments. This result was also supported by the performed FEM analysis.

Accordingly, shelves can be simulated structurally under the actual realization of computer-aided analysis such as SolidWorks FEA for cost reduction and for the prevention of material damage likely to occur. The filament type used in the tests and the fill ratios of these filaments were 1.3261 for MDF shelf material and 1.6029 for PB material in the deflection test results. The results showed that the material type, filament fill, and filament material type were significant.

The adequacy of models was evaluated by the *R*-square (R^2) and adjusted *R*-square (adj-R^2) values. The results for these values were 96.1% and 94.2%, respectively.

REFERENCES

Afrose MF, Masood SH, Nikzad M, Iovenitti P (2014) Effects of build orientations on tensile properties of PLA material processed by FDM. Adv Mater Res 1044-1045:31-34. https://doi.org/10.4028/www.scientific.net/AMR.1044-1045.31.

Ayrilmis N (2018) Effect of layer thickness on surface properties of 3D printed materials produced from wood flour/PLA filament. Polym Test 71:163-166.

Blok LG, Longana ML, Yu H, Woods BKS (2018) An investigation into 3D printing of fibre reinforced thermoplastic composites, Bristol Composites Institute (ACCIS), University of Bristol, Bristol, BS8 1TR, UK.

Bouzouita A, Samuel C, Cuvier DN, Odent J, Lauro F, Dubois P, Raquez JM (2016) Design of highly tough poly (L-lactide)-based ternary blends for automotive applications. J Appl Polym Sci 133(19):1-9. https://doi.org/10.1002/app.43402.

BS EN 16122 (2012) Domestic and non-domestic storage furniture—Test methods for the determination of strength, durability and stability. BSI Standards Publication, Test procedures for movable parts, Strength of pivoted doors. Vertical load of pivoted doors.

Chacón JM, Caminero MA, García-Plaza E, Núñez PJ (2017) Additive manufacturing of PLA structures using fused deposition modelling: Effect of process parameters on mechanical properties and their optimal selection. Mater Des 124:143-157. https://doi.org/10.1016/j.matdes.2017.03.065.

Compton BG, Lewis JA (2014) 3D-Printing of lightweight cellular composites. Adv Mater 26(34):5930-5935. https://doi.org/10.1002/adma.201401804.

Czuba L (2014) Handbook of Polymer Applications in Medicine and Medical Devices. Elsevier 9-19. https://doi.org/10.1016/B978-0-323-22805-3.00002-5.

Deb D, Jafferson JM (2021) Natural fibers reinforced FDM 3D printing filaments. Mater Today Proc 46: 1308-1318.

Dizon JRC, Espera AH, Chen Q, Advincula RC (2018) Mechanical characterization of 3D-printed polymers. Addit Manuf 20:44-67.

Drumright RE, Gruber PR, Henton DE (2000) Polylactic acid technology. Adv Mater 12(23):1841-1846. https://doi.org/10.1002/1521-4095.(200012)12:23≤1841::AID-ADMA1841≥3.0.CO;2-E

Eckelman CA (2003) Textbook of product engineering and strength design of furniture. Pages 65-67 *in* Chapter IV implified methods of furniture analysis, Purdue University, West Lafayette, Indiana.

Garlotta D (2002) Literature review of poly (lactic acid). J Polym Environ 9(2):63-84.

Garric X, Garreau H, Vert M, Moles JP (2008) Behaviors of keratinocytes and fibroblasts on films of PLA50–PEO–PLA50 triblock copolymers with various PLA segment lengths. J Mater Sci Mater Med 19(4): 1645-1651.

Guntekin E (2003) Performance of ready to assemble (RTA) furniture, Suleyman Demirel University, Faculty of Forestry, pp. 37-48.

Harris A, Lee E (2010) Heat and humidity performance of injection molded PLA for durable applications. J Appl Polym Sci 115(3):1380-1389. https://doi.org/10.1002/app.

Imirzi HO (2008) Strength properties of box type furniture manufactured with different construction techniques and different thicknesses of boards. PhD thesis, Gazi University, Ankara.

Jivkov V, Yordanov Y, Marinova A (2010) Improving by reinforcement the deflection of shelves made of PB and MDF. Pages 205-208 *in* PTF BPI on Processing Technologies for the Forest and Biobased Products Industries, Salzburg University, Kusch Austria.

Koprnicky J, Najman P, Safka J (2017) 3D printed bionic prosthetic hands. *in* 2017 IEEE International Workshop of Electronics, Control, Measurement, Signals and their Application to Mechatronics (ECMSM), DOI: 10.1109/ECMSM.2017.7945898.

Kuşkun T, Kasal A, Çağlayan G, Ceylan E, Bulca M, Smardzewski J (2023) Optimization of the cross-sectional geometry of auxetic dowels for furniture joints. Materials 16(7):2838. https://doi.org/10.3390/ma16072838.

Lanzotti A, Grasso M, Staiano G, Martorelli M (2015) The impact of process parameters on mechanical properties of parts fabricated in PLA with an Open-Source 3-D Printer. Rapid Prototype J 21(5):604-617. https://doi.org/10.1108/RPJ-09-2014-0135.

Lopes MS, Jardini AL, Filho RM (2012) Poly (lactic acid) production for tissue engineering applications, *in* 20th International Congress of Chemical and Process Engineering CHISA, Prague, Cezch Republic.

Mannoor MS, Jiang Z, James T, Kong YL, Malatesta KA, Soboyejo WO, Verma N, Gracias DH, McAlpine MC (2013) 3D printed bionic ears. Nano Lett 13(6):2634-2639. doi: 10.1021/nl4007744.

Nagarajan V, Mohanty AK, Misra M (2016) Perspective on polylactic acid (PLA) based sustainable materials for durable applications: Focus on toughness and heat resistance. ACS Sustainable Chem Eng 4(6):2899-2916. https://doi.org/10.1021/acssuschemeng.6b00321.

Nagib R, Farkas AZ, Szuhanek C (2023) FEM analysis of individualized polymeric 3D printed guide for orthodontic mini-implant insertion as temporary crown support in the anterior maxillary area. Polymers (Basel) 15(4):879; https://doi.org/10.3390/polym15040879.

Notta-Cuvier D, Odent J, Delille R, Murariu M, Lauro F, Raquez JM, Bennani B, Dubois P (2014) Tailoring polylactide (PLA) properties for automotive applications: Effect of addition of designed additives on main mechanical properties. Polym Test 36:1-9. https://doi.org/10.1016/j.polymertesting.2014.03.007.

Notta-Cuvier D, Murariu M, Odent J, Delille R, Bouzouita A, Raquez M, Lauro F, Dubois P (2015) Tailoring polylactide properties for automotive applications: Effects of co-addition of halloysite nanotubes and selected plasticizer. Macromol Mater Eng 300(7):684-698. https://doi.org/10.1002/mame.201500032.

Pandzic A, Hodzic D, Milovanovic A (2019) Influence of material colour on mechanical properties of PLA material in FDM technology. Pages 75 *in* 30th DAAAM International Symposium on Intelligent Manufacturing and Automation, Vienna, Austria. 555-561.

Perce JM (2017) Building research equipment with free, open-source hardware. Science 337:1303-1304. https://doi.org/10.1126/science.1228183.

Pearce JM, Morris Blair C, Laciak KJ, Andrews R, Nosrat A, Zelenika-Zovko I (2010) 3-D Printing of open-source appropriate technologies for self-directed sustainable development. J Sustain Dev 3(4):17-29. https://doi.org/10.5539/jsd.v3n4p17.

Song Y, Li Y, Song W, Yee K, Lee KY, Tagarielli VL (2017) Measurements of the mechanical response of unidirectional 3D-printed PLA. Mater Des 123:154-164. https://doi.org/10.1016/j.matdes.2017.03.051.

Tankut ND, Tankut AN, Eckelman CA (2008) Improving the deflection characteristics of shelves and side walls in panel-based cabinet furnıture. For Prod Soc J 53(10): 56-64.

TS EN 9215 (2005) This standard comprises strength and balance tests for wooden furniture. 1-55.

Tymrak BM, Kreiger M, Pearce JM (2014) Mechanical properties of components fabricated with open-source 3-D printers under realistic environmental conditions. Mater Des 58:242-246. https://doi.org/10.1016/j.matdes.2014.02.038.

Wang L, Gramlich WM, Gardner DJ (2017) Improving the impact strength of poly (lactic acid) (PLA) in fused layer modeling (FLM). Polymer (Guildf) 114:242-248. https://doi.org/10.1016/j.polymer.2017.03.011.

Wertz JT, Mauldin TC, Boday DJ (2014) Polylactic acid with improved heat deflection temperatures and self-healing properties for durable goods applications. ACS Appl Mater Interfaces 6(21):18511-18516. https://doi.org/10.1021/am5058713.

Yildirim MN, Karaman A, Doruk S (2019) Use of "T" Type fasteners produced in 3D Printer in furniture corner joints. *in* 3rd International Symposium on Multidisciplinary Studies and Innovative Technologies, Ankara, Turkey.

Zhang X, Chen L, Mulholland T, Osswald TA (2019) Characterization of mechanical properties and fracture mode of PLA and copper/PLA composite part manufactured by fused deposition modeling. SN Appl Sci 1(6): 616. https://link.springer.com/article/10.1007/s42452-019-0639-5.